Master thesis

2018/2019

The uptake of nickel in *Arabidopsis thaliana*

Cindy Lainé

Title page illustration:

- The photo (Open pit mining) at the top came from the website ABC news (https://www.abc.net.au/news/2016-01-21/wach-western-areas-nickel-mine/7103634).
- The second photo (*Arabidopsis thaliana*) was taken by Mr. Peter Greenwood.
- The third figure (DNA) came from the website TBR Newsmedia (http://tbrnewsmedia.com/life-lines-its-in-my-dna/)
- The fourth photo (*Pycnandra acuminata)* was taken by Mr. Antony Van der Ent (Jaffré, Reeves, Baker, Schat, and Ent, 2018).

The uptake of Ni in *Arabidopsis thaliana*

Cindy Michele Suzanne Lainé

Reg. no.: 921208-496-260

MSc Plant Biotechnology, specialization Molecular Plant Breeding and Pathology

Supervisor: Jitpanu Yamjabok

Examiner: Prof.dr. Mark Aarts

MSc Thesis Genetics (GEN-80436)

Laboratory of Genetics, Wageningen University

August 2018- February 2019

WAGENINGEN
UNIVERSITY & RESEARCH

Table of Contents

Abstract

Background and aims: The physiological and genetic mechanisms behind Ni uptake, translocation, sequestration, and tolerance in plants are still unknown and unexplored. Genes and transporters involved in Ni hyperaccumulation are not species specific, but expressed and regulated at different levels, and can therefore be compared to non-hyperaccumulating species such as *Arabidopsis thaliana*. In this thesis, I aimed to characterize the potential contribution of calcium channels in Ni uptake and determine natural variation for Ni tolerance in *A. thaliana*.

Methods: Nickel and calcium concentrations in roots and shoots of *A. thaliana* plants grown with and without the calcium channel blocker verapamil and with and without Ni supplemented in the nutrient solution were determined in . To estimate Ni tolerance, root growth was measured automatically, with BRAT software for five natural accessions. Secondly, root growth was measured manual for 350 natural accessions (HapMap) to perform a GWAS. GWAS was performed on root growth decrease and residuals and with two SNPs Set (215.000SNPs set and an imputed data set of 1 million SNPs). Nickel tolerance was determined by measuring root growth in Ni excess and control condition for *A. thaliana* accessions from serpentine soils (Pra), knockout mutants for *NICOTIANAMINE SYNTHASE* (*NAS)*genes.

Results: Ca concentration decreased by ± 70% in roots with a high verapamil concentration which confirmed that verapamil blocks most of the calcium channels in A. thaliana. In contrary, Ni concentration was not affected by verapamil in shoots and roots. I observed that BRAT did not detect all plants nor measure the roots accurately. The GWAS displayed several QTLs and genes, such as NRAMP6, a gene that might be associated with Ni tolerance*. A. thaliana* accessions from serpentine soils (Pra) displayed Ni tolerance. Knockout mutant *nas1,2,3,4* showed the highest root decrease with Ni excess.

Conclusions: I deduced that nickel is not predominantly taken up through calcium channels. The BRAT software is not reliable for root measurements in a set-up with Ni excess. The gene *NRAMP6* is the most promising candidate gene detected by the GWAS because its homologs (*NRAMP3* and *NRAMP4*) are involved in Ni translocation to the vacuole. All genes detected by the GWAS still require validation by screening T-DNA mutant lines. Natural variation for Ni tolerance is confirmed by the GWAS results and the natural accessions (Pra). Nicotianamine reduces the Ni toxicity in *A. thaliana.*

1. Introduction

Nickel in plants

Nickel (Ni) is an essential micronutrient for plants and is required for a few enzyme activities. For instance, Ni is needed to hydrolyze urea by the chloroplast enzyme urease (Marschner 1995; Sachan and Lal 2017). This enzyme hydrolyzes urea which is an important source of nitrogen. Moreover, Ni increases the resistance to disease because it helps the production of secondary metabolites (Sachan and Lal 2017). Consequently, Ni deficiency is harmful to plants (**Figure 1A**). Ni is needed at a normal concentration ranging from 0.01 to 10 µg/g dry weight (DW) in the shoot (Brooks et al., 1977). A Ni concentration lower than 0.01 µg/g dry weight (DW) is regarded as deficient for plants (Marschner 1995). At first, Ni can be found in three different forms in the soil and therefore is absorbed differently to roots. Ni soluble (Ni H_2O) is transported by passive diffusion from the soil to roots (Ahmad and Ashraf 2011). Chelate Ni is absorbed via active transport in roots. Insoluble Ni, which is not the common form for plant absorption, is absorbed meanly through endocytosis (Ahmad and Ashraf 2011; Yusuf et al., 2011). Then, Ni is translocated from the roots to the shoots through the xylem. Once Ni is in the shoots, plants accumulate Ni in leaves and stem, essentially in the epidermal cells and in vacuoles or are re-translocated to the flowers and seeds (Ahmad and Ashraf 2011; Yusuf et al., 2011).

Although Ni deficiency causes a growth disturbance, a Ni excess is more problematic. First of all, Ni excess disturbs biochemical processes and general plant physiology. For instance, it leads to the production of reactive oxygen species, which are toxic in high quantities for the plant. Ni disturbs photosynthesis due to the inhibition of enzymes involved in the synthesis of chlorophyll (**Figure 1B**) (Sachan and Lal 2017). Ni creates metabolic disturbance and leads to a deficiency of other metals because of its high affinity to bind sulfhydryl (-SH) groups and disulfide. Secondly, the consumption of contaminated food is dangerous for humans. Nickel is known to be carcinogenic. Therefore, Ni contamination is a dilemma for agriculture (Alloway 1995). Ni excess is due to high Ni concentrations in the soil. The agricultural soil with the highest Ni concentration in Europe is found in Greece, where its concentration is up to 2475 mg/kg (Albanese et al., 2015). Most of the soils in Europe have Ni concentrations lower than 48 mg/kg. A high Ni concentration can originate from environmental conditions or from anthropogenic activities (Sachan and Lal 2017). For instance, it is caused by industrial pollution, disposal of household waste or the utilization of phosphate fertilizers (Nziguheba and Smolders 2008).

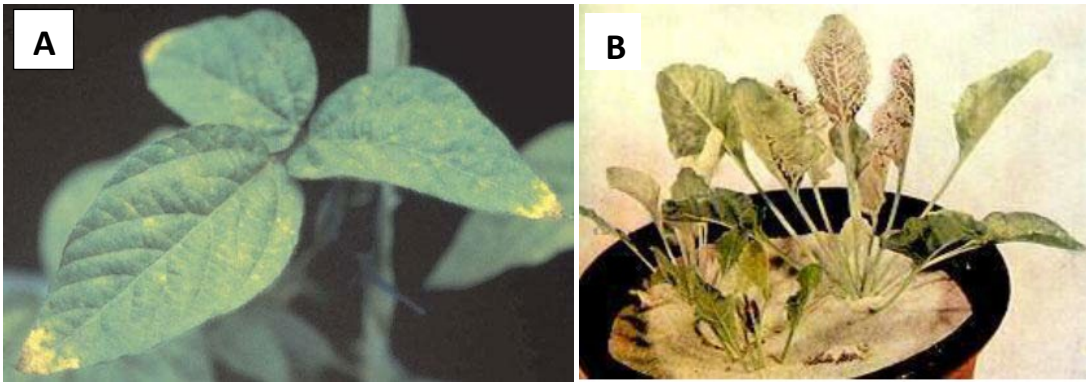

Figure 1: *Effect of Ni deficiency (A) resulting in necrosis at the tip of the leaves in soybean or Ni toxicity (B) in sugar beet leaves (figure taken from Sachan and Lal, 2017).*

Nickel phytomining

Endowed with a rich combination of properties and infinitely recyclable, nickel is an important metal on the market. Ni is mainly used for the development of stainless steel because of steel rusts without Ni. Over about 8% Ni is needed for stainless steel ('Stainless Steel - General Information - Alloying Elements in Stainless Steel'). Nickel's value on the market is up to 13,000 USD per ton which is significantly higher than the price of copper (6,000 USD/Ton), zinc (2,000 USD/Ton) or aluminum (2,000 USD/Ton) (Markets Insider, 2019). Nickel provides interesting investment on the market for Ni investor but the only method to obtain Ni is extraction by open-pit mining. Such a method is unsatisfactory because it requires extensive stripping that generates problems of soil erosion, water flow disruption, watercourse pollution and loss of biodiversity (L'Huillier and Edighoffer 1996). To overcome these problems, it is clear that a new method of Ni extraction is required. I suggest the use of a new method which would decrease pollution and its effect on biodiversity. One such method is phytomining which is the process of extracting metal, such as Ni, from the soil by plants (Anderson et al., 1999). Phytomining, at first, consists of the use of plants that absorb metal contained in the soil and concentrate it in their harvestable parts (leaves, stems). Then, the plants can be harvested and incinerated into ash. Finally, this ash is smelted and refined to recover the accumulated metals (Ni). This method could create a more sustainable situation for biodiversity and decrease pollution. It is demonstrated that, through phytomining, around 100 kg Ni/ha could be extracted (Anderson et al., 1999). Phytomining requires a suitable crop able to hyperaccumulate Ni in shoot parts and tolerate its toxicity. This suitable crop can be improved by overexpressing natural genes involved in Ni tolerance, hyperaccumulation, and translocation (Cherian and Oliveira 2005). Although phytomining represents an ideal method to extract Ni, the physiological mechanisms and genes needed to improve a suitable crop for a large-scale phytomining are still unknown and unexplored. These mechanisms and genes

involved in Ni hyperaccumulation are not specific for each species but are rather regulated and expressed at different levels.

Ni hyperaccumulator

There are species, Ni hyperaccumulators, able to accumulate naturally extreme amount of nickel at a concentration higher than 1,000 µg/g DW and to tolerate its toxicity (Brooks et al., 1977). For instance, two known species of Ni hyperaccumulators are *Alyssum bertolonii* from Italy and *Berkheya coddii* from South Africa which accumulates up to 17,000 and 13,400 µg Ni /g DW, respectively (Anderson et al., 1999). Another Ni hyperaccumulator, *Sebertia (Pycnandra) acuminata from New Caledonia*, accumulates 257,400 µg/g DW Ni in the phloem sap (Jaffré 1996). Although hyperaccumulator represents a suitable candidate for phytomining, they have generally a long-life cycle and low yield biomass.

Noccaea caerulescens (N. caerulescens) is a well-studied heavy metal hyperaccumulator from the *Brassicaceae* family (Visioli, Gullì, and Marmiroli 2014). This species grows on metalliferous and non-metalliferous soils. However, *N. caerulescens* is able to hyperaccumulate several metals such as Zn, Cd, and Ni and its genome have not been sequenced yet which make its study more difficult. Another species, from the same family and closely related, is *Arabidopsis thaliana* (*A. thaliana*) which is a non-hyperacumulator. However, its genome has been fully sequenced. In addition to that, many studies suggest that the genes involved in hyperaccumulation are not specific for each species but are rather regulated and expressed at different levels, compared to non-hyperaccumulating species. The same mechanisms are involved in the homeostasis of toxic trace elements in non-hyper-accumulative plants such as *A. thaliana*.

Arabidopsis thaliana a model plant in genetics

Arabidopsis thaliana is a plant model used in genetics for several physiological, geographic and practical reasons (Meyerowitz 2001; Serino and Marzi 2018). First of all, it has a lifetime of three months and its method of reproduction by self-fertilization make this species a plant really easy to grow (Agrawal et al., 2012). In addition to that, this species produces a high amount of seeds at each generation (Serino and Marzi 2018). Moreover, its genome is small, simple, sequenced and publically available (Serino and Marzi 2018). Finally, it has a significant genetic variation due to its adaptation to growing around the world. More than 350 natural accessions of *A. thaliana* are spread around the world (Al-Shehbaz and O'Kane 2002). Therefore, I decided that A. thaliana is a suitable species to study Ni uptake and genes conferring Ni tolerance.

Ni homeostasis and tolerance in plants

Ni homeostasis is explained by four different mechanism ; the Ni uptake from the soil to the roots, the Ni translocation from the roots to the shoots, the Ni sequestration in the leaves and the Ni tolerance.

About the Ni uptake from the soil to the root, it is known that the *IRON (FE) RELATED TRANSPORTER* (*IRT1*) is involved in *A. thaliana* (Nishida et al., 2011). When *A. thaliana* is in a medium with nickel excess, the expression of the gene *IRT1*, is higher than in normal condition. This suggests that *IRT1* is involved in the uptake of Ni from the soil to the roots (Nishida et al., 2011).

Nickel can be chelated by three different Ni binding ligands. First of all, histidine is an important chelator of nickel. The *ATP phosphoribosyltransferase* (*ATP –PRT*) regulates the pool of histidine and was found to be more expressed in hyperaccumulator plants (Ingle et al., 2005; Rees, Ingle, and Smith 2009). Overexpression of *ATP-PRT* in *A. thaliana* increased the production of histidine significantly (Ingle et al., 2005). Secondly, nicotianamine (NA) is another Ni binding ligand (Suyeon Kim et al., 2005). With an excess of nickel, the expression of four *NICOTIANAMINE SYNTHASE* genes is induced in *A. thaliana (NAS1, NAS2, NAS3,* and *NAS4*) in order to produce a higher amount of NA to tolerate Ni toxicity (Suyeon Kim et al., 2005). Finally, malate is another binding ligand involved in Ni detoxification by reducing the reactive oxygen species in the roots (Agrawal et al., 2012). By proving that root growth was indicator of Ni tolerance, Agrawal et al., 2012 demonstrated that the *A. thaliana* accession named Landsberg erecta (Ler-0) was Ni tolerant (Agrawal et al., 2012). Ler-0 was suggested to be resistant to Ni toxicity by accumulating a larger amount of Ni amount in leaves and not in roots (Agrawal et al., 2012). The *AtALMT1 gene*, encoding a plasma membrane-located malic acid transporter, was found to be involved in the detoxification of Ni by chelation.

The *Metallionein 1B* (*MT1B*) plays a role in the chelation of nickel, conferring tolerance to Ni toxicity in the plant (Visioli, Gullì, and Marmiroli 2014; J. Zhou and Goldsbrough 1995; Zimeri et al., 2005). The level of the gene expression of *MT1B* increases in the condition of high Ni concentration in the soil in the hyperaccumulator *Noccaea caerulescens* (Visioli, Gullì, and Marmiroli 2014).

Nickel translocation involves several transporters. Firstly, YELLOW STRIPE-LIKE family of proteins (YSL) transports nicotianamine-nickel/ Iron/ Zn or other element chelates in the hyperaccumulator *Noccaea caerulescens* (*N. caerulescens*) and many other plant species (Gendre et al., 2007). The expression of *YSL3* stays unchanged in *A. thaliana* upon exposure to heavy metals (Chu et al., 2010; Gendre et al., 2007). The level of expression of *YSL5* and *YSL7* was higher in *N. caerulescens*

than *A. thaliana* in the presence of nickel (Gendre et al., 2007). Secondly, it was demonstrated in *A. thaliana* that ARABIDOPSIS THALIANA IRON-REGULATED PROTEIN (AtIREG2) is a transporter of nickel across the vacuolar membrane to the vacuole (Liu et al., 2014, 2012; Schaaf et al., 2006). It was found that the ZINC FINGER TRANSCRIPTION FACTOR in *A. thaliana* (At*ZAT11)* downregulates the expression of *AtIREG2* (Liu et al., 2014, 2012). It was suggested that *ZAT11* is negatively regulated with the Ni tolerance in the plant (Liu et al., 2014, 2012). The *Multidrug resistance-associated protein* (*AtMRP3*) was found that its promoter activity increases under nickel stress, suggesting that also *AtMRP3* is involved in the Ni homeostasis in *A. thaliana* (Zientara et al., 2009). The *NATURAL RESISTANCE-ASSOCIATED MACROPHAGE PROTEIN* genes *NRAMP3* and *NRAMP4* have a higher expression in hyperaccumulator (Visioli, Gullì, and Marmiroli 2014). They are vacuolar membrane metal transporter suggesting its involvement in Ni translocation to the vacuole (Visioli, Gullì, and Marmiroli 2014).

Calcium channel transports several metals, including Ni (Cheng et al., 2002; Mei et al., 2007). It was demonstrated in tobacco that calcium transporter influences Ni fluctuation (Mei et al., 2007). The *ARABIDOPSIS THALIANA CATION EXCHANGER 1* (*CAX1*) plays a role in the regulation of Ca^{2+}/ H^{+}. When this exchanger is activated, an increase of nickel occurs. *CAX1*, *CAX3,* and *CAX4* have their levels of expression increasing with different nickel concentrations (Cheng et al., 2002). The transporter *CAX1* and *CAX2* seemed to have a redundant function (Hirschi 1999); meaning that if one is mutated and non-functional, the phenotype is unchanged in *A. thaliana* (Agorio et al., 2017; Pottier et al., 2015).

Calcium channel blocker to investigate Ni uptake in plants

Research on heavy metals homeostasis, including Ni, is difficult in plants because several types of the protein channel are involved as previously demonstrated. Some of these channels are “metal specific” and transport only one type of metal. Calcium channels, by contrast, are “ non-metal-specific” (Yusuf et al., 2011) and transport several metals, including Ni (Cheng et al., 2002; Mei et al., 2007). It was demonstrated that Ni was taken up mostly through calcium channel in the two Ni hyperaccumulator species *Odontarrhena bracteata (O. bracteata)* and *Odontarrhena inflata* (O. inflata) (formerly *Alyssum* section *Odontarrhena*) (Mohseni, Ghaderian, and Schat 2018). Due to the fact that calcium channel might also transport most Ni in non-hyperaccumulator plants, it is difficult to study Ni uptake. One approach to study Ni uptake through other channels is to block the calcium channel. Calcium channel blockers prevent or reduce the opening of channels. Verapamil is a calcium channel blocker from the phenylalkylamine group, developed in Germany in 1962 (Spedding and Paoletti 1992). Verapamil blocks or reduces calcium entry into the cells, through calcium channels, thereby inhibiting calcium effects and the Ni transport in plants (Cosio, Martinoia, and Keller 2004). It

was proved that verapamil blocks efficiently calcium channel in the two Ni hyperaccumulator species *O. bracteata* and *O. inflata* (Mohseni, Ghaderian, and Schat 2018).

Verapamil is used in this study to block the calcium channel in plants and, therefore, to investigate the Ni uptake in plants. To perform an experiment using verapamil, several parameters require investigation beforehand. First of all, verapamil is concentration dependent. For instance, if its concentration is too low (2 µM), it might not close a significant amount of channels (Piñeros and Tester, 1997). A concentration of 30-50 µM of verapamil is the minimum concentration required to close an important number of channels (Iriti et al., 2006; Piñeros and Tester 1997; Singh, Sharma, and Prasad 2011). Secondly, the duration of incubation is also important. If the exposure of verapamil is too long, it might be lethal for the plant. An inoculation over the night should be efficient enough to allow the blocker to bind the channels and not bind nickel (Singh, Sharma, and Prasad 2011).

- *Genome-wide association study association to define candidate genes*

Quantitative Trait Loci (QTL) needs to be identified, to unravel genes involved in Ni homeostasis. The Genome-Wide Association Study (GWAS) is an approach that can identify QTLs related to Ni homeostasis. This approach associates phenotypic traits with genotype variation, essentially single nucleotide polymorphisms (SNPs) in a large population resulting in a list of significant SNPs (Korte and Farlow 2013). The phenotypic traits analyzed in this study are the relative change in root growth as an indicator of Ni tolerance and, second, the residuals calculated with the regression of root growth from plants grown in control condition with plants grown with Ni excess. A GWAS results in the log(p) value per SNP related to the associated trait. When these log(p) values are plotted, a, so called, Manhattan plot is created. This is called a Manhattan plot, because it represents the skyline of Manhattan. This Manhattan plot also displays for each SNP its position on the physical map. The p-value is determined by a t-test comparing the call and non-call genotype (Lamy et al. 2006). The region of SNPs, that are above the threshold for significance, are identified as QTL for a trait. These QTL are selected for more detailed analysis and candidate genes are selected.

In order to increase the statistical power of the GWAS, a large population is required and a wide distribution of SNPs along the genome for this population. The HapMap population is the one utilized in this study, because of two reasons. Firstly, the HapMap consists of 350 *A. thaliana* accessions from all over the world. Therefore, it is a global population and has a high natural genetic variation. This high genetic variation comes from the adaption to different environments. The drawback of this significant genetic variation is that some associations could not be detected, because of the

heterogeneity of the genotype (Korte and Farlow 2013). A trait controlled by many common variants each having only a small phenotypic effect, is an example of this and it will be difficult to identify the causal trait. However, a global population benefits to GWAS due to a lower risk of finding false positive (Korte and Farlow 2013). Secondly, there are two large sets of SNPs for the HapMap population. This population was genotyped by a chip array, which has 215.000 SNPs spreading over the genome when there was no whole-genome sequencing available yet. Meanwhile, 143 accessions of the HapMap have been sequenced. Therefore, an imputed data set has been made, combining the sequence data of the 143 accessions and the chip array data for all 350 accessions (Bader, unpublished). The data were imputed for the remaining lines (Bader, unpublished). These two set of SNPs require a different way to run a GWAS and, therefore, their outputs are slightly different. For this reason, both sets are used in this study.

Once significant SNPs are discovered to be associated with the phenotype, the region of Linkage Disequilibrium (LD) is determined. Linkage disequilibrium is the non-random association of alleles at different loci in a given population (The International HapMap Consortium, Altshuler, and Donnelly 2005). A maximum LD (LD= 1) is found when only one haplotype is present in combination with the significant SNP. If there is a complete equilibrium, there is no LD. In this study, the r square (r^2) is used as a measure of the LD. This r^2 is a measure of the linkage between two SNPs (Altshuler, and Donnelly, 2005). It will result in an estimation of an LD region. In this significant LD region (threshold is arbitrary) of a discovered SNP by the GWAS, all genes are potential candidate genes. To make a selection of these potential candidate genes, a selection can be made, for example by known function and by their Gene Ontology. Then, the validation of these candidate genes is possible with T-DNA mutant lines. T-DNA lines contain a DNA insertion in a specific gene which will alter the expression of the gene. There is a T-DNA line library for *A. thaliana*. This library contains for almost all genes a T-DNA mutant line (O'Malley, Barragan, and Ecker 2015). By comparing and analyzing the phenotype of T-DNA lines in a control condition with a treatment, such as Ni excess, it is possible to narrow down the number of candidate genes and validate their correlation with the phenotypic traits. Further analysis is required to fully validate the role of a candidate gene in correlation with specific traits.

2. Aim and objectives

The aim of this thesis is to characterize the importance of calcium channel in Ni uptake and determine natural variation for Ni tolerance in *Arabidopsis thaliana*.

Objectives:

1. Define the Ni uptake by *A. thaliana* Columbia accessions growing under different conditions (-Ni/-verapamil, +Ni/-verapamil, -Ni/+verapamil, +Ni/+verapamil) in order to block calcium channels.

2. Determine natural variation for Ni tolerance in *A. thaliana* by measuring automatically root growth with the software BRAT for the HapMap population

3. Discover significant QTLs associated with Ni tolerance by performing a GWAS across 350 *A. thaliana* accessions from the HapMap population.

3. Materials and methods

Nickel was used in the form of Ni $SO_4.6H_2O$ for all experiment in this thesis (**Supplemental Data 1**)

Plant material

The HapMap population is composed of 5,810 natural accessions of *A. thaliana* spread around the world (Platt et al., 2010). A core of 350 accessions from this HapMap was made in order to reduce the number of accessions and redundancy of the genotypes but by keeping genetic variation (Li et al., 2010). These 350 accessions from the HapMap population were furnished by the Laboratory of Genetics at Wageningen University.

Arabidopsis thaliana knock-out mutants (*nas* 1,2,3 / *nas* 1,2,4 / *nas* 1,3,4 / *nas* 2,3,4 / *nas* 1,2,3,4) came from the Laboratory of Genetics at Wageningen University.

Seeds of *A. thaliana* mutants transformed by ion beam were provided by Dr. Michiko Takahashi from the Utsunomiya in Japan (*At* 60 Gy 39 and At 30 Gy 26). Crosses were made by Prof.dr. Mark Aarts (Laboratory of Genetics at Wageningen University) (*At* 60 Gy 39 x Col-0 / *At* 60 Gy 39 x No-0). The F1 seeds from these crosses were utilized in this study.

A. thaliana wild type lines (Pra 1, Pra2, Pra 3, Pra 4, Pra 5, Pra 6) were collected in serpentine soil by Dr. Sylvain Merlot from The National Center for Scientific Research (CNRS) de Gif sur Yvette in Paris, France. Seeds from selfing were kindly provided for research (Pra 1, Pra 3, Pra 4, Pra 5, Pra 6). Seeds obtained from selfing from two of these accessions were used (Pra 4 and Pra 6) (Generation T2).

Seed sterilization

Seeds were surface-sterilized using the vapor-phase method in order to avoid bacterial contamination (Clough and Bent 1998). They were transferred to open 1.5ml Eppendorf tubes and incubated in a desiccator jar containing two beakers filled with 50 ml bleach and 1.5 ml HCl. These products are toxic by inhaling and, therefore the desiccator was placed inside a fume hood and sealed with parafilm. Seeds remained in the desiccator for 3 h. Thereafter, the tubes were placed over the night with the lid open in a flow cabinet in order to get rid of the toxic vapor.

Growing condition on MS agar plates

i. Pilot experiment for germination rate on agar plate with Nickel

Seeds were surface vapour-sterilized (Clough and Bent 1998). They were sowed on 92 x 16 mm petri-dish (Greiner Bio-One®) containing half-strength Murashige and Skoog medium (MS) with 0.8% Daishin agar (Murashige and Skoog, 1962). Five Ni concentration was used for this pilot experiment

which was 0, 10, 50, 75 and 100 µM Ni). Plates were sealed with parafilm and placed for four days in a dark room and at 4 °C. Thereafter, plates were transferred to a growth chamber with a cycle set up a 16h/8h light/dark cycle and at 24 °C. At Day 5 After Germination (DAG), the germination rate was calculated for each plate. At DAG 10, the germination rate was observed in the case of late germination. In total, twelve seeds of a specific genotype were planted on petri-dish plates. Three plates per treatment for each genotype were used. The *A. thaliana* accessions were chosen according to their possible Ni tolerance or sensitivity from publications (Agrawal, Lakshmanan, Kaushik, and Bais, 2012; Fischer, Spielau, and Clemens, 2017)(**Table 1**).

***Table 1**: Five wild type A. thaliana accessions with their specificity in Ni tolerance and Ni sensitivity*

Full name	Abbreviation	Specificity	Literature
Columbia (from the WUR)	Col-0	Control	/
Landsberg erecta	Ler-1	Ni tolerant	(Agrawal, Lakshmanan, Kaushik, and Bais, 2012)
Bensheim	Be-1	Ni sensitive	
C24	C24	Ni sensitive	
JEA	JEA	Zn sensitive	(Fischer, Spielau, and Clemens 2017)
Cape Verde Islands	Cvi-0	Zn tolerant	

ii. Pilot experiment to determine a suitable Nickel concentration on agar plate

A. thaliana seeds were vapor-sterilized and planted on MS medium with 1% Daishin agar and determined concentration of Nickel (0, 10, 20, 30, 40, 50, 60, 70, 80, 90, 100 µM $NiSO_4H_2O$) (Murashige and Skoog, 1962). Square plates were used (120 x 120 x 17 mm) (Greiner Bio-One®) and filled with exactly 50 ml of MS medium in order to have the same thickness of solidified agar for the screening analysis. Thereafter, plates were sealed with parafilm and were stratified for 3 days in the dark and at 4°C. Then, they were placed vertically in the growth chamber set up a 16h/8h light/dark cycle and at 24 °C for 10 days. There were four replicates of agar plates for each treatment (**Figure 2 and 3**). Each genotype was selected according to their Ni sensitivity and Ni tolerance (Agrawal et al., 2012; Fischer et al., 2017) (**Table 2**).

***Table 2**: Five wild type A. thaliana accessions with their specificity in Ni tolerance and Ni sensitivity. Two Col-0 were used in order to check which one will be the most homogeneous and suits the best for the following experiments*

Full name	Abbreviation	Specificity	Literature
Columbia (from the WUR)	Col-0b	Control	/
Columbia (from the Hapmap)	Col-0c	Control	/
Landsberg erecta	Ler-1	Ni tolerant	(Agrawal, Lakshmanan, Kaushik, and Bais, 2012)
Bensheim	Be-1	Ni sensitive	
C24	C24	Ni sensitive	
Cape Verde Islands	Cvi-0	Zn tolerant	(Fischer, Spielau, and Clemens 2017)

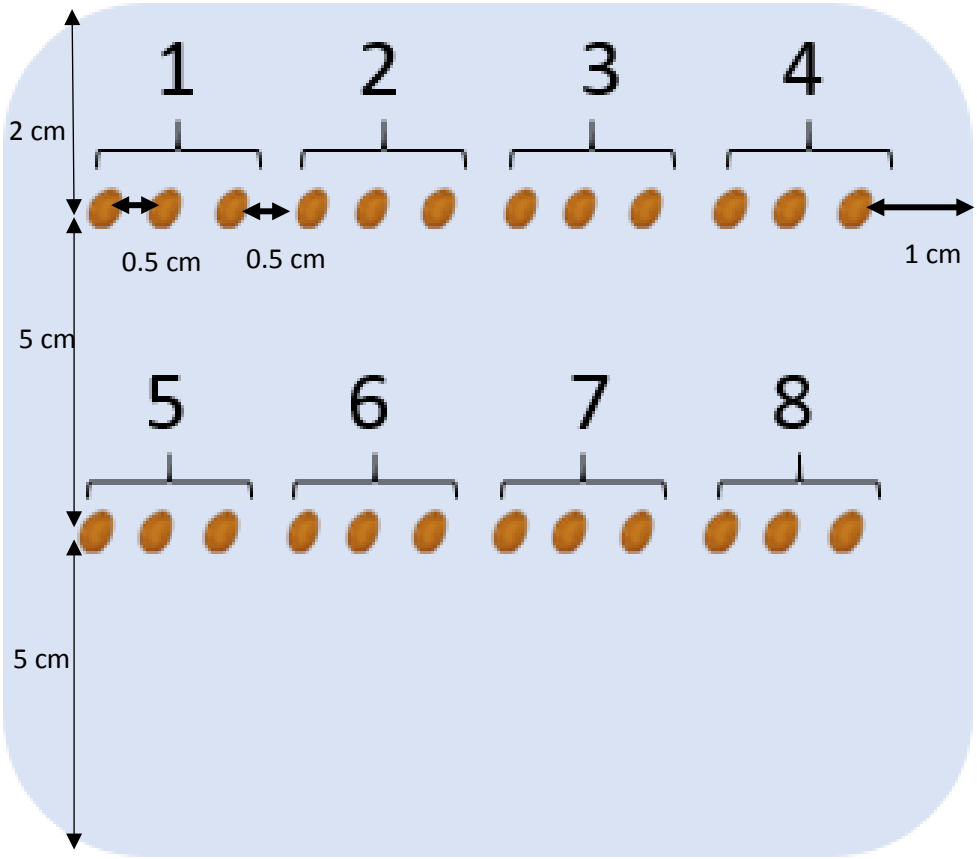

Figure 2: Template showing the position of the seeds on each agar plate. Twelves seeds were planted in two rows and at equal distance of 0.5cm from each other. There were eight sections and each of them represented a specific genotype. The accession Columbia was not on a fixed position.

		Sections							
		1	2	3	4	5	6	7	8
Plates	1	AAA	BBB	CCC	DDD	EEE	FFF	GGG	HHH
	2	BBB	AAA	DDD	CCC	FFF	EEE	HHH	GGG
	3	HHH	GGG	FFF	EEE	DDD	CCC	BBB	AAA
	4	GGG	HHH	EEE	FFF	CCC	DDD	AAA	BBB

***Figure 3**: Scheme for square plates displaying the position of each genotype. Each letter presents a different genotype.*

Hydroponic growing condition

Seeds were sowed on 1.5 ml tube which had the bottom cut off filled with half-strength MS medium and 0.8% Daishin agar (Murashige and Skoog, 1962). The pH of the medium was adjusted to 5.7 and the agar medium was autoclaved. The tubes were placed into 600 ml box filled with half-strength Hoagland's solution (**Table 3)** (Schat, Vooijs, and Kuiper 1996).

Table 3: Stock solutions of macronutrients, micronutrients and Fe(Na)EDTA or Fe-EDDHA.

Macronutrients	**Stock (M)**	**Volume required for 1L of Half strength Hoagland's solution (ml)**
KNO_3	1.00	3.0
$Ca(NO_3)_2.4H_2O$	1.00	2.0
$NH_4H_2PO_4$	1.00	1.0
$MgSO_4.7H_2O$	1.00	1.0

Micronutrients (1 X)	**Stock (mM)**	**Volume required for 1L of Half strength Hoagland's solution (ml)**
KCl	1.00	1.0
H_3BO_3	25.00	
$MnSO_4.4H_2O$	2.00	
$ZnSO_4.7H_2O$	2.00	
$CuSO_4.5H_2O$	0.10	
$(NH_4)_6Mo_7O_{24}.4H_2O$	0.10	
$ZnSO_4.7H_2O$	0.02	

Other	**Stock (mM)**	**Volume required for 1L of Half strength Hoagland's solution (ml)**
Fe(Na)EDTA	20	1
Fe-EDDHA	20	1

In order to prepare half-strength Hoagland's solution, a buffer solution was first prepared and required to adjust the pH. This buffer solution contains 2 mM 2-[N-morpholino] ethanesulfonic acid (MES). The MES was placed in an Erlenmeyer flask with 1 L demi-water and the pH was adjusted up to 5.5 with KOH. The solution was poured into 20 L container and filled with demi water up to half of the container. The stock solution of each nutrient was added and the volume was adjusted with demi water to the desired level.

Once the 600ml boxes were filled with half-strength Hoagland's nutrient solution, the agar tubes were placed inside the boxes. Seeds were sown delicately on the surface of the agar and at the middle of the tube.

For homogenous germination of seeds, seeds were stratified for 3 to 5 days in a dark room and at 4 °C. Then, plants were placed in a growing room with a 12h/12h light/dark cycle at 20 °C/15 °C temperature at day/night and 70% humidity. At three DAG (Day After Germination), the boxes were slightly opened in order to keep the humidity and permit the plant to slowly adapt to the dry air. At eight DAG, the lids were fully opened. At nine DAG, plants were transferred into 600 ml or 1 L pots or into 10 L trays depending on the experiment. Each week, the nutrient solution was changed with half-strength Hoagland's solution.

i. Pilot experiment for verapamil and nickel experiment

A. thaliana accession Columbia (Col-0) were vapor sterilized and grown in hydroponic condition as described above. The half-strength Hoagland solution was prepared with Fe-EDTA. One plant per pot was grown. Two pots per treatment were used. At 26 DAG, the half-strength Hoagland's solution was changed and verapamil was added to the solution at determined concentrations (**Table 4**). Verapamil is soluble in water according to ChemWatch (https://www.chemwatch.net/) which facilitates its addition to the Hoagland solution (Omega.chemwatch.net 2015). At 27 DAG, nickel was added to the nutrient solution as a series of concentration (**Table 4**). At 29 DAG, plants were harvested for Ni and Ca content.

***Table 4**: Concentration of verapamil and nickel were exposed to sample in order to define the most suitable concentration for the future experiments. There are 25 different treatments. For each treatment, two pots of 600ml were used and one A. thaliana plant was grown per pot.*

Treatment	**1**	**2**	**3**	**4**	**5**	**6**	**7**	**8**	**9**	**10**	**11**	**12**	**13**	**14**	**15**
Verapamil (µM)	0					25					50				
Nickel (µM)	0	5	10	25	50	0	5	10	25	50	0	5	10	25	50

Treatment	**16**	**17**	**18**	**19**	**20**	**21**	**22**	**23**	**24**	**25**
Verapamil (µM)	75					100				
Nickel (µM)	0	5	10	25	50	0	5	10	25	50

For the following hydroponic experiments (ii) and (iii), half-strength Hoagland solution was prepared with Fe-EDDHA and not with Fe-EDTA. The reason is that Fe-EDTA has a much lower affinity with iron (Fe) than with Ni and, therefore, it binds to Ni and Fe precipitate at the bottom of the pot. On the contrary, Fe-EDDHA has a higher affinity for Fe than Ni and, by consequence, it binds to Fe.

ii. Pilot experiment to define the median effective concentration 50

A. thaliana accession Col-0 were vapor sterilized and grown in hydroponic condition as previously described. Plants were grown in 1 L pots with half-strength Hoagland's solution (Schat, Vooijs, and Kuiper, 1996). At day 17 DAG, the treatment with active carbon started when roots were dipped into finely powdered activated charcoal (Schat and Bookum 1992). This solution stained the roots into a black color. Then, roots were rinsed with deionized water to remove excess charcoal on the roots. Immediately after, plants were placed back into the pots containing new half-strength Hoagland's solution with eight different Ni concentration 0 µM, 0.5 µM, 1 µM, 2 µM, 4 µM, 8 µM, 16 µM. After 4 days of Ni exposure, at 21 DAG, manual measurement of the unstained roots was performed with a ruler in order to calculate the median effective concentration value (EC50). The EC50 is the concentration of a substance that caused a reduction of growth, such as root growth, by 50 % (Cho, Chardonnens, and Dietz 2003; Schat and Bookum 1992). The average of the three plants per pot was taken for the statistical analysis. Three pots were used per treatment.

The same experiment was executed with a series of Ni concentration at increasing concentration: 0 µM, 16 µM, 32 µM, 64 µM, 128 µM, 256 µM. For this experiment, one Columbia accession was grown per pot and three pot were used for each treatment.

iii. Experiment to perform a GWAS with the HapMap population

A set of 350 accessions from the HapMap population was grown in hydroponic condition with half-strength Hoagland's solution on trays with a capacity of 70 plants (Schat et al., 1996). The seeds were not vapor-sterilized. All plants grew in the control condition without nickel until day 20 (DAG). Then, roots were dipped into active carbon and, thereafter, all plants were transferred to a new half-strength Hoagland's solution. Half of the plants received a nickel excess treatment with the effective concentration (EC50) (44 µM Ni) and the other half continued growing in normal condition. The EC50 is the concentration of a substance that caused a reduction of growth, such as root growth, by 50 % (Cho, Chardonnens, and Dietz 2003; Schat and Bookum 1992). At 24 DAG, after Ni exposure, root growth was measured.

iv. Analysing Ni tolerance with root growth for *A. thaliana* natural accessions, mutants and genes knockout

The following selective set of *A. thaliana* was grown in normal hydroponic condition:

- Columbia (Col-0) and Nossen (No-0)
- Knock-out mutants (*nas* 1,2,3 / *nas* 1,2,4 / *nas* 1,3,4 / *nas* 2,3,4 / *nas* 1,2,3,4)
- Mutant At 60 Gy 39 and At 30 Gy 26 for Ni tolerance control
- F1 from the crosses At 60 Gy 39 x Col-0 and At 60 Gy 39 x No-0

Plants grew into 10L tray. Three trays per treatment were used and two plants per genotype and per tray were grown. At 18 DAG, roots from all plants were dipped into active carbon and immediately after placed back into the nutrient solution with the EC50 (44 µM) Ni for half of the plants and without Ni for the other half. At 22 DAG, plants were harvested and root length was measured with a ruler.

Growing condition on Rockwool

Non-sterilised seeds were sown on 50-mm-diameter filter paper discs placed inside a petri dish with 0.5 ml demi water. These Petri-dishes were transferred to the dark room at 4 °C for 3 days for stratification. Thereafter, these Petri-dishes were placed in a growing chamber with a 16h/8h light/dark cycle and 24 °C for germination. One day after germination, seedlings were moved from filter papers to Hyponex-soaked Rockwool. Each seedling was delicately taken with a thin wet brush and placed at the center on top of a Rockwool block. Plants grew in a greenhouse with a 16h/8h day/night cycle and 20 °C /18 °C day/night and 70% humidity. Plants received hyponex water (liquid fertilizers for intensive horticulture) once a week (**Supplemental Table S1**).

Plant harvesting

Plants were sown for propagation after selfing or crossing grew on Rockwool in the greenhouse. After they flowered and produced siliques, no nutrient solution was given anymore. Thereafter plants drought, seeds from every single plant were collected and placed into separate plastic bags.

Plant collection for nickel analysis

Plants grown in hydroponics were harvested at 29 DAG. Plants were harvested and roots and shoots were separated. The fresh weight of the shoots was measured. The shoots were placed into paper bags. The roots were desorbed in 10 mM EDTA for 10 minutes. Thereafter, they were rinsed with demi water, blotted with filter paper and placed into paper bags. Plant material was placed in the oven at 60°C for 2 days. Dry plant material was powdered with mortar and pestle.

Nickel measurement

Roots from two plants were pooled together in order to have the required weight of material (> 50mg) for the digestion. Samples of powdered plant materials (50 – 100 mg) were digested (7h at 140°C) in 2 mL of a 4:1 mixture of concentrated HNO_3 (65%) and HCl (37%), in Teflon bombs (**Figure 4**). After cooling down to room temperature, the bombs were opened and, after adding 8 mL of demineralized water, poured over into polycarbonate tubes. The nickel concentrations were measured using an atomic absorption spectrophotometer (AAS, Perkin Elmer AAnalyst 100). The Ni concentrations in the dry plant materials were calculated as:

$$\frac{[\text{AAS}]\ \text{x}\ 10\ \text{ml}\ \text{x}\ 1000}{\text{dry weight (mg)}} = \frac{\mu\text{M}}{\text{g}} = \frac{\text{mg}}{kg} = ppm$$

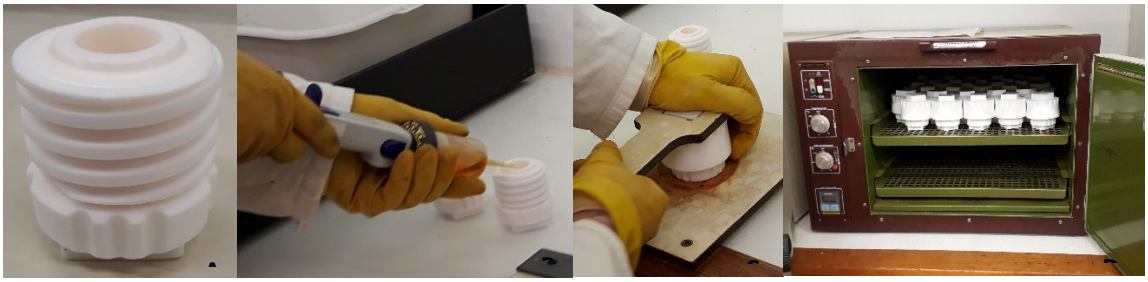

Figure 4: *Photos representing the different steps required for the digestion of plant material to measure metal content.*

Automatic root measurement with Brat software

Phenotyping accurately is required for mapping population at a high resolution. Phenotyping consists in the evaluation of observable traits in plants. Most phenotypes are difficult to estimate because they are complex and require an adequate instrument to measure them. Slovak et al., (2014) present a revolutionary software named BRAT version one (BRAT V1) (Slovak et al., 2014). BRAT V1 allows its user to phenotype several measurements of the plants relating to the root part. For instance, the software detects the length of the longest root, the relative root growth rate and the width of roots. The plant species used for in their experiment to phenotype traits on roots is *A. thaliana*. 160 accessions were chosen for this study. They were grown in square agar plates with a specific design for the position of the seeds on the plate. According to the method, 24 seeds must be placed per plates in two rows with equal distance between the seeds. These positions are important for both the detection of the roots by the software and the statistical analysis. The detection was obtained by segmentation by the software. Thereafter, the software is able to measure the different phenotypes on roots. The statistical analysis demonstrated the high accuracy of the software to measure the different traits. The evidence from this study suggests that the software helps researchers to phenotype faster and to obtain a more accurate measurement. Another version of BRAT was developed for phenotyping roots in *Lotus Japonicus*, a plant legume, to prove its utility with different plant species (Giovannetti et al., 2017). The software BRAT V1 was improved into a second version, BRAT V2, for more accurate results and faster results. Its efficiency was demonstrated as well (Satbhai, Göschl, and Busch 2017). For this reason, BRAT V1 and Brat V2 software were used in this study to phenotype root in *A. thaliana*.

Plants grew vertically on agar plates as previously explained. At day 10 (DAG), photos of each plate were taken with an Expression/STD 1600 scanner (Epson) for high-quality image acquisition. While photos were taken, all lights in the room were turned off, curtains were closed and scanners were placed with the lid opened in order to improve contrast. Each photo was scanned for root length (length of the longest root of each plant) by the software Busch-lab Root Analysis Toolchain (BRAT version 1 or BRAT version 2) provided by the Busch laboratory, Gregor Mendel Institute of Molecular Plant Biology (http://www.plant-image-analysis.org/software/brat). The experiment was executed by following the protocols provided by Busch Laboratory (Satbhai, Göschl, and Busch 2017; Slovak et al., 2014).

Manual root growth measurement

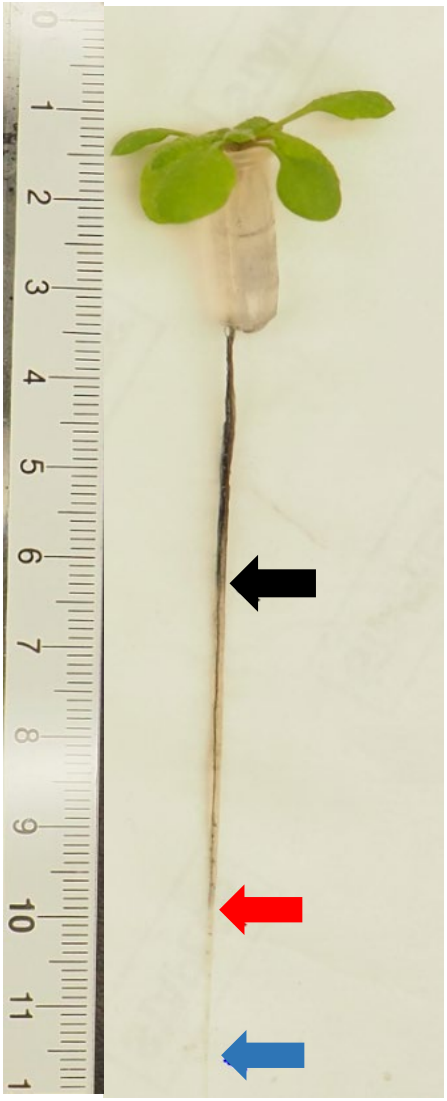

For plants grown in hydroponic condition as previously described, root measurement was performed manually with a ruler (**Figure 5**). Plants were placed on a white paper next to a ruler.

Figure 5: *Manual measurement of A. thaliana accession Col grown in hydroponic condition at four days after active charcoal staining. Three regions can be distinct on the root. The arrows mark the end of the respective staining as seen from the top. The darkly stained region represents the root growth until the active carbon is applied (black arrow). The greyish stained region represents the cells elongation (red arrow). The white region shows the cells division zone (blue arrow). The cell division zone was measured as a reference for root growth for all experiment.*

Statistical analysis

Ionome profile was analyzed with Microsoft Excel (2016).

Root length obtained with the automatic roots screen was analyzed with R studio (x64 3.5). One way-ANOVA, post hoc tests (Bonferroni and Tukey test) and boxplots were obtained with R studio (x64 3.5). Graphics of p-values and Pearson-correlation were performed with Microsoft Excel (2016).

The EC50 calculation and designed graphics were executed with Microsoft Excel (2016).

The relative change in root growth (root growth decrease) was calculated with Microsoft Excel (2016).

The Genome-Wide Association Study was performed with a set of 215.000 SNPs run with an R script provided by Dr. Willem Kruijer from the Laboratory of Genetics at Wageningen University (**Supplemental Figure S1**) (Kruijer et al., 2015) and with an imputed data of 1 million SNPs with GEMMA (**Supplemental Figure S2)** (Zhou and Stephens, 2012)**.** The LD measure (r^2) was defined with the software Plink and ran through a command line for both sets of SNPs (**Supplemental Figure S3**) (Purcell et al., 2007).

i. Heritability calculation

The broad sense heritability (H^2) was calculated with Microsoft Excel (2016) and with the following equation (Kruijer et al., 2015):

If H^2 is equal to 1, the phenotypic variance is explained by the genotypic variation. If H^2 is equal to 0, the phenotypic variance is explained by the variation of the environment.

$$\text{Heritability } (H^2) = \frac{\text{V genotype}}{\text{V genotype} + \text{V environment}}$$

V genotype is equal to the average of the variance between root growth in control and in treatment.

V environment is equal to the variance of the average between root growth in control and in treatment.

ii. Residuals calculation

The residuals are the vertical deviation from the y value of the actual scatter plot point (**Figure 6A and 7A**) and the y value of the regression equation at this point (Cantor, Lange, and Sinsheimer 2010). In another term, they are the difference between the observed value (coordinate of root growth in treatment by root growth in Ni excess) and the expected value (determined by the equation of the linear regression) for each accession. The sum of these residuals is equals to 0. The residuals were calculated with IBM SPSS Statistics (version 23) (VSN International; www.vsni.co.uk/software/genstat/).

The residuals can be calculated in two different way. If root length in control condition is plotted on the X-axis and root length in Ni excess is plotted in Y-axis, I obtained “Residuals_control” (**Figure 6B**). If root length in Ni excess is plotted on the X-axis and root length in control condition is plotted in Y-axis, I obtained “Residuals_treatment” (**Figure 7B**). These residuals gave different results and, therefore, I decided to make a distinction between them.

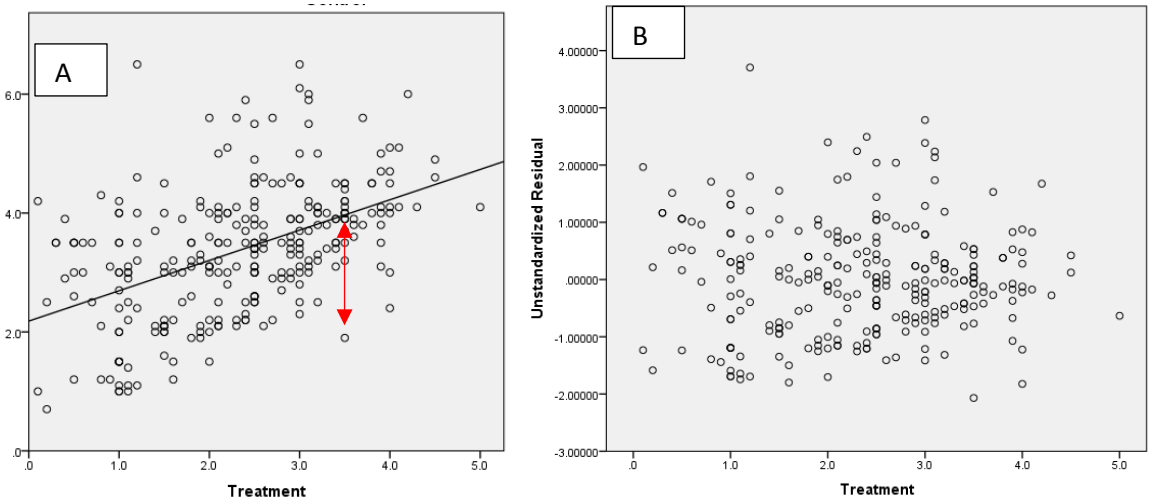

***Figure 6**: Linear regression on the observed value and calculation of the residuals. Each circle represents the value per accession. The X-axis represents the root length (cm) per accession in Ni excess. (A) the black line displays the linear regression calculated by SPSS. The Y-axis represents the root length (cm) per accession in the control condition. The red arrow displays the distance between the y value of the actual scatter plot point and the y value of the regression equation at this point (B) The Y-axis represents the calculated value of the residuals_control per accession from the scatterplot 6A.*

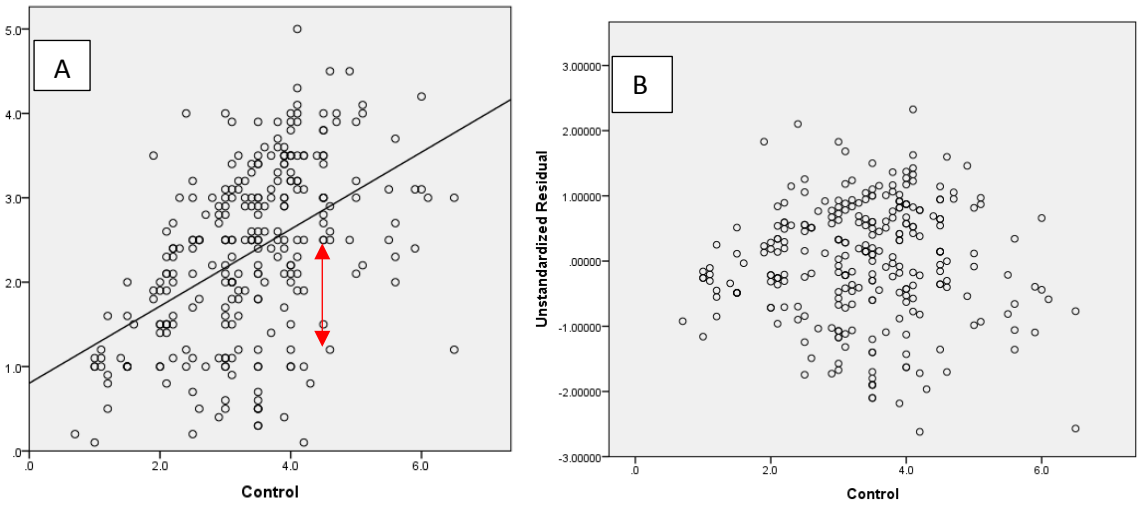

***Figure 7**: Linear regression on the observed value and calculation of the residuals. Each circle represents the value for one accession. The X-axis represents the root length (cm) per accession in the control condition. (A) the black line displays the linear regression calculated by SPSS. The Y-axis represents the root length (cm) per accession in Ni excess. The red arrow displays the distance between the y value of the actual scatter plot point and the y value of the regression equation at this point (B) The Y-axis represents the calculated value of the residuals_treatment per accession from the scatterplot 7A.*

For statistical analysis, a quantile-quantile(Q-Q)plot (Q-Q plot) of the root growth decrease, residuals_treatment and residuals_control was performed in order to check their distribution (Das and Imon 2016). This QQplot displays a normal symmetric distribution (**Supplemental Figure S4, S5 and S6**). A test for homogeneity of error variance for the residuals distribution is also required (Das and Imon 2016). Therefore, a scatterplot was realized. This scatterplot display 0 as the center of the trend and, consequently, the linearity assumption is accepted **(Supplemented Figure S5 and S6).**

4. Results

Calcium content is lower in roots with verapamil

Due to the high Ni uptake through calcium channel, studying other Ni transporter is difficult. In this experiment, calcium channels were blocked with the calcium channel transporter, verapamil. Verapamil is known as a calcium channel blocker (Piñeros and Tester, 1997). Therefore, it is expected that less Ca is absorbed in plants by roots and translocated to shoots in verapamil treatment. Plants grew in hydroponic condition in order to harvest roots and shoot for Ca concentration measurement. At 26 DAG, plants were incubated with verapamil and at 27 DAG Ni was added to the medium. At 29 DAG, plants were harvested to measure Ca concentration in shoots. Calcium concentration decreases by 70% in roots with a 100 µM verapamil concentration in the medium **(Figure 8A)**. Verapamil has an effect on Ca concentration in roots and blocks calcium channels in roots. While in shoots, there is no statistically significant alteration of Ca concentration with a higher verapamil concentration (**Figure 8B**).

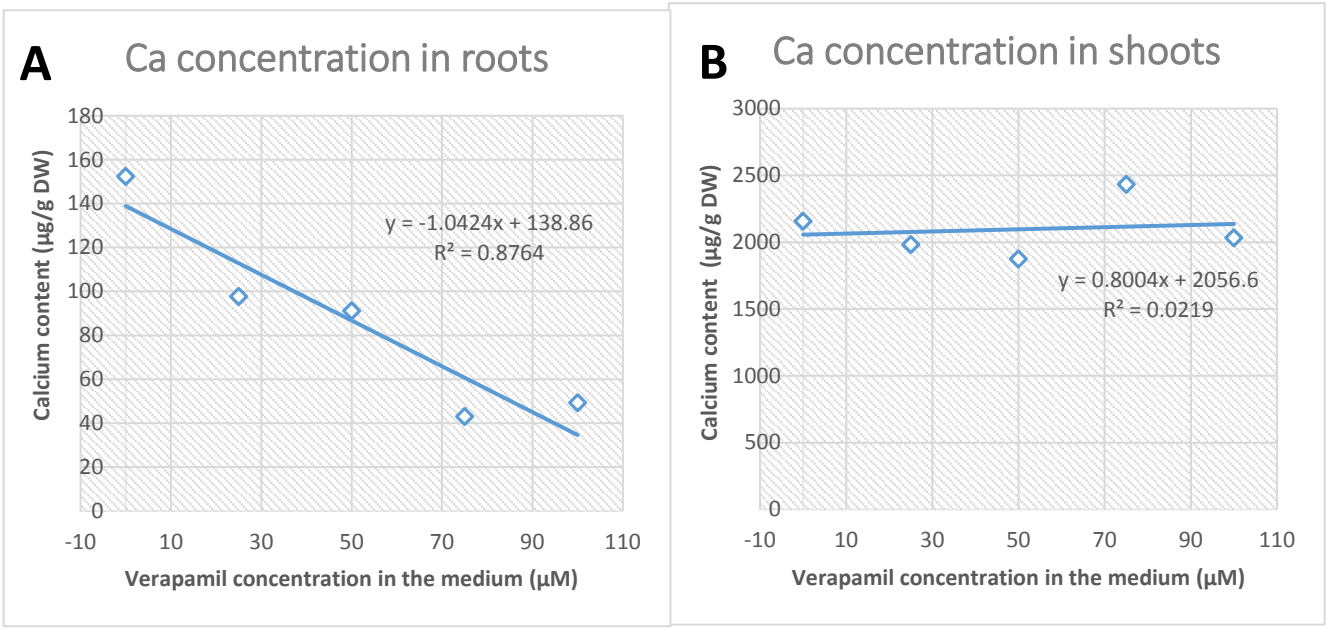

Figure 8: *Calcium concentration (µg / g dry weight) of A. thaliana (Col-0) exposed to five concentrations of verapamil. Plants were grown in hydroponic condition and measurements were effectuated in (A) roots and (B) shoots by Atomic Absorption Spectrophotometer (AAS).*

Nickel content stays unchanged in shoots and roots with verapamil

Ni concentration was determined in an AAS in both shoots and roots for the Columbia accession. Ni concentration was measured in roots **(Figure 9).** For each treatment, the roots of two plants were

pooled together for sufficient biomass (> 50 mg) required for AAS. I observe that a higher Ni concentration in Hoagland's solution significantly increases Ni concentration in roots. With a higher verapamil concentration in the medium, root Ni concentrations seem to increase with verapamil which is opposite to hypothesis. In conclusion, verapamil has no effect on Ni concentration in roots.

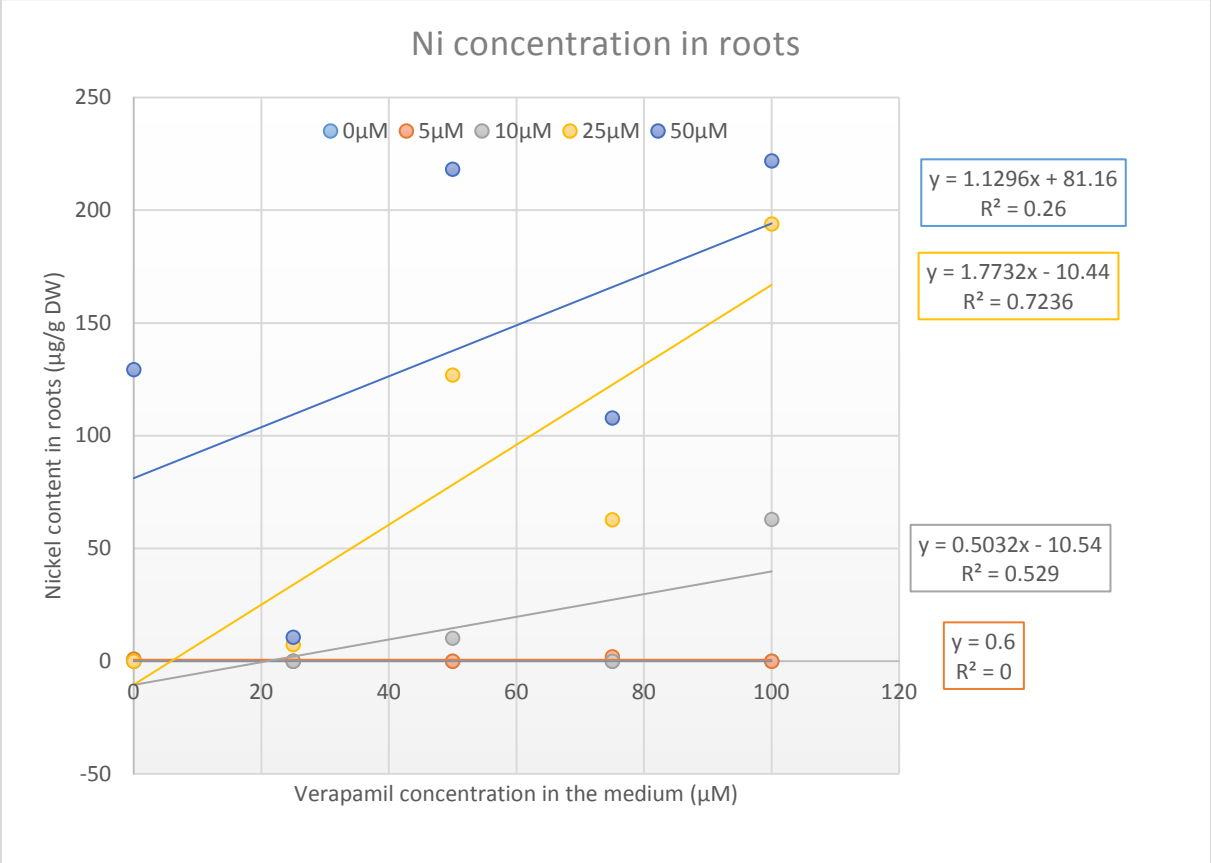

Figure 9: *Ni concentration means (µg / g dry weight) in roots of wild-type (Col-0) A. thaliana plants (33 days old). Each dot represents means calculated from two pooled plants of each treatment. These two plants were grown in two different pots. The different color refers to the different nickel concentration in the hydroponic solution. Equations to the right refer to the linear trend line for each nickel treatment.*

The average Ni concentration was taken for statistical analysis in shoots. Higher Ni concentration in Hoagland's solution significantly increases Ni concentration in shoots (**Figure 10**). For instance, I observe that Ni concentration increases, with a four-fold change, with 25 µM Ni in the medium compared with 5 µM Ni in the medium (20 µg Ni/g DW). While, at higher verapamil concentration, shoot Ni concentration is not significantly different. Ni concentration with different verapamil concentration cannot be distinguished from the Ni concentration without verapamil. Therefore, verapamil does not affect shoot Ni concentration.

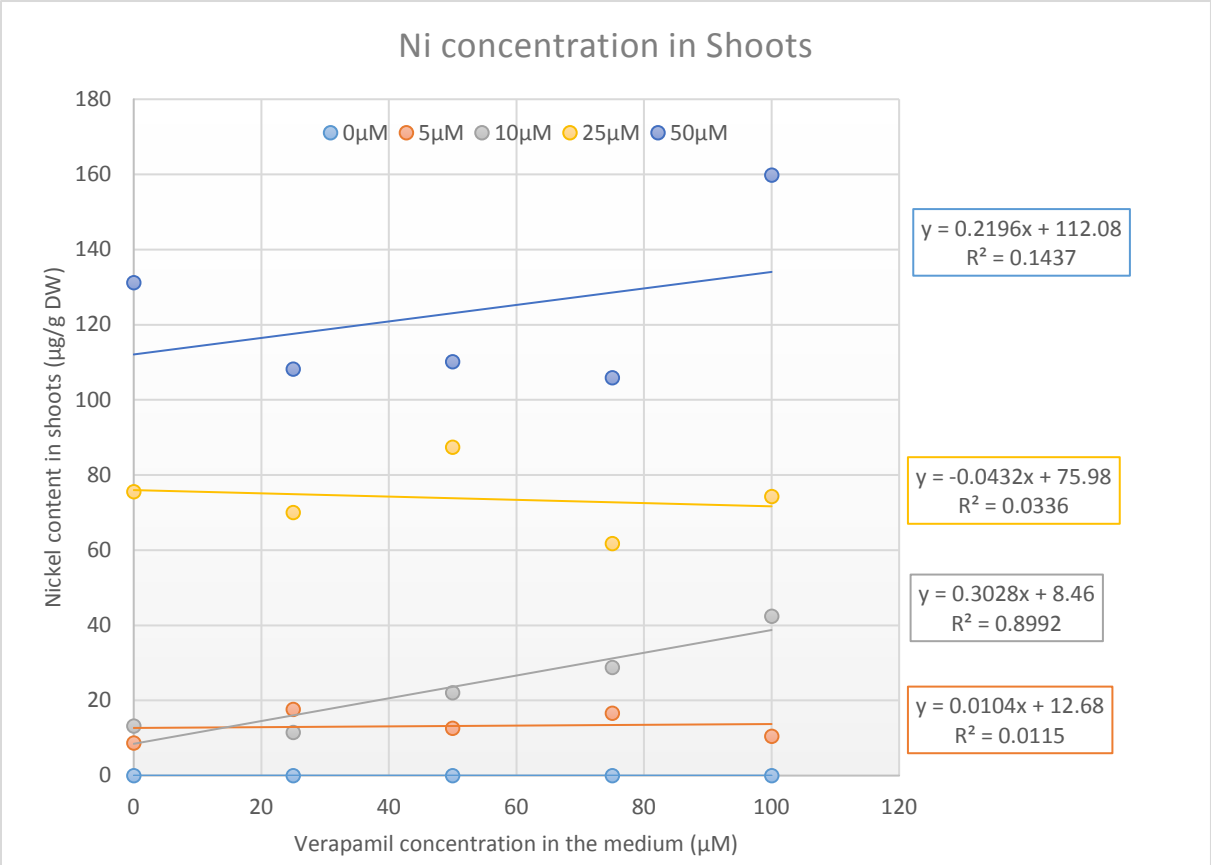

Figure 10: *Ni concentration means (µg / g dry weight) in shoots of wild-type (Col-0) A. thaliana plants exposing to different concentration of verapamil and Ni. Each dot represents means calculated from two pooled plants of each treatment. The different color refers to the different nickel concentration in the hydroponic solution. Equations to the right refer to the linear trend line for each nickel treatment.*

Germination rate is not affected by nickel on agar plate

The germination rate was determined in order to know if *A. thaliana* accessions were able to germinate directly on an agar plate with nickel for a practical reason. The reason is that if A. thaliana accessions (Ni sensitive and Ni tolerant) are able to germinate immediately on an agar plate with Ni supplemented, there will be no need to germinate them at first on agar plate without Ni and, then, to be transferred them on a plate with Ni. To identify the germination rate on agar plate supplemented by Ni, five *A. thaliana* accessions with specificity in nickel tolerance or sensitivity were planted (**Table 1**). The germination rate was counted at 5 days after germination. There is no significant difference in germination rate for the different Ni concentration **(Figure 11).** Additionally, for *A. thaliana* Ni sensitive (Be-1) shows no significant difference between 0 µM Ni and 100 µM Ni for germination rate. *A. thaliana* seems to be capable of germinating on agar plate supplemented by Ni up to 100 µM Ni and, therefore,

for the following experiments, plants grown on agar plate were germinated instantly with Ni. **Figure 11** shows that the accession JEA has a significant lower germination rate (40% lower) in control conditions and (20% lower) in treatment with Ni excess compared with the other genotypes. Consequently, the genotype JEA was not further used for experiments.

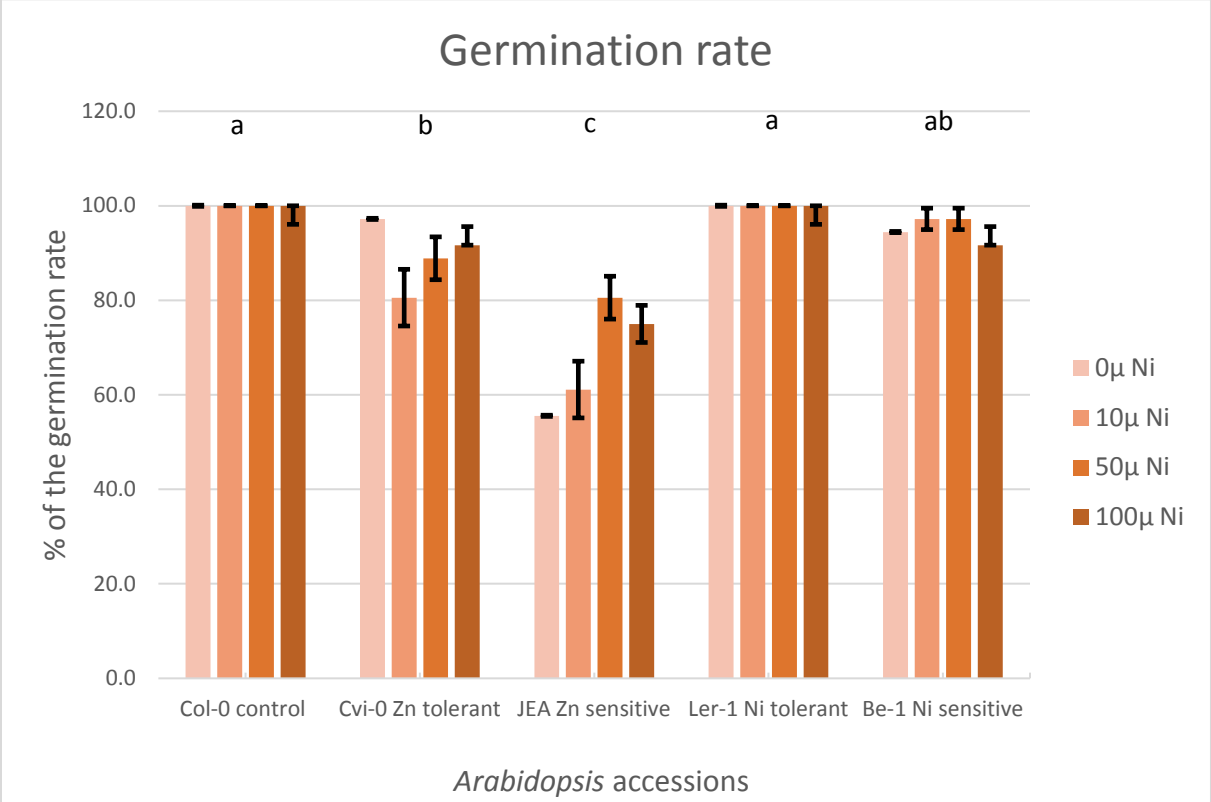

Figure 11: *Germination rate of* five *A. thaliana (5 days old) accessions. Lower case upper the bars define significantly different group between genotypes. One way ANOVA, two-way ANOVA and Tukey post hoc test (α = 0.05) were performed for genotypes, treatments and interaction genotype x treatment with R studio* ***(Supplemental Table S2).*** *The black bars represent the standard error per accession and treatment.*

Automatic root length measurement

The objective of this experiment was to display natural variation in root growth of Ni-stress *A. thalian*. Beforehand, I needed to determine the most suitable Ni concentration required to induce the differences between accessions on plants that grew on vertical agar plates. In order to achieve this objective, eight *A. thaliana* accessions were grown on vertical squared agar plates with determined Ni concentration (0, 10, 20, 30, 40, 50, 60, 70, 80, 90, 100 µM Ni). The eight accessions chosen were

related to metal tolerance explained in the materials and methods **(Table 2).** When plants were 10 days old, photos of each plate were scanned. Each photo was segmented by both Brat version 1 (V1) and Brat version 2 (V2) for an automatic roots length measurement (Satbhai, Göschl, and Busch 2017; Slovak et al., 2014).

To determine statistically significant differences between genotype per treatment, one-way ANOVA was performed for every treatment in between genotypes. P-values from these tests were analyzed in order to define which Ni treatment is the most suitable to compare genotypes (**Figure 12**). P-values lower than 0.05 correspond to a significant difference between genotypes. At 0 µM Ni and 10 µM Ni, no significant difference is observed between genotypes according to their p-values of 0.162 and 0.0916 respectively. Nickel concentration is insufficient to induce a significant reduction in root growth. At 20, 30, 40, 80 and 90 µM Ni, there is a significant difference among genotypes as their p-value is below 0.05 (**Supplemental Figure S7 and S8**). However, three intermediate Ni concentrations (at 50, 60 and 70 µM Ni) show no significant difference, which is contradicting to the normal stress response curve. For this reason, statistical analysis cannot be performed on the output data given by this software. I decided to continue with an analysis of the efficiency of the automatic segmentation by BRAT V1 and BRAT V2.

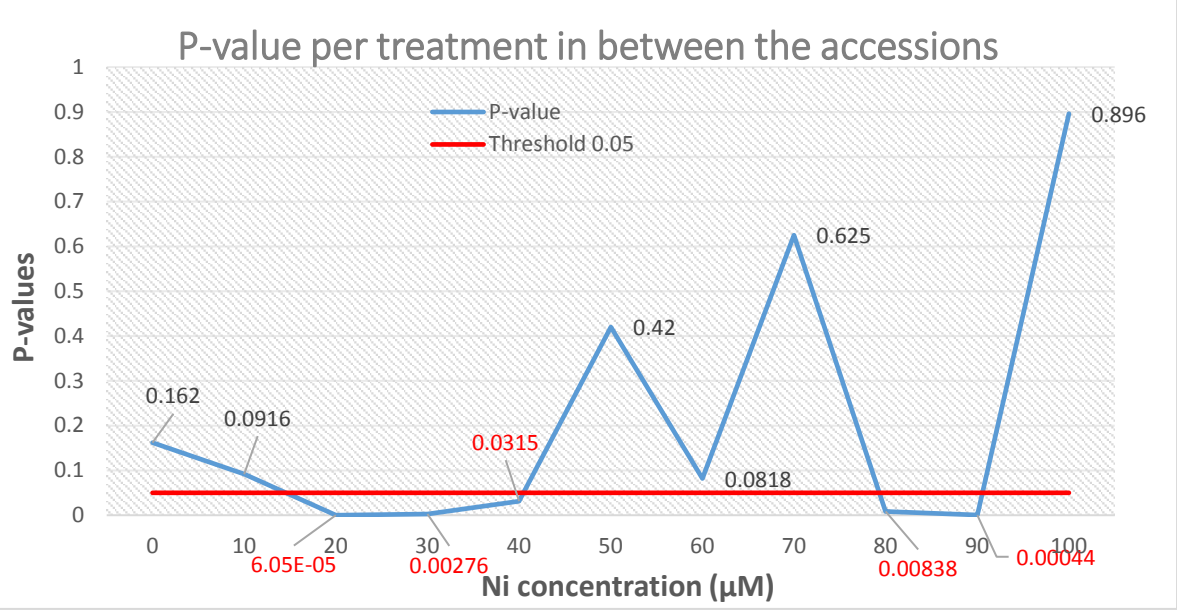

Figure 12: *Comparison of p-values from one-way ANOVA tests for root growth response of different A. thaliana to series of Ni concentration. The phenotype is the longest root length given by BRAT V1. The red line represents the threshold of p-value=0.05. Every p-value upper this threshold was not considered as significant.*

I can observe that accessions grown in control condition have a different number of plants measured by BRAT V1 (**Figure 13**). For instance, the genotype Be-1 has five root measurements while the genotype Cvi-0 has only two. In fact, twelve plants were grown in total for each genotype. There are 58 % to 83% of missing root measurement for control condition. Therefore, it is clear that BRAT V1 does not detect all plants on plates (**Figure 14A**). Moreover, BRAT V2, which is a more recent version of BRAT V1, also shows the same problem for plant segmentation in control condition (**Figure 14B**) *(Satbhai, Göschl, and Busch 2017)*.

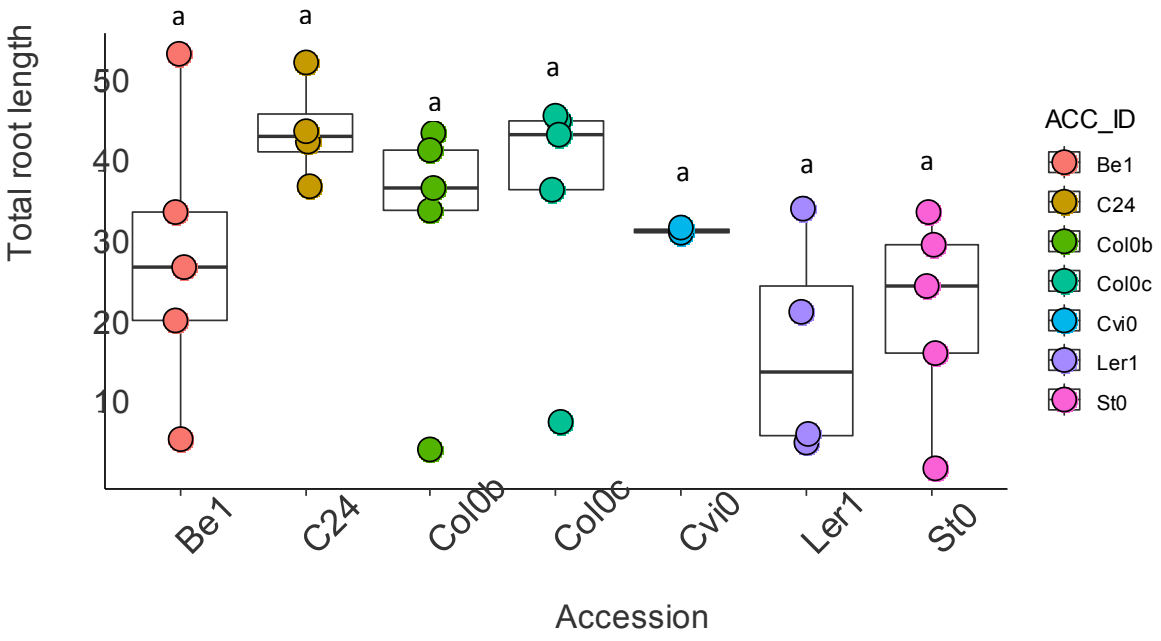

Figure 13: *Boxplot representing the length of the longest root (mm) of seven A. thaliana accessions measured by BRAT V1. Plants grew in the control condition without Ni on vertical square agar plates. Measurements were performed when plants were 10 days old. Each color illustrates a genotype and each dot represents a measurement from one plant. Mean and error bar are calculated based on every plant measured. Statistical significance is defined by one-way ANOVA test (α=0.05) in between genotype.*

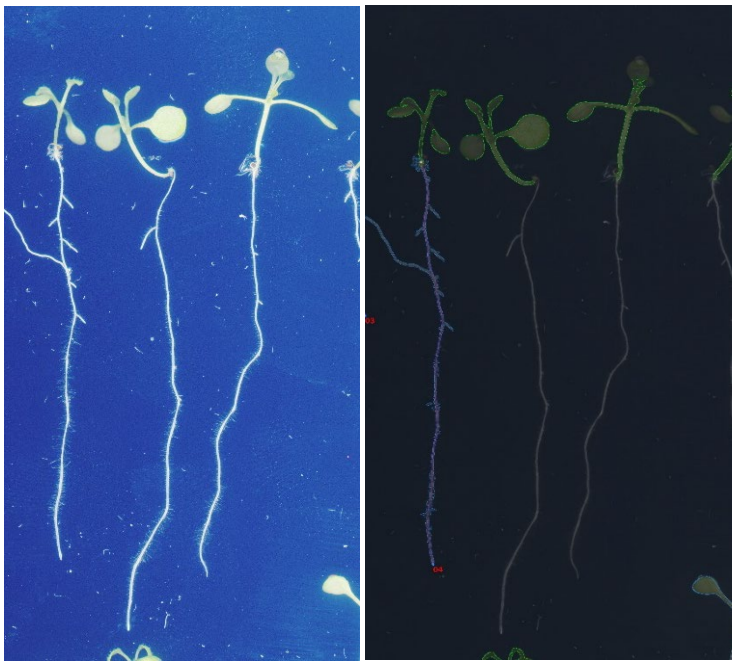

***Figure 14**: Root detection by BRAT V1 (A) and BRAT V2 (B) of three A. thaliana plants (10 days old) Col-0b (WUR) grown in control condition on the vertical agar plate #1. When a plant is detected, a number in red at the tip of the root is written and the shape of the longest root is drawn (left plant on the B image).*

After finding that not every plant is automatically detected, the total number of plants detected by both software BRATV1 and BRAT V2 was analyzed. In total, 1,056 plants (8 genotypes x 3 plants repeat x 4 plates x 11 treatments) were grown on vertical agar plates. Brat V1 detects only 36% of the plants while BRATV2 detects 52% of the plants (**Figure 15**). Perhaps, non-detected plants do not conform to rules for plants detection. However, these rules cannot be applied for all failed detection because both software does not detect all same plants. Only 193 common plants are identified by both BRAT V1 and BRAT V2.

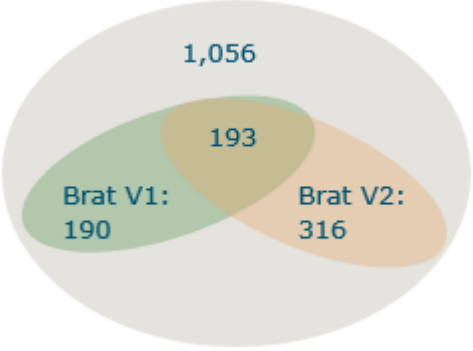

***Figure 15**: Number total of plants grown on the top, the number of plants detected by BRAT V1 and the ones by BRAT V2 and the number of same plants detected by both software.*

By analyzing the detection of a single plant, root measurements seem to be disparate from BRAT 1 to BRAT 2 (**Figure 16**). I observe that the position of the beginning of the roots and stems is different. This difference is not negligible as it results in two different measurements. BRAT V1 measures 4.07 mm for the longest root while BRAT V2 measures 6.46 mm.

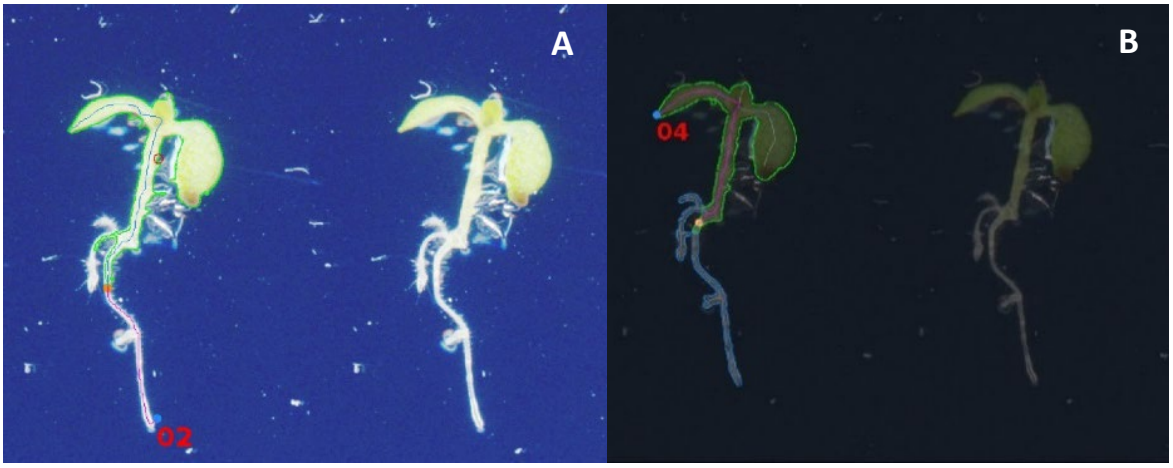

***Figure 16**: A. thaliana accession Be-1 (10 days old) grown on agar plates with 90 µM Ni. Plant segmentation by (A) BRAT V1 and (B) BRAT V2. The starting point of the roots detected by the software is indicated by an orange dot. The number written next to the plant (2 or 4) is a speculate position by the software. On the right of each of this photo represents the original image before detection and on the left is after root detection.*

To study the correlation between the outputs given by BRAT V1 and BRAT V2, all roots 193 measurements originating from the exact same plant and same scanned photo were compared (**Figure 17**). It is expected that every root length has an equal value with BRAT V1 and BRAT V2. However, I can observe that values on the scatterplot do not lie into an ascending line which indicates that a significant amount of measurements differ from one to the other version of the software. Moreover, Pearson correlation (r) for the 193 plants detected by both software is equal to 0.66 (**Figure 17)**. If r is equal to 0, it means that the two variables do not follow a linear function. If r is equal to 1, it means that the two variables are perfectly related and follow a linear relationship. Therefore, BRAT V1 and BRAT V2 do not deliver the same output. This suggests that at least one of this software does not measure precisely and incorrectly. By checking photos generated after segmentation, it is obvious that BRAT V1 and BRAT V2 measure sometimes precisely and right; however, sometimes absolutely inaccurate and

false (**Supplemental Figure S9**). For this reason, experiments using automatic measurement with BRAT software were not continued.

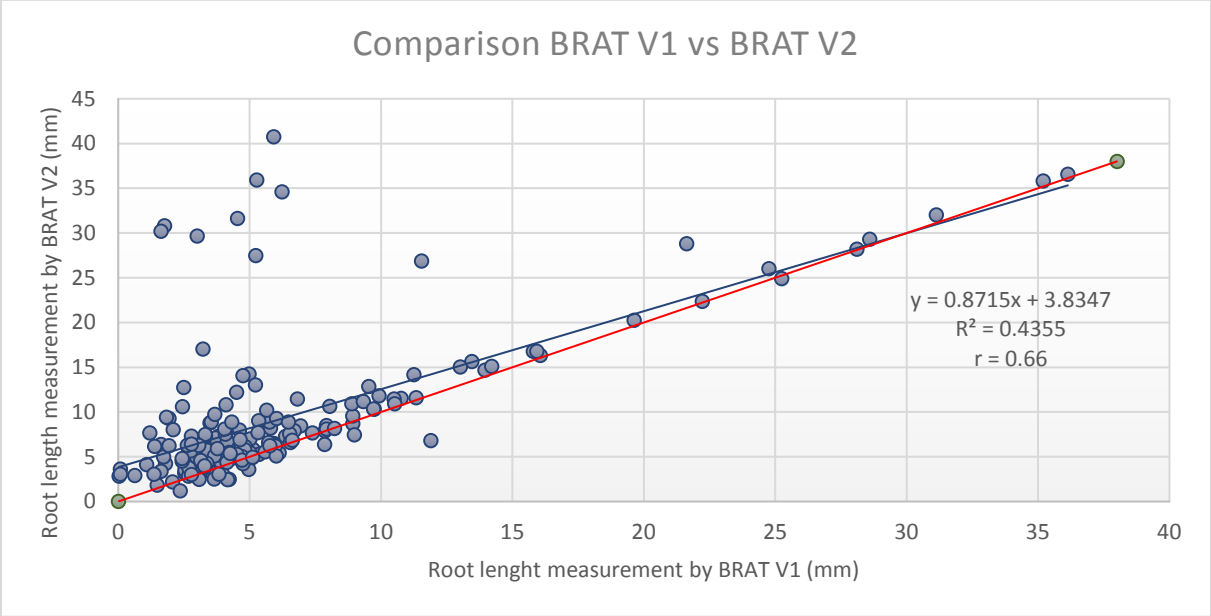

***Figure 17**: Scatterplot comparing the 193 A. thaliana (10 days old) root length measured between BRAT 1 and BRAT 2. Plants grew on agar plates and each plate was scanned. Each same scan was segmented for root detection by both BRAT V1 and BRAT V2. The blue line represents the trend line according to the data points and the red line displays the expected correlation between the two software.*

Determination of the nickel median effective concentration 50 % for root growth in hydroponic condition

Regarding the precedent experiments, I decided to measure root growth manually with a ruler. The goal of this experiment was to define which Ni concentration will be the most suitable to grow the 350 *A. thaliana* accessions in order to see variation for Ni tolerance. This concentration should reduce root growth enough to see a significant difference with plants in control condition and should not completely stop root growth to find a significant difference between accessions. Therefore, the median effective concentration, which is the Ni concentration that reduces root growth by 50% (EC50) (Cho, Chardonnens, and Dietz 2003; Schat and Bookum 1992), was determined by the following experiments.

First, *A. thaliana* plants (Col-0) were grown in pots in hydroponic condition until 17 DAG. Then, roots were dipped into active charcoal to stain them into a black color. Immediately after, I applied

different Ni concentration for each treatment in the Hoagland solution (0 µM, 0.5 µM, 0.75 µM, 1 µM, 1.5 µM, 1.75 µM, 2 µM, 3 µM, 4 µM, 8 µM and 16 µM). Finally, the cell division part of the root length was measured for each plant. By comparing root growth in the control condition to Ni excess treatment, I observe that root growth is not reduced significantly by 50 % (**Figure 18**). The nickel treatment requires a Ni concentration higher than 16 µM Ni. However, according to the value of R^2 (0.19), the data does not fit properly the exponential model. The correlation between root growth and Ni content is expected to be exponential because roots will stop growing and get a value close to 0 when Ni excess will start to be too toxic for the plants. For this reason, Ni concentration values were transformed with a logarithm function (**Figure 19**). These points were transformed into a linear model because it fits the experimental design. This linear model confirms the exponential relationship between the Ni concentration and the root growth. This relationship is explained by 40% according to the R^2 value (0.4) which is acceptable. Therefore, it is possible to calculate a prediction of the EC50 from this model.

Calculation maximum root growth

$$y= - 0.7871* \log (0 + 0.5) + 2.5201 = - 0.7871* (-0.3) + 2.5201 = 2.75623 \text{ cm}$$

Prediction of the EC50

Maximum root growth / 2 = -0.7871 x + 2.5201

2.75623/2 = - 0.7871x + 2.5201

X= (1.378115-2.5201) / -0.7871= 1.45087

10^x = 28.2407

The predicted value of EC50 is 28.24 µM nickel

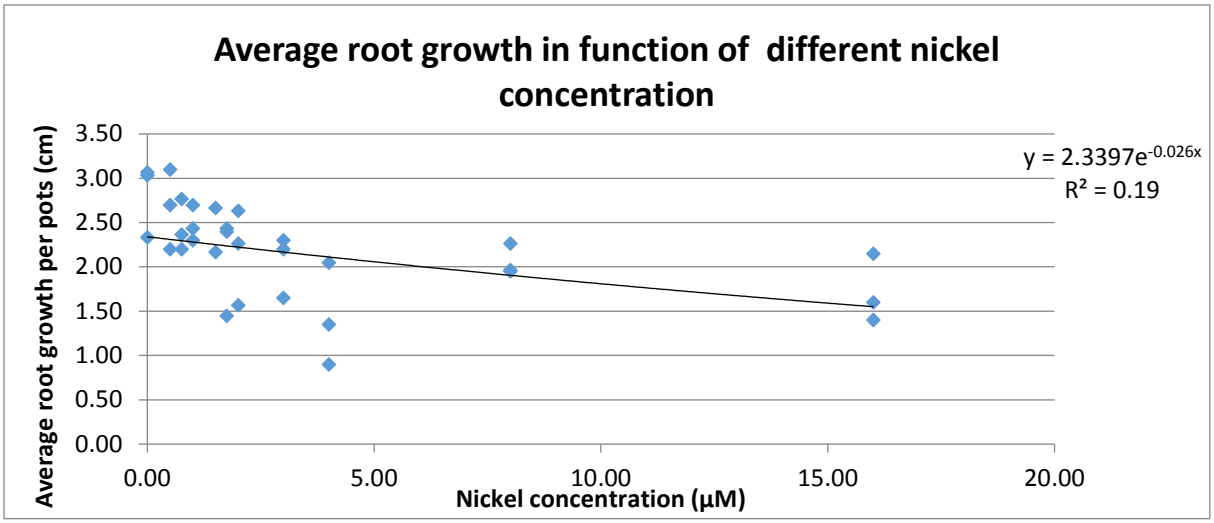

Figure 18: *Average root growth of A. thaliana (Col-0) plants (4 days after charcoal staining) per pots in function of different Ni concentration. Three pots per treatment were used and three plants grew per pots. The measurement of root growth per pot was pooled and the average was taken. An exponential trend line was drawn with Excel (2016) and its function and R^2 were determined.*

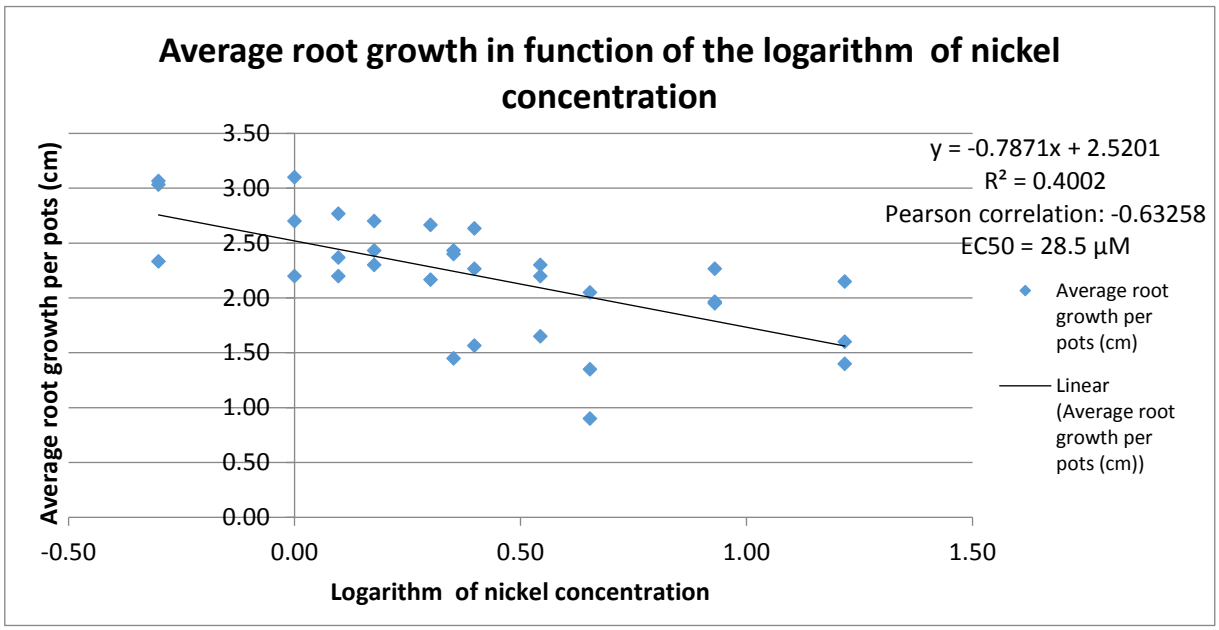

Figure 19: *Linear model of root growth in the function of the logarithm value of Ni concentration. Each dot represents the average of root growth of A. thaliana (Col-0) plants (4 days after charcoal staining) per pots. Three pots per treatment were used and three plants grew per pots. The measurement of root growth per pot was pooled and the average was taken. An exponential trend line was drawn with Excel (2016) and its function and R^2 were determined. Pearson correlation was established by comparing the expected value to the observed value.*

According to the predicted value obtained for the EC50 (28 µM), I decided to perform a second pilot experiment in order to confirm this prediction. Plants were grown in the exact same hydroponic condition and root growth was measured four days after active charcoal staining. Different Ni concentrations were chosen for this experiment (0 µM, 16 µM, 32 µM, 64 µM, 128 µM, 156 µM). I observed that the exponential model fits the data with an R^2 equal to 0.75 (**Figure 20**). Data points at 128 µM and 256 µM Ni was removed because roots stopped growing with this Ni excess and, thus, only values of 0 cm were measured on the roots. It is not possible to calculate exponential zero as it is equal to infinite. For this reason, values for these two treatments (128 µM and 256 µM Ni) could not fit in the exponential model. However, the EC50 can be determined following the equation of the exponential model. The EC50 appears to be equal to 43.3 µM Ni which is significantly higher than the EC50 predicted (28 µM).

In order to use all data points obtained, Ni concentration was transformed with a logarithm function. Data points show that a linear model does not completely fit the data distribution and its EC50 (25 µM) is significantly lower than the EC50 define with the exponential model (43 µM) (**Supplemental Figure S10**). In contrast, a polynomial model displayed a perfect match with the data distribution and its EC50 (44 µM) is not significantly different from the EC50 defined with the exponential model (43 µM) (**Supplemental Figure S11**). Consequently, I decided to opt for an EC50 equal to 44 µM Ni for the following experiments.

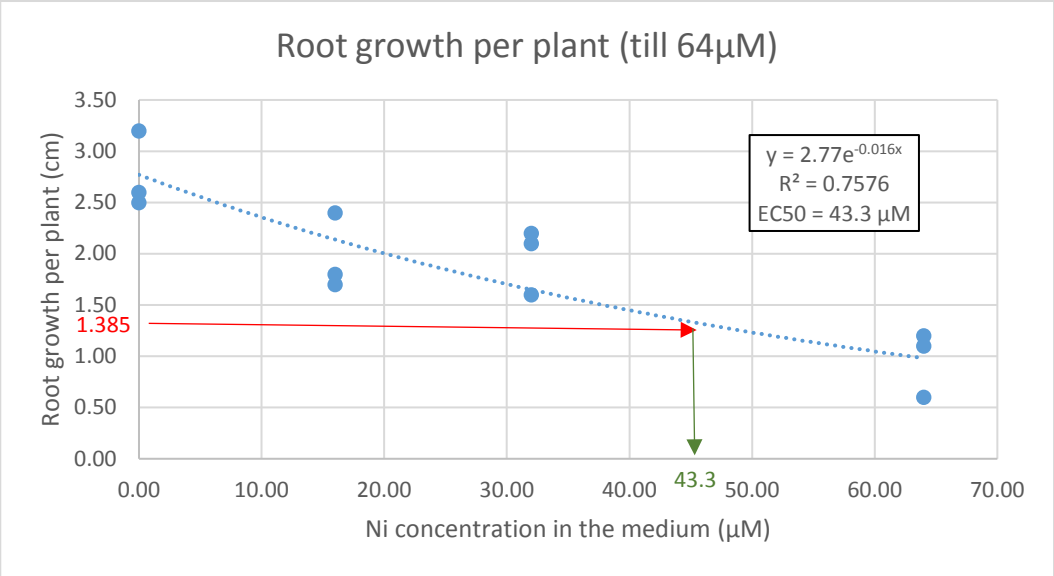

***Figure 20**: EC50 determination with the data distribution of root growth in the function of the logarithm Ni concentration with a linear model. Each data point represents the root growth measurement of one plant in one pot along different logarithm Ni concentration. With only three repeats per treatment, it was decided to set up the intercept (maximum root growth) of the equation at 2.77 which represents the average of the three root growth measurements in the control condition. The equation and R^2 were determined with Excel (2016) and the EC50 were calculated with the equation of the linear model. The red arrow represents the 50% of root growth (1.385cm) and the green arrow displays the EC50 (43.3 µM).*

Associated QTLs detected with GWAS for Ni tolerance

To discover QTLs with possible genes involved in Ni tolerance, a GWAS was performed with a focus on root growth in *A. thaliana* for Ni tolerance. This approach associates phenotypic traits, such as root growth, with genetic variants. It is a way to discover SNPs associated with a phenotypic trait. As GWAS required a large population to obtain significant results, the 350 accessions from the HapMap population were chosen to perform this experiment for two reasons. Firstly, the HapMap is defined as a global population, accessions are found all around the world requiring adaptation to the different environmental condition and, therefore, the genetic variation within *A. thaliana* is important. Secondly, the HapMap has been genotyped by a chiparray, which has 215,000 SNPs spread over the entire genome which is representative of the genome. The HapMap was grown in the hydroponic control condition to measure root growth. Four days before root measurements, all roots were dipped into active charcoal and an EC50 of 44 µM Ni was added in the medium for half of the plants.

A first GWAS was performed using, as a phenotypic trait, the relative change in roots (root growth decrease) calculated by the following equation:

$$\text{Relative change in roots (\%)} = \frac{[\text{Root growth control} - \text{root growth treatment}] \text{ x } 100}{\text{Root growth control}}$$

The data was transformed with this equation in order to represent more accurately the HapMap population because natural variation exists in root growth between the accessions in the control condition (**Figure 21**). When comparing the accession Fja1-5 to TDr-1 for Ni sensitivity, they show no significant difference according to **Figure 21 D** but display significant difference regarding **Figure 21 C**. The reason for this difference is that Fja1-5 has a natural root growth four times higher than TDr-1 in control condition (**Figure 21 A**).

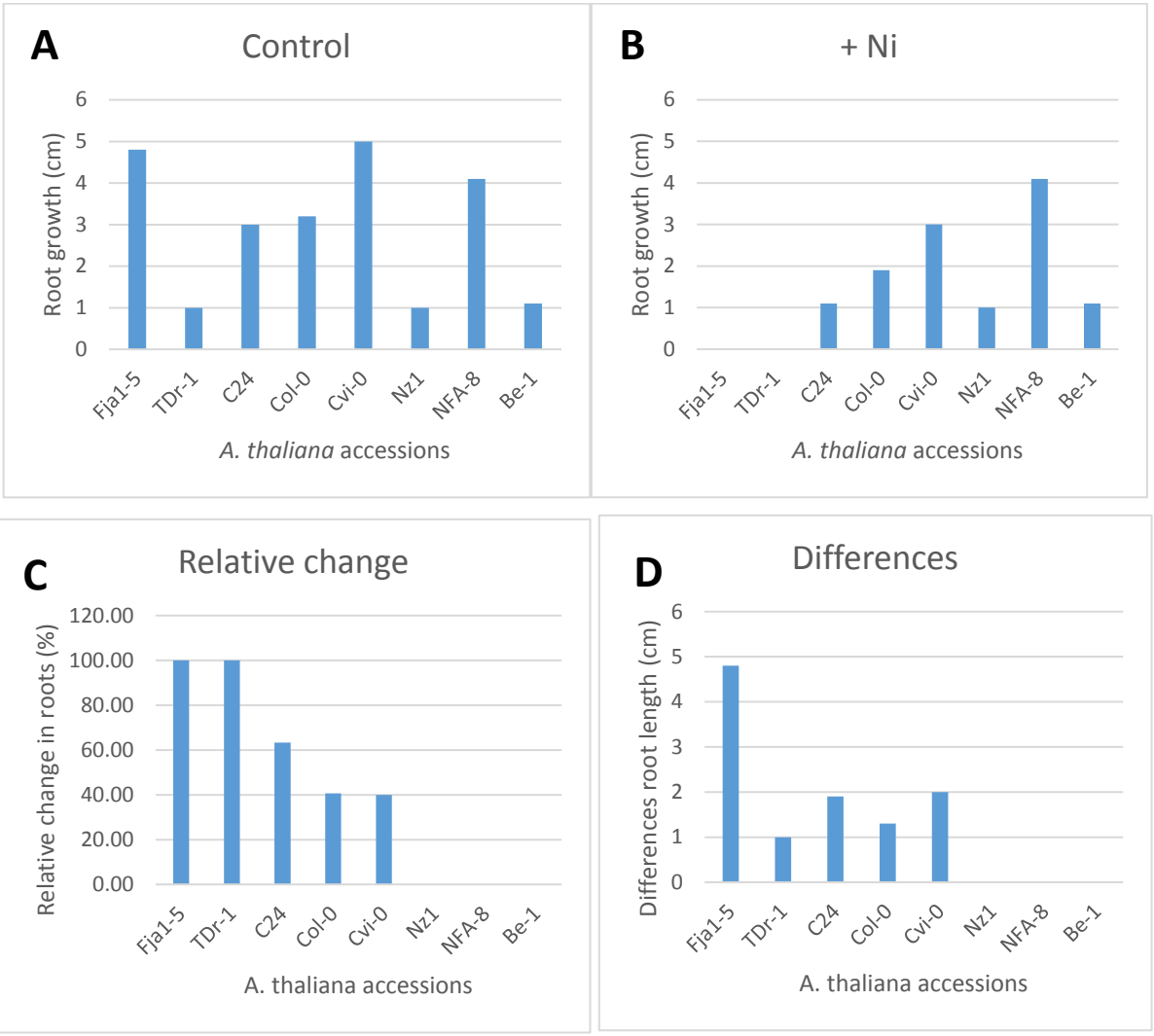

***Figure 21**: Comparison between root growth in the control condition or in nickel excess and between the relative change and differences. Root growth for eight accessions of the HapMap population from the GWAS experiment chosen according to their root phenotype. Plants (24 days old) were grown in hydroponic condition and root length was measured 4 days after dipping roots in active charcoal., (A) Root growth for plants grown in the control condition. (B) Root growth for plants grown 4 days in Ni excess. (C) Relative change in root growth showing the percentage of decrease of root growth while growing in Ni excess. (D) Difference calculated between root growth in control by root growth in Ni excess. As there is only one plant per treatment and per genotype, no statistical analysis is possible.*

By looking at the distribution of the relative change in root growth across 296 *A. thaliana* accessions, I observe that variation in Ni tolerance (**Figure 22**). Columbia has a root growth decrease of 41% which was expected as the EC50 was calculated with the same accession. Shahdera has a root growth increase of 33% in Ni excess which means that Sha is more Ni tolerance than Col-0. C24 has a root growth decrease of 86% which suggests that C24 is more Ni sensitive than Sha and Col-0.

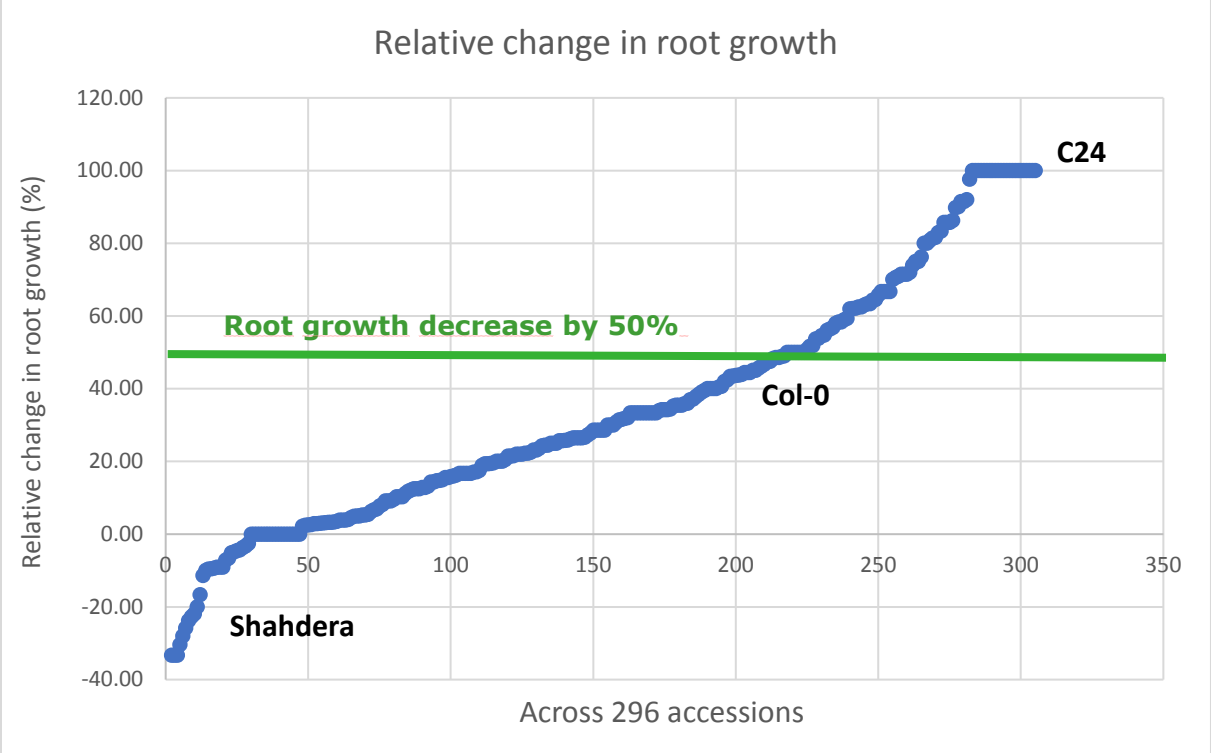

***Figure 22:** Relative change in root growth across 296 A. thaliana accessions. The green line delimits the accession with a root growth decrease higher or lower than 50%. All accessions located upper this limit will be seen as more Ni sensitive (C24) and every accession located below this limit are more Ni tolerant (Shahdara).*

At first, a QQplot of the relative change in root growth was produced to check the distribution of the data (**Supplemental Figure S4**). This QQplot shows a normal symmetric distribution with some outliers which is acceptable. Then, the GWAS on the relative change in root growth was run on both R studio and Gemma as explained in methods (Zhou and Stephens, 2012). According to the Manhattan plots representing the GWAS results, no SNPs met the Bonferroni threshold (**Figure 23, 24 and 25**). Therefore, it was decided to set an arbitrary -log(p) threshold at 4. Six significant QTLs were detected, that might be linked to the relative root growth (**Figure 23A**) (Korte and Farlow 2013). The QTL4 is detected by both GWAS (**Figure 23A and B**). The GWAS with the imputed data is more truthful as it contains a considerable amount of SNPs so it covers more the genome. Therefore, I suggested continuing by studying this QTL. The other QTLs (QTL2, QTL5, and QTL6) will not be considered as associated with the phenotypic trait.

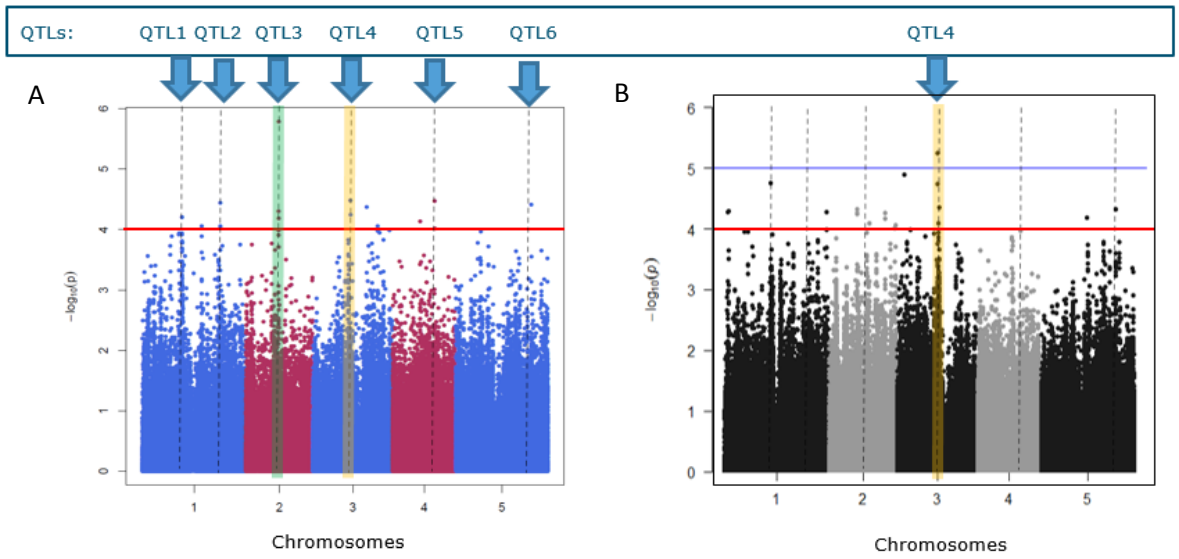

***Figure 23**: Manhattan plot representing the GWAS on the relative change in roots across 296 accessions of the HapMap population with a set of 215.000 SNPs (A) and an imputed data of one million SNPs (B). Each dot represents the p-value of an SNP in function of its position on the chromosome. The chromosomes are indicated on the X-axis and by different color/contrast. The red line displays an arbitrary threshold for the log10 (p-value) which is set up at 4. Significant QTLs (according to the arbitrary threshold) are indicated by a blue arrow at the top, dot lines show interesting peaks for (A). Common peaks for both images (A and B) are represented in yellow (QTL4). The green line represents a common peak with GWAS run with root growth decrease, residuals_control and residuals_treatment (QTL3). The minor allele frequency (MAF) was set up at a minimum of 5%.*

A second GWAS was performed using the residuals_treatment of the data. After normality and linearity were checked, GWAS was performed with both sets of 215.000 SNPs and imputed data. Results are displayed with Manhattan plots (**Figure 24**). For the GWAS with 215.000 SNPs, five loci (QTL7, QTL3, QTL8, QTL9 and QTL 10) are detected and seem to be associated with the phenotypic trait. By comparing these peaks with the GWAS with the imputed data, only one locus (QTL7) is consistent. Therefore, this QTL7 is selected for further study. Apart from this QTL, the Manhattan plot displays two other interesting QTL (QTL11 and QTL12) and not detected by the other GWAS. For the reason that imputed data is more accurate and trustful, this QTL will be analyzed. Regarding the QTL3, it is detected by both GWAS on root growth decrease and residuals_treatment. For this reason, I decided that it might be an interesting QTL. For the three last QTLs (QTL8, QTL9 and QTL10), there are no common peaks with the other GWAS and, therefore, they were no longer studied.

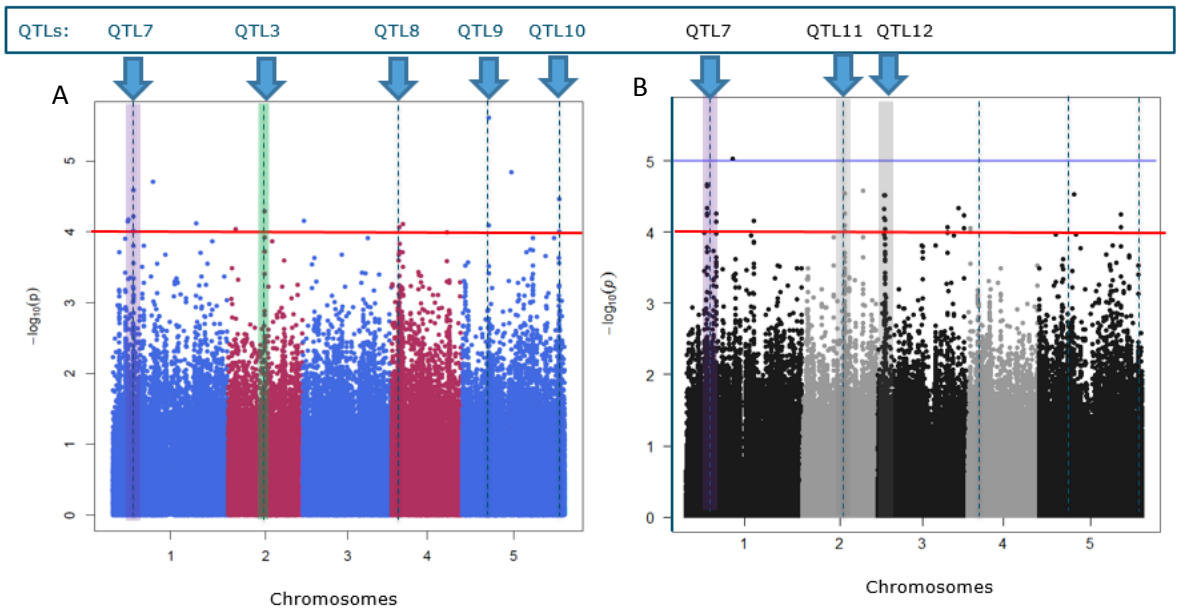

***Figure 24**: Manhattan plot representing the GWAS with the residuals_treatment as a phenotypic trait across 296 accessions of the HapMap population with a set of 215.000 SNPs (A) and an imputed data of one million SNPs (B). Each dot represents the p-value of an SNP in function of its position on the chromosome. The chromosomes are indicated on the X-axis and by different color/contrast. The red line displays an arbitrary threshold for the log10 (p-value) which is set up at 4. Significant QTLs (according to the arbitrary threshold) are indicated by a blue arrow at the top, dot lines show interesting peaks for (A). Common peaks for both images (A and B) are represented in purple (QTL7).*

The green line represents a common peak with GWAS run with root growth decrease, residuals_control and residuals_treatment (QTL3). The minor allele frequency (MAF) was set up at a minimum of 5%.

A third GWAS was performed using the residuals_control as a phenotypic trait. After normality and linearity were checked, GWAS was performed with both sets of 215.000 SNPs and imputed data. Results are displayed with Manhattan plots (**Figure 25**). The QTL3 and QTL4 and detected also. The QTL4, QTL15 and QTL16 have a high –log(p-value) and, therefore, they are selected as interesting QTLs.

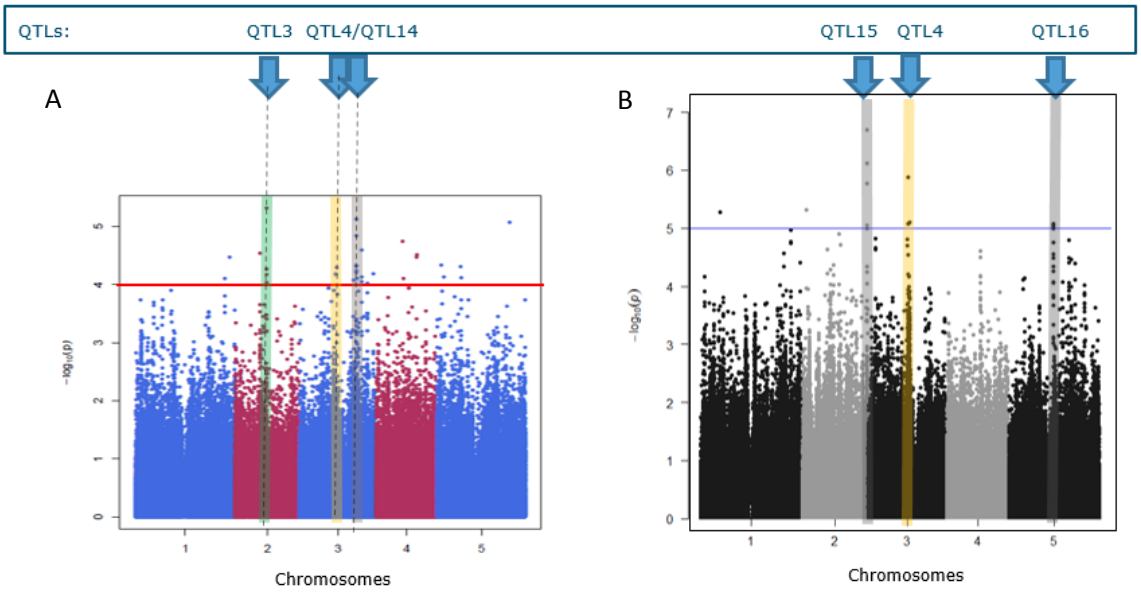

***Figure 25**: Manhattan plot representing the GWAS with the residuals_control as a phenotypic trait in roots across 296 accessions of the HapMap population with a set of 215.000 SNPs (A) and an imputed data of one million SNPs (B). Each dot represents the p-value of an SNP in function of its position on the chromosome. The chromosomes are indicated on the X-axis and by different color/contrast. The red line displays an arbitrary threshold for the log10 (p-value) which is set up at 4. Significant QTLs (according to the arbitrary threshold) are indicated by a blue arrow at the top, dot lines show interesting peaks for (A). Common peaks for both images (A and B) are represented in yellow (QTL4). The green line represents a common peak with GWAS run with root growth decrease, residuals_control and residuals_treatment (QTL3). The minor allele frequency (MAF) was set up at a minimum of 5%.*

The results from the GWAS display eight QTLs possibly associated with Ni tolerance. However, some QTLs might be a false positive because the LOD threshold chosen (4) might not be high enough.

For each QTL, the LD region was checked in order to determine all possible candidate genes (**Supplemental Figure S12**). The LD region was determined with r2 which displays the correlation

between the significant SNP and the other SNPs. LD region was checked within 5 kb in both sides of the SNP detected (Sung Kim et al., 2007). The genes located in the LD region are found with the website TAIR Gene (**Supplemental Figure S13 and Table S3**). In total 115 genes were detected to be potential genes involved in Ni tolerance (**Supplemental Table S3**). The following table represents the most promising genes for further studies (**Table 6**).

***Table 6**: Description of two of the genes obtained from the GWAS results. The information related to the genes came from the website The Arabidopsis Information Resource (Tair) (https://www.arabidopsis.org/index.jsp), National Center for Biotechnology Information (NCBI) (https://www.ncbi.nlm.nih.gov/) and UniProt (https://www.uniprot.org/).*

QTLs	Chrom osome	Position	Log	Genes	Name of the gene	The function of the gene	Gene expression
QTL3	2	9649576	5.76	AT2G22680	WAVH1	Metal ion binding (zinc), ubiquitin-protein transferase activity, involved in root gravitropism (regulation of root growth)	Expressed in root tips and leaf primordia
QTL7	1	5486002	4.56	AT1G15960	NRAMP6	Metal transporter, Probable intracellular cadmium (Cd) transporter that participates in the distribution or availability of Cd within the cell.	Expressed in the vascular bundles of shoots, cotyledons, young leaves, sepals and petals, at the top of the flower stem and in the style. Expressed in the peduncle of developing siliques as well as in the septum and the funiculi.

A large number of genes are discovered with a potential role in Ni tolerance (**Supplemental Table S3**). No conclusion can be done on their role without a first validation. This validation can be established by growing T-DNA mutant lines for these genes. T-DNA mutant lines have a DNA insertion into a selected gene, modifying its function. By comparing the root growth of T-DNA lines in the control condition with Ni excess treatment, validation on the role of the candidate genes can be defined.

Natural variation in A. thaliana for Ni tolerance

For the following results, heritability was calculated for the control condition and for the Ni excess (**Table 7**). These values are acceptable and mean that most of the phenotypic variation observed for each genotype is explained mostly by the genotypic variance and not the environment.

***Table 7**: Heritability along the A. thaliana natural accessions (Col-0, No-0, Pra-1, Pra-3, Pra-4, Pra-5, and Pra-6), the mutant At60Gy39, the F1 progeny from the crosses (At60Gy39 x Col-0) and (At60Gy39 x No-0) and the knockout mutant (nas 1,2,3/ nas 1,2,4/ nas 1,3,4/ nas 2,3,4/ nas 1,2,3,4) in control condition and in Ni excess.*

	Control	Ni excess
V environment	0.52	0.47
V genotype	0.82	0.80
Heritability	0.61	0.63

I observe that root growth in Col-0 significantly decreases of more than 50% in Ni excess (p-value = 0.009 < 0.05) (**Figure 24, 25 and 26**). The mutant At60Gy39 (control for Ni tolerance) does not show any significant difference in root growth in control condition and in Ni excess (p-value = 0.158 > 0.05).

i. Serpentine accessions

The goal of this experiment was to prove that some *A. thaliana* natural accessions are Ni tolerant. Accessions collected on serpentine soil, which has high Ni concentration, grew in hydroponic condition with or without Ni and their root length was measured in order to determine root growth.

By comparing the behavior of Pra accessions with these two controls, I observe that root growth for all Pra accessions (Pra-1, Pra-3, Pra-4, Pra-5, and Pra-6) does not significantly change in control compared to Ni excess (**Figure 26**). This suggests that all Pra accessions are naturally Ni tolerant.

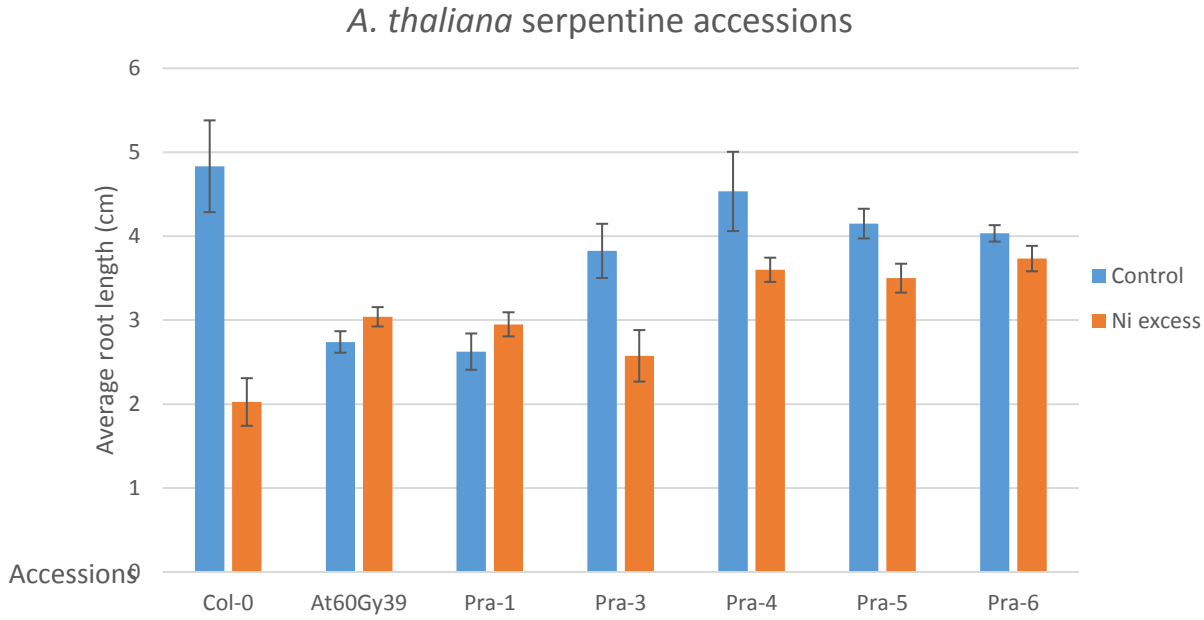

P-value	0.009	0.158	0.320	0.051	0.096	0.121	0.246

***Figure 26**: Comparison of root growth in between control and Ni excess for six natural A. thaliana accessions from serpentine soils and the mutant At60Gy39 which is a control for Ni tolerance. The bars represent the average root length per accession and per treatment. The black bars represent the standard error. P-values (below the graphic) were calculated from a t-test per accession to compare root length in control and in Ni excess. The color bars represent the average of root growth from 3 to 6 plants per treatment and genotype.*

ii. Contribution of NAS genes for Ni tolerance

This experiment was performed in order to determine the contribution of *NICOTIANAMINE SYNTHASE* (*NAS)* genes (*NAS1, NAS2, NAS3, NAS4*) in Ni tolerance (**Figure 27**). It was demonstrated that Nicotianamine (NA) is an important binding ligand that chelates to Ni conferring tolerance to Ni toxicity (Suyeon Kim et al., 2005). The expression of four *NICOTIANAMINE SYNTHASE* genes *(NAS1, NAS2, NAS3,* and *NAS4*) is induced by Ni excess in *A. thaliana* in order to produce a higher amount of NA to tolerate Ni toxicity (Suyeon Kim et al., 2005).

A. thaliana knockout mutants were grown in hydroponic condition. Half of the plants received Ni supplemented in the nutrient solution (Ni excess) and the other half grew without Ni. The knockout mutants (*nas1,2,3* and *nas1,2,3,4*) plants did not germinate or were infected with fungi. Therefore, there were no enough repeats to include them for the heritability calculation and to perform a t-test.

Root growth for these mutants (*nas1,2,3* and *nas1,2,3,4*) shows a considerable decrease (59% and 94%) but, in reason of the lack of repeats, I cannot confirm that these results are significant. I observe that root growth for the mutant *nas 2,3,4* significantly decreases by 66% in Ni excess. In contrary, root growth for the mutant *nas1,2,4* has no significant decrease in Ni excess but it might be caused by environmental variation. I observe a reduction in root growth of 46% for the mutant *nas1,3,4* in Ni excess. I deduce that the gene *NAS3* seems to be the most involved in Ni tolerance because of all genotypes with this gene knockout show root growth decrease in Ni excess. It seems that the *NAS4* gene has the most contribution in Ni tolerance because a knockout of this gene results in a higher root decrease compared to Col-0. I observe also that the higher root decrease in Ni excess is when all four *NAS* genes are knockout and, therefore, all these genes might increase Ni tolerance.

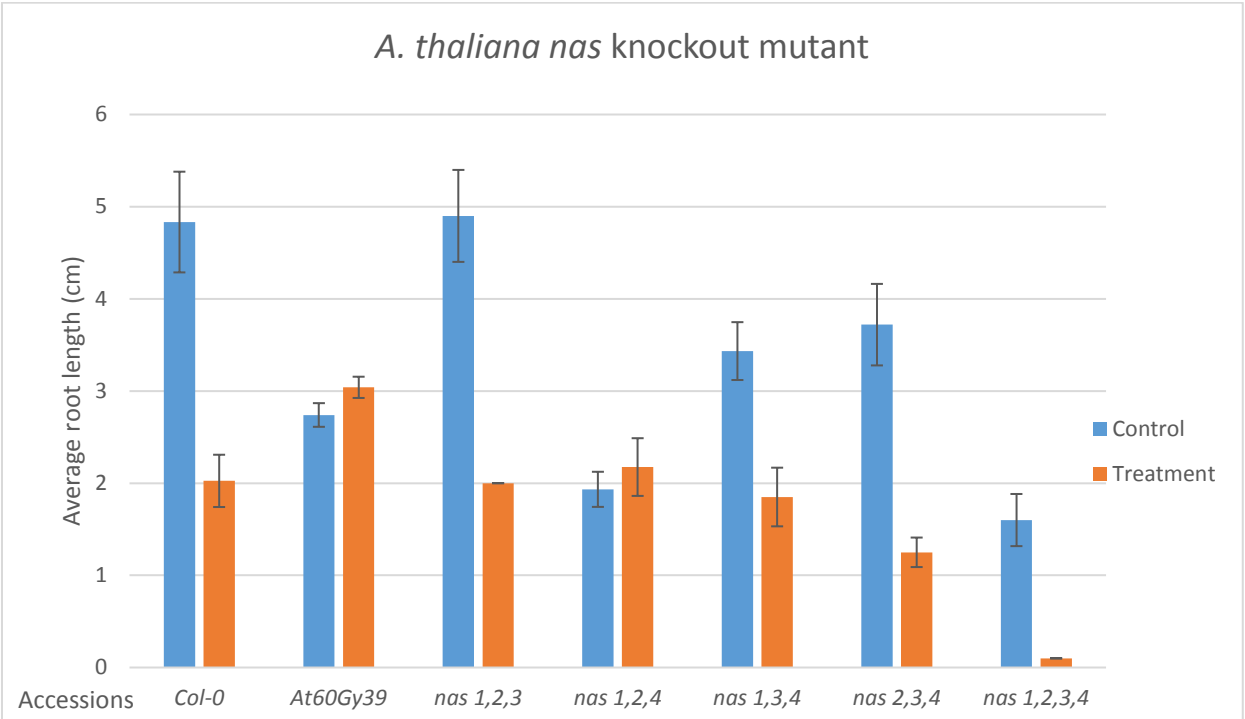

P-value	0.009	0.158	/	0.629	0.077	0.004	/
Root growth decrease (%)	58	-11	59	-13	46	66	94

***Figure 27**: Comparison of root growth in between control and Ni excess for A. thaliana knockout mutant (nas 1,2,3/ nas 1,2,4/ nas 1,3,4/ nas 2,3,4/ nas 1,2,3,4), the natural accession Col-0 and the mutant At60Gy39. The bars represent the average root length per accession and per treatment. The black bars represent the standard error. P-values (below the graphic) were calculated from a t-test per accession to compare root length in control and in Ni excess. The color bars represent the average of root growth from 1 to 6 plants per treatment and genotype. The root growth decrease was calculated with the average of the root growth.*

iii. Characterization of induced mutation involved Ni tolerance

The aim of this experiment was to determine if induced mutation involved in Ni tolerance are recessive of dominant (**Figure 28**). The mutant At60Gy39 was made by ion beam irradiation and by two series of growth on Ni excess (400 µM)(Hase et al., 2010). Plants which could grow on Ni excess were selected each time as the next generation resulting in *A. thaliana* Ni tolerant. Crosses were made in between this mutant At60Gy39 and Col-0 or No-0. The progeny from this crosses (F1) is heterozygote. If the mutation conferring Ni tolerance is recessive, it is expected that 100% of the progeny will be Ni sensitive as the parent Col-0 and No-0 (Delhaize 1996). In contrast, if the mutation is conferring Ni tolerance is dominant, it is expected that 100% of the progeny is Ni tolerant as the parent At60Gy39 (Yi and Richards 2008). I observe that root growth for the F1 progeny from both crosses (At60Gy39 x Col-0) and (At60Gy39 x No-0) does not significantly decrease with Ni excess.

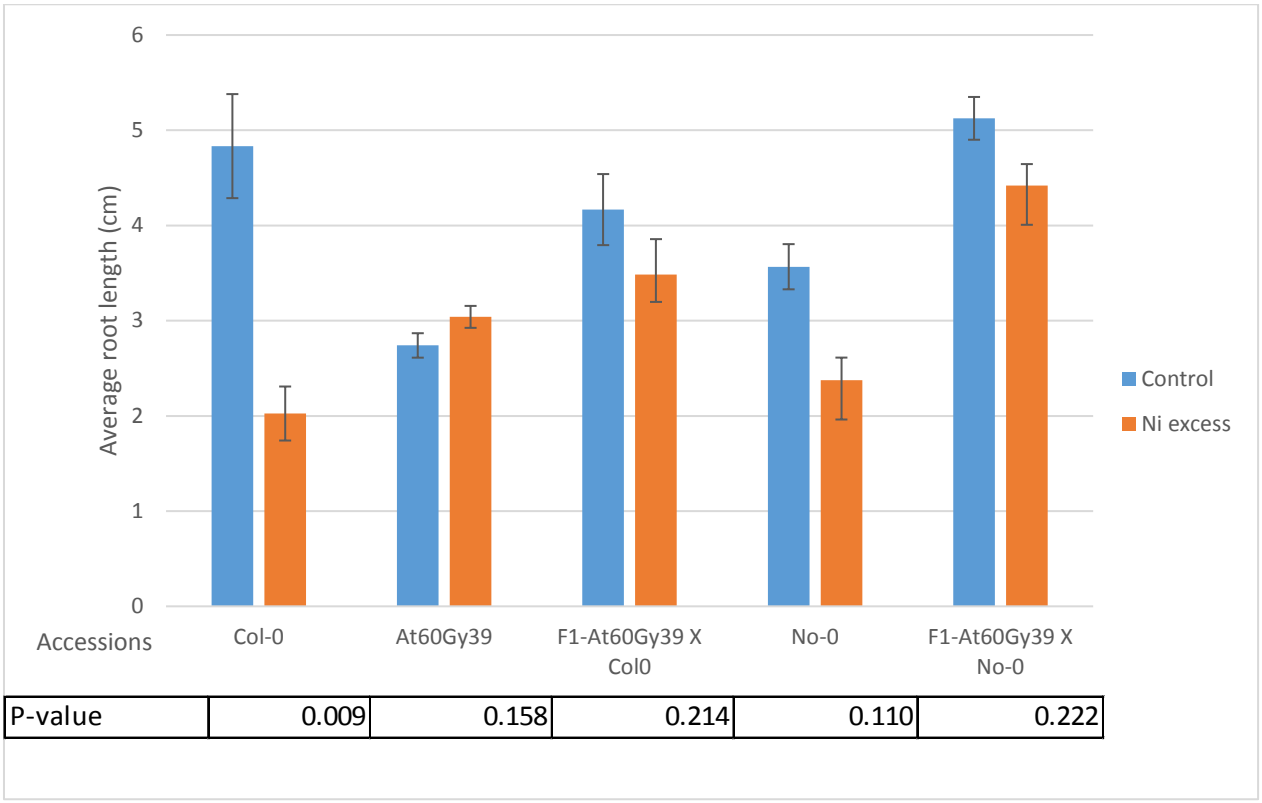

P-value	0.009	0.158	0.214	0.110	0.222

***Figure 28**: Comparison of root growth in between control and Ni excess for A. thaliana mutant (At60Gy39), natural accession Col-0 and Nossen (No-0) and for F1 progeny from the crosses (At60Gy39 x Col-0) and (At60Gy39 x No-0). The bars represent the average root length per accession and per treatment. The black bars represent the standard error. P-values (below the graphic) were calculated from a t-test per accession to compare root length in control and in Ni excess. The colour bars represent the average of root growth from 3 to 6 plants per treatment and genotype.*

5. Discussion

The aim of this thesis is to characterize the importance of calcium channel in Ni uptake and determine natural variation for Ni tolerance in *A. thaliana*.

The purpose of adding verapamil, while growing *A. thaliana*, was to characterize the contribution of calcium channel for Ni uptake. In a recent paper, it was demonstrated that in the two Ni hyperaccumulator *O. bracteata* and *O. inflate* Ni was taken up predominantly through calcium channel (Mohseni, Ghaderian, and Schat 2018). I suggested that the same Ni uptake occurs in *A. thaliana*. Due to the fact that most Ni is taken up through calcium channel, it is more difficult to study other transporter involved in Ni uptake. For this reason, I decided to block calcium channel to study easier other Ni transporters. Calcium channels were blocked with the calcium channel blocker named verapamil (Cosio, Martinoia, and Keller 2004; Spedding and Paoletti 1992). Results from this study showed that (i) after 3 days with high verapamil concentration, calcium content decreases in roots by ± 70% which proves that verapamil blocks most of the calcium channels. However, it was observed that (ii) Ca concentration in shoots stayed unchanged with or without verapamil. This suggests that either verapamil does not block calcium translocation from roots to shoots or that there is enough Ca in roots to meet the demand of shoots for this short duration. It is known that Ca channels are implicated in root-shoot transport (White and Broadley 2003). For this reason, the second solution is the most probable as it was demonstrated that verapamil blocks calcium channel in plants, in animals and in fungi (Bergson et al., 2011; Singh, Sharma, and Prasad 2011; Yu et al., 2014). (iii) Ni content in shoots and roots did not show a difference between plants growing with or without verapamil. This indicates that verapamil has much less effect on Ni content than on Ca in the plants. In conclusion, Ni is not predominantly taken up through calcium channel in *A. thaliana*.

Root growth was proved to be an indicator of Ni tolerance in *A. thaliana* (Agrawal et al., 2012). For this reason, root growth was analyzed in this study. In order to phenotype root growth, it was first decided to measure automatically root length from *A. thaliana* plants grown on vertical agar plates (measurement of the longest root) with the revolutionary software BRAT. It was demonstrated that BRATV1, BRATV2, and version of Lotus BRAT, could measure accurately root length in *A. thaliana* and in *Lotus Japonicus* (Giovannetti et al., 2017; Satbhai, Göschl, and Busch 2017; Slovak et al., 2014). In this study, *A. thaliana* roots were automatically measured by both BRATV1 and BRATV2. The results showed four important aspects: (i) germination rate was not influenced by Ni concentration (100 µM Ni) on agar plates; (ii) BRATV1 and BRATV2 did not detect roots from every plant; (iii) BRATV1 and BRATV2 had a low Pearson correlation for their roots measurement ($r = 0.66$); (iv) BRATV1 and BRATV2

did not measure root length accurately. The first observation was helpful for growing plants on agar plates directly with Ni. The second observation suggested that it is more difficult to perform statistical analysis and to obtain significant results when a number of samples per treatment and per genotype are not equilibrated. The third observation showed that at least one of the two BRAT version does not measure correctly root length. The last observation confirmed that BRAT software measures root length wrongly and, therefore, automatic measurement with BRAT software is not reliable and suitable for this experiment. Consequently, the direction of the thesis for studying roots turned into a manual measurement of root growth. Perhaps, if BRAT software allows placing the coordinate of the beginning of the root and the tip of it, the measurements might be a more accurate and a considerable amount of non-detected plants may be measured. One of the reasons why BRAT software was not suitable for this experiment might be the stress treatment chosen. It is known that, in heavy metal excess condition, the root architecture change considerably. For instance, there is a higher lateral root density with an excess of cadmium and copper than in control in *A. thaliana* in order to reach non heavy metal contaminated zone (Remans et al. 2012). For this reason, the primary root is more difficult to be detected and measured accurately by the BRAT software.

The goal of the following experiment was to define the median effective concentration in hydroponic condition for root growth in order to detect Ni sensitive and Ni tolerant plants. If Ni excess is too toxic for plants, none might survive (Sachan and Lal 2017). On the contrary, if Ni does not affect considerably root growth, no Ni sensitive or Ni tolerant may be detected. It was thought that the EC50 should be close to 1 µM Ni (Weng et al., 2003). However, the results showed an unexpectedly high value for the EC50 (44 µM Ni) (See Supplemental Data 1, 2 and 3 for calculation). One of the reasons for this high Ni value might be the pH.

The pH is one important factor involved in Ni uptake by the plant. When pH is neutral in the nutrient solution, Ni uptake increases considerably in hyperaccumulator plants, such as *Alyssum corsicum* (Kukier et al., 2004). In contrast, when the pH raised from 4.0 to 7.0 in hydroponic condition, Ni uptake decreases significantly in non-hyperaccumulator plants, such as oath (Weng et al., 2003). Weng demonstrated that the EC50 for shoot growth in oath decreases from 23 to 1.7 µM Ni in hydroponic condition when pH increases from 4.0 to 7.0 respectively in the nutrient solution (Weng et al., 2003). This theory does not correspond with the value of the EC50 found for root growth and the pH used in this study. The EC50 for root growth is significantly high (44 µM Ni) for non-hyperaccumulator plants (*A. thaliana*) and the pH is acidic (5.5).

Another reason that could explain this high EC50 value is the use of Fe-EDDHA in the nutrient solution. At first, Fe-EDDHA was utilized instead of Fe-EDTA because Fe-EDTA has a much lower affinity with Fe than Ni when the pH > 5.5 and, therefore, Ni replaces Fe on Fe-EDTA. EDDHA has a high affinity for Fe than Ni and does not bind Ni. Thus, Ni is more available in the medium. However, Bin et al., (2016) demonstrated that Fe-EDDHA can be dissociated from Fe and binds Ni (Bin, Weng, and Bugter 2016). Consequently, there might be less Ni available in the nutrient solution for plants and the Ni uptake could decrease. Instead of Fe-EDDHA, Fe-HBED (di-hydroxybenzoyl-ethyl-enediaminediacetate) could be utilized in nutrient solution because it has a significantly higher affinity with Fe and, even with high Ni concentration, it cannot be dissociated from Fe and without Fe deficiency in plants (Bin, Weng, and Bugter 2016).

To discover candidate genes associated with Ni tolerance, a GWAS was performed on two phenotypic traits (relative change in root growth and the residuals). I observed six significant QTLs. From these QTLs, no conclusion can be drawn regarding the involvement of these candidate genes in Ni tolerance (**Supplemented Table 3**). However, there could be a hypothesis regarding the role of the gene AT1G15960 found on QTL12. This gene is a *NATURAL RESISTANCE-ASSOCIATED MACROPHAGE PROTEIN 6 (NRAMP6).* It was demonstrated that genes *NRAMP3* and *NRAMP4* have a higher expression in hyperaccumulator plants with Ni in the medium (Visioli, Gullì, and Marmiroli 2014). They are vacuole membrane metal transporter suggesting their involvement in Ni translocation to the vacuole (Visioli, Gullì, and Marmiroli 2014). Moreover, it was proved that NRAMP homologs may be involved in Ni transport (Mizuno et al., 2005). For this reason, NRAMP6 might be an important candidate gene. However, its role in Ni tolerance can be not confirmed yet and must be validated with T-DNA mutant lines. One of the other genes that might be associated with the Ni excess response is the WAVY gene because this gene controls the gravitropic response in *A. thaliana* roots and it is known that root architecture is influenced by heavy metals (Remans et al. 2012; Sakai et al. 2012). Every gene located in the significant QTLs and in the LD region requires T-DNA mutant lines screening to validate their potential role in Ni tolerance.

Meanwhile, by comparing the results of GWAS, I observe that some QTLs detected on the Manhattan plots are identical (same region and/or SNPs), as expected, for R studio and GEMMA but some also are located in the different region. This difference can be explained for several reasons.

The first explanation is the choice of the number of SNPs. GWAS run through R studio was executed with a set of 215.000 SNPs and corrected by a kinship produced from this same set. The

kinship is a matrix explaining the correlation between each genotype with each other (Davila Olivas et al., 2017). GWAS run though GEMMA was performed with an imputed data set of 1 million SNPs and corrected by a kinship derived from the imputed data set. Therefore, the difference in kinship might be the reason for diverse QTLs. A Pearson correlation can be tested in between both kinships to check whether they are significantly different and if their difference could influence considerably to the output of a GWAS. QTLs should be chosen according to the imputed data set because it has more SNPs and, therefore, its kinship might be more reliable.

Secondly, the SNPs sets mentioned before were not obtained in the same way. The 215.000 SNPs was generated by alignment to the 215.000 SNPs and the imputed data aligns all scaffolds to Columbia which does not result obligatory into the same markers.

The third explanation is related to the data analysis platform chosen. GEMMA and script R. Studio (Dr. Willem Kruijer) produce a GWAS with a different algorithm which might be the reason for different QTLs observed (Zhou and Stephens, 2012). The GWAS with the imputed data was executed through GEMMA in this study but cannot run on R. Studio which has not enough capacity and power. On the contrary, the GWAS with the 215.000 SNPs set was performed with R. Studio and can be executed with GEMMA (**Table 8**). The resulting output from this other GWAS (215.000 SNPs set with GEMMA) could give more confidence in the choice of QTLs.

***Table 8**: Representation of the different possibilities to execute a GWAS according to the algorithm and the SNPs set chosen. The green V shows the GWAS performed already and the red crosses represent the incompatibility between the algorithm and the SNPs set.*

		SNPs set		
		215.000 SNPs	1 Million SNPs	All SNPs
Different algorithms	Script R studio (Dr. Willem Kruijer)	V	X	X
	GEMMA (Zhou and Stephens, 2012)	Possible	V	X
	GWAPP (Seren et al., 2012)	X	X	Possible

The fourth explanation relates to the LOD threshold. I observe that with a LOD threshold of 4, there is no selection on false positive. Therefore, a higher LOD threshold might be required to select against false positive.

The last explanation could be related to the low number of replicates used. Only one plant per accession and per treatment was used which is not enough to calculate the heritability to know if the phenotypic variation observed is more related to the genotypic variation or to the variation environmental. This is why, I suggest to perform this experiment a second time with maybe fewer accessions (around 200) and more repeats.

In conclusion, several factors influence the QTLs detected and selected on the Manhattan plot. By generating several GWAS with a different combination of these factors, significant QTLs could be selected with more confidence and less false positive may be chosen. For instance, GWAS could also be executed with the website GWAPP which contains all SNPs (Seren et al., 2012).

In the last experiments, I aimed to confirm natural variation for Ni tolerance in *A. thaliana* by phenotyping and comparing root growth in Ni excess and control condition for the natural accessions collected on serpentine soils (Pra). The characteristic of serpentine soils is their high level of Ni concentration (Sağlam 2017). Due to this high Ni level in soils, Ni hyperaccumulator can be easily detected. For instance, *Noccaea camlikensis* and *Alyssum peltarioides* from Brassicaceae family are Ni hyperaccumulator plants which accumulate 4472 mg Ni /kg DW and 3209 mg Ni /kg DW respectively (Sağlam 2017). From the *A. thaliana* plants collected on serpentine soils, I observed that all five Pra accessions (Pra1, Pra-3, Pra-4, Pra-5, and Pra-6) displayed no significant root growth decrease in Ni excess compared with the control condition. I deduced that these accessions are Ni tolerant. This observation confirms the precedent results in this thesis and the work from Agrawal et al., 2012 that there is a natural variation for Ni tolerance *in A. thaliana* (Agrawal et al., 2012).

To characterize the contribution of the NAS genes in Ni tolerance, I compared root growth of *A. thaliana* knockout mutant of NAS genes (*nas 1,2,3/ nas 1,2,4/ nas 1,3,4/ nas 2,3,4/ nas 1,2,3,4*) in control and Ni excess. It was demonstrated that NA is an important binding ligand that chelates to Ni conferring tolerance to Ni toxicity (Suyeon Kim et al., 2005). From the results obtained in this thesis, I observed that root decrease for the mutant *nas 1,2,3,4* is the highest compared to the other genotypes. I deduced that higher production of nicotianamine reduces Ni toxicity in plants which are in accord with Suyeon Kim et al., 2005.

To determine if the mutation conferring Ni tolerance in the mutant At60Gy39 is recessive or dominant, crosses were made from (At60Gy39 x Col-0) and (At60Gy39 x No-0) and root growth of their F1 progeny was studied in control condition and Ni excess. Results show that root growth for both F1 progenies does not decrease significantly with Ni excess. I deduced that F1 progeny is Ni tolerant and, therefore, the mutation conferring it Ni tolerance is not recessive but dominant.

6. Conclusion

From my observation on the effect of verapamil, it suggests that verapamil does affect calcium in roots and, therefore, verapamil blocks most calcium channels and reduces calcium uptake from the nutrient solution to roots. On the contrary, verapamil had no effect on Ni content both shoots and roots. This suggests that Ni is not predominantly transported by calcium channel in plants and is taken up mostly through other transporters.

Regarding the efficiency of BRAT software, for plants grown on agar plates, it was deduced that the automatic measurement of roots with BRATV1 and BRATV2 is not reliable and suitable for this study. For plants grown in hydroponic condition, manual measurement of root growth with active charcoal seemed to be sufficiently efficient.

After the results of the EC50, I suggest the use of Fe-HBED, instead of Fe-EDTHA, because of its higher affinity with Fe.

The GWAS results let suppose that determining which QTL is significant is difficult and require a comparison between the same peaks coming across the different GWAS executed with different SNPs set, or analysis platform or another factor. They also proved the natural variation for Ni tolerance in *A. thaliana*. Natural variation for Ni tolerance is confirmed by the GWAS results and the natural accessions which display Ni tolerance (Pra).

From the last experiments, root growth for the knockout mutant *nas1,2,3,4* decreases the most and it confirms that more production of nicotianamine reduces the Ni toxicity in *A. thaliana*. The induced mutation in the Ni tolerant At60Gy39 seems to be dominant.

7. Suggestions for future experiments

According to the result of the EC50, *A. thaliana* seems to not uptake a significant amount of Ni with a low pH. On the contrary, publications proved that non-hyperaccumulator uptakes less Ni with a high pH. It might be interesting to grow *A. thaliana* in a series of pH from 3 to 8 to see how the pH influence the Ni uptake in hydroponic condition.

Quantitative trait locus can be analyzed by phenotyping a Recombinant Inbred Lines (RIL) of the most Ni tolerant and Ni sensitive plants observed in this study (El-Lithy et al., 2006). There are RIL available for the crosses (C24 x Col-0) and (Sha x Col-0) which were some of the extreme phenotypes (Ni sensitive and Ni tolerant respectively).

In order to validate significant QTLs after a GWAS, GWAS can be run by different method and software. For instance, GWAS can be performed through R studio, Gemma, on the GWAPP website, or even with REMMA (additivity module) to select the peaks that come out across these different methods. This will give more confidence in some QTLs and get rid of the false positive.

Then, in order to narrow down the number of candidate genes which might be involved in Ni tolerance, a screening of T-DNA lines can be used. By comparing the phenotype of T-DNA lines grown in a control condition with Ni treatment, the involvement of candidate genes in Ni tolerance can be validated.

To discover where are localized the mutations in mutated *A. thaliana* plants which are Ni tolerant, a SHOREmap approach can be performed (Schneeberger et al., 2009).

8. References

Agorio, Astrid, Jérôme Giraudat, Michele Wolfe Bianchi, Jessica Marion, Christelle Espagne, Loren Castaings, Françoise Lelièvre, Catherine Curie, Sébastien Thomine, and Sylvain Merlot. 2017. 'Phosphatidylinositol 3-Phosphate-Binding Protein AtPH1 Controls the Localization of the Metal Transporter NRAMP1 in Arabidopsis'. *Proceedings of the National Academy of Sciences of the United States of America* 114 (16): E3354–63. https://doi.org/10.1073/pnas.1702975114.

Agrawal, Bhavana, Venkatachalam Lakshmanan, Shail Kaushik, and Harsh P. Bais. 2012a. 'Natural Variation among Arabidopsis Accessions Reveals Malic Acid as a Key Mediator of Nickel (Ni) Tolerance'. *Planta* 236 (2): 477–89. https://doi.org/10.1007/s00425-012-1621-2.

Ahmad, Muhammad Sajid Aqeel, and Muhammad Ashraf. 2011. 'Essential Roles and Hazardous Effects of Nickel in Plants'. *Reviews of Environmental Contamination and Toxicology* 214: 125–67. https://doi.org/10.1007/978-1-4614-0668-6_6.

Albanese, Stefano, Martiya Sadeghi, Annamaria Lima, Domenico Cicchella, Enrico Dinelli, Paolo Valera, Marco Falconi, Alecos Demetriades, and Benedetto De Vivo. 2015. 'GEMAS: Cobalt, Cr, Cu and Ni Distribution in Agricultural and Grazing Land Soil of Europe'. *Journal of Geochemical Exploration*, Continental, regional and local scale geochemical mapping, 154 (July): 81–93. https://doi.org/10.1016/j.gexplo.2015.01.004.

Alloway, B. J., ed. 1995. *Heavy Metals in Soils*. 2nd ed. Springer Netherlands. //www.springer.com/gp/book/9789401045865.

Al-Shehbaz, Ihsan A., and Steve L. O'Kane. 2002. 'Taxonomy and Phylogeny of Arabidopsis (Brassicaceae)'. *The Arabidopsis Book / American Society of Plant Biologists* 1 (September). https://doi.org/10.1199/tab.0001.

Anderson, C. W. N, R. R Brooks, A Chiarucci, C. J LaCoste, M Leblanc, B. H Robinson, R Simcock, and R. B Stewart. 1999. 'Phytomining for Nickel, Thallium and Gold'. *Journal of Geochemical Exploration* 67 (1): 407–15. https://doi.org/10.1016/S0375-6742(99)00055-2.

Bergson, Pamela, Gregory Lipkind, Steven P. Lee, Mark-Eugene Duban, and Dorothy A. Hanck. 2011. 'Verapamil Block of T-Type Calcium Channels'. *Molecular Pharmacology* 79 (3): 411–19. https://doi.org/10.1124/mol.110.069492.

Bin, Levi M., Liping Weng, and Marcel H. J. Bugter. 2016. 'Effectiveness of FeEDDHA, FeEDDHMA, and FeHBED in Preventing Iron-Deficiency Chlorosis in Soybean'. *Journal of Agricultural and Food Chemistry* 64 (44): 8273–81. https://doi.org/10.1021/acs.jafc.6b01382.

Brooks, R. R, J Lee, R. D Reeves, and T Jaffre. 1977. 'Detection of Nickeliferous Rocks by Analysis of Herbarium Specimens of Indicator Plants'. *Journal of Geochemical Exploration* 7 (January): 49–57. https://doi.org/10.1016/0375-6742(77)90074-7.

Cantor, Rita M., Kenneth Lange, and Janet S. Sinsheimer. 2010. 'Prioritizing GWAS Results: A Review of Statistical Methods and Recommendations for Their Application'. *American Journal of Human Genetics* 86 (1): 6–22. https://doi.org/10.1016/j.ajhg.2009.11.017.

Cheng, Ning-hui, Jon K. Pittman, Toshiro Shigaki, and Kendal D. Hirschi. 2002. 'Characterization of CAX4, an Arabidopsis H+/Cation Antiporter'. *Plant Physiology* 128 (4): 1245–54. https://doi.org/10.1104/pp.010857.

Cherian, Sam, and M. Margarida Oliveira. 2005. 'Transgenic Plants in Phytoremediation: Recent Advances and New Possibilities'. *Environmental Science & Technology* 39 (24): 9377–90. https://doi.org/10.1021/es051134l.

Cho, Misuk, Agnes N. Chardonnens, and Karl-Josef Dietz. 2003. 'Differential Heavy Metal Tolerance of Arabidopsis Halleri and Arabidopsis Thaliana: A Leaf Slice Test'. *New Phytologist* 158 (2): 287–93. https://doi.org/10.1046/j.1469-8137.2003.00746.x.

Chu, Heng-Hsuan, Jeff Chiecko, Tracy Punshon, Antonio Lanzirotti, Brett Lahner, David E. Salt, and Elsbeth L. Walker. 2010. 'Successful Reproduction Requires the Function of Arabidopsis Yellow Stripe-Like1 and Yellow Stripe-Like3 Metal-Nicotianamine Transporters in Both Vegetative and Reproductive Structures'. *Plant Physiology* 154 (1): 197–210. https://doi.org/10.1104/pp.110.159103.

Clough, S. J., and A. F. Bent. 1998. 'Floral Dip: A Simplified Method for Agrobacterium-Mediated Transformation of Arabidopsis Thaliana'. *The Plant Journal: For Cell and Molecular Biology* 16 (6): 735–43.

Cosio, Claudia, Enrico Martinoia, and Catherine Keller. 2004. 'Hyperaccumulation of Cadmium and Zinc in Thlaspi Caerulescens and Arabidopsis Halleri at the Leaf Cellular Level'. *Plant Physiology* 134 (2): 716–25. https://doi.org/10.1104/pp.103.031948.

Das, Keya Rani, and A. H. M. Rahmatullah Imon. 2016. 'A Brief Review of Tests for Normality'. *American Journal of Theoretical and Applied Statistics* 5 (1): 5. https://doi.org/10.11648/j.ajtas.20160501.12.

Davila Olivas, Nelson H., Enric Frago, Manus P. M. Thoen, Karen J. Kloth, Frank F. M. Becker, Joop J. A. van Loon, Gerrit Gort, Joost J. B. Keurentjes, Joost van Heerwaarden, and Marcel Dicke. 2017. 'Natural Variation in Life History Strategy of Arabidopsis Thaliana Determines Stress Responses to Drought and Insects of Different Feeding Guilds'. *Molecular Ecology* 26 (11): 2959–77. https://doi.org/10.1111/mec.14100.

Delhaize, E. 1996. 'A Metal-Accumulator Mutant of Arabidopsis Thaliana.' *Plant Physiology* 111 (3): 849–55.

El-Lithy, Mohamed E., Leónie Bentsink, Corrie J. Hanhart, Gerda J. Ruys, Daniela Rovito, José L. M. Broekhof, Hein J. A. van der Poel, Michiel J. T. van Eijk, Dick Vreugdenhil, and Maarten Koornneef. 2006. 'New Arabidopsis Recombinant Inbred Line Populations Genotyped Using SNPWave and Their Use for Mapping Flowering-Time Quantitative Trait Loci'. *Genetics* 172 (3): 1867–76. https://doi.org/10.1534/genetics.105.050617.

Fischer, Sina, Thomas Spielau, and Stephan Clemens. 2017. 'Natural Variation in Arabidopsis Thaliana Cd Responses and the Detection of Quantitative Trait Loci Affecting Cd Tolerance'. *Scientific Reports* 7 (1): 3693. https://doi.org/10.1038/s41598-017-03540-z.

Gendre, Delphine, Pierre Czernic, Geneviève Conéjéro, Katia Pianelli, Jean-François Briat, Michel Lebrun, and Stéphane Mari. 2007. 'TcYSL3, a Member of the YSL Gene Family from the Hyper-Accumulator Thlaspi Caerulescens, Encodes a Nicotianamine-Ni/Fe Transporter'. *The Plant Journal: For Cell and Molecular Biology* 49 (1): 1–15. https://doi.org/10.1111/j.1365-313X.2006.02937.x.

Giovannetti, Marco, Anna Małolepszy, Christian Göschl, and Wolfgang Busch. 2017. 'Large-Scale Phenotyping of Root Traits in the Model Legume Lotus Japonicus'. *Methods in Molecular Biology (Clifton, N.J.)* 1610: 155–67. https://doi.org/10.1007/978-1-4939-7003-2_11.

Hase, Yoshihiro, Masachika Okamura, Daigaku Takeshita, Issay Narumi, and Atsushi Tanaka. 2010. 'Efficient Induction of Flower-Color Mutants by Ion Beam Irradiation in Petunia Seedlings

Treated with High Sucrose Concentration'. *Plant Biotechnology* 27 (1): 99–103. https://doi.org/10.5511/plantbiotechnology.27.99.

Hirschi, K. D. 1999. 'Expression of Arabidopsis CAX1 in Tobacco: Altered Calcium Homeostasis and Increased Stress Sensitivity'. *The Plant Cell* 11 (11): 2113–22.

Ingle, Robert A., Sam T. Mugford, Jonathan D. Rees, Malcolm M. Campbell, and J. Andrew C. Smith. 2005. 'Constitutively High Expression of the Histidine Biosynthetic Pathway Contributes to Nickel Tolerance in Hyperaccumulator Plants'. *The Plant Cell* 17 (7): 2089–2106. https://doi.org/10.1105/tpc.104.030577.

Iriti, M., M. Sironi, S. Gomarasca, A. P. Casazza, C. Soave, and F. Faoro. 2006. 'Cell Death-Mediated Antiviral Effect of Chitosan in Tobacco'. *Plant Physiology and Biochemistry: PPB* 44 (11–12): 893–900. https://doi.org/10.1016/j.plaphy.2006.10.009.

Jaffré, Tanguy. 1996. 'Etude comparative des formations végétales et des flores des roches ultramafiques de Nouvelle-Calédonie et d'autres régions tropicales du monde'. In *Phytogéographie tropicale : réalités et perspectives*, edited by Jean-Louis Guillaumet, M. Belin, and H. Puig, 137–49. Colloques et Séminaires. Paris: ORSTOM. http://www.documentation.ird.fr/hor/fdi:010009688.

Kim, Sung, Vincent Plagnol, Tina T. Hu, Christopher Toomajian, Richard M. Clark, Stephan Ossowski, Joseph R. Ecker, Detlef Weigel, and Magnus Nordborg. 2007. 'Recombination and Linkage Disequilibrium in Arabidopsis Thaliana'. *Nature Genetics* 39 (9): 1151–55. https://doi.org/10.1038/ng2115.

Kim, Suyeon, Michiko Takahashi, Kyoko Higuchi, Kyoko Tsunoda, Hiromi Nakanishi, Etsuro Yoshimura, Satoshi Mori, and Naoko K. Nishizawa. 2005. 'Increased Nicotianamine Biosynthesis Confers Enhanced Tolerance of High Levels of Metals, in Particular Nickel, to Plants'. *Plant & Cell Physiology* 46 (11): 1809–18. https://doi.org/10.1093/pcp/pci196.

Korte, Arthur, and Ashley Farlow. 2013. 'The Advantages and Limitations of Trait Analysis with GWAS: A Review'. *Plant Methods* 9 (July): 29. https://doi.org/10.1186/1746-4811-9-29.

Kruijer, Willem, Martin P. Boer, Marcos Malosetti, Pádraic J. Flood, Bas Engel, Rik Kooke, Joost J. B. Keurentjes, and Fred A. van Eeuwijk. 2015. 'Marker-Based Estimation of Heritability in Immortal Populations'. *Genetics* 199 (2): 379–98. https://doi.org/10.1534/genetics.114.167916.

Kukier, Urszula, Carinne A. Peters, Rufus L. Chaney, J. Scott Angle, and Richard J. Roseberg. 2004. 'The Effect of PH on Metal Accumulation in Two Alyssum Species'. *Journal of Environmental Quality* 33 (6): 2090–2102.

Lamy, Philippe, Claus L. Andersen, Friedrik P. Wikman, and Carsten Wiuf. 2006. 'Genotyping and Annotation of Affymetrix SNP Arrays'. *Nucleic Acids Research* 34 (14): e100. https://doi.org/10.1093/nar/gkl475.

L'Huillier, L., and S. Edighoffer. 1996. 'Extractability of Nickel and Its Concentration in Cultivated Plants in Ni Rich Ultramafic Soils of New Caledonia'. *Plant and Soil* 186 (2): 255–64. https://doi.org/10.1007/BF02415521.

Li, Yan, Yu Huang, Joy Bergelson, Magnus Nordborg, and Justin O. Borevitz. 2010. 'Association Mapping of Local Climate-Sensitive Quantitative Trait Loci in Arabidopsis Thaliana'. *Proceedings of the National Academy of Sciences of the United States of America* 107 (49): 21199–204. https://doi.org/10.1073/pnas.1007431107.

Liu, Xiao-Min, Jonguk An, Hay Ju Han, Sun Ho Kim, Chae Oh Lim, Dae-Jin Yun, and Woo Sik Chung. 2014. 'ZAT11, a Zinc Finger Transcription Factor, Is a Negative Regulator of Nickel Ion Tolerance in Arabidopsis'. *Plant Cell Reports* 33 (12): 2015–21. https://doi.org/10.1007/s00299-014-1675-7.

Liu, Xiao-Min, Hay Ju Han, Kyung Eun Kim, Hyeong Cheol Park, Jong Chan Hong, Dae-Jin Yun, and Woo Sik Chung. 2012. 'WITHDRAWN: Overexpression of a C2H2-Type Zinc Finger Protein Gene, ZAT11, Leads to Enhanced Primary Root Growth and Increased Nickel Ion Sensitivity in Arabidopsis'. *Biochemical and Biophysical Research Communications*, December. https://doi.org/10.1016/j.bbrc.2012.11.115.

Marschner, Horst. 1995. *Mineral Nutrition of Higher Plants*. https://www.elsevier.com/books/mineral-nutrition-of-higher-plants/marschner/978-0-12-473542-2.

Mei, Hui, Jian Zhao, Jon K. Pittman, Jinesh Lachmansingh, Sunghun Park, and Kendal D. Hirschi. 2007. 'In Planta Regulation of the Arabidopsis Ca2+/H+ Antiporter CAX1'. *Journal of Experimental Botany* 58 (12): 3419–27. https://doi.org/10.1093/jxb/erm190.

Meyerowitz, Elliot M. 2001. 'Prehistory and History of Arabidopsis Research'. *Plant Physiology* 125 (1): 15–19. https://doi.org/10.1104/pp.125.1.15.

Mizuno, Takafumi, Koji Usui, Kenji Horie, Shiro Nosaka, Naoharu Mizuno, and Hitoshi Obata. 2005. 'Cloning of Three ZIP/Nramp Transporter Genes from a Ni Hyperaccumulator Plant Thlaspi Japonicum and Their Ni2+-Transport Abilities'. *Plant Physiology and Biochemistry* 43 (8): 793–801. https://doi.org/10.1016/j.plaphy.2005.07.006.

Mohseni, Roshanak, Seyed Majid Ghaderian, and Henk Schat. 2018. 'Nickel Uptake Mechanisms in Two Iranian Nickel Hyperaccumulators, Odontarrhena Bracteata and Odontarrhena Inflata'. *Plant and Soil* 434: 263–69. https://doi.org/10.1007/s11104-018-3814-3.

Murashige, Toshio, and Folke Skoog. 1962. 'A Revised Medium for Rapid Growth and Bio Assays with Tobacco Tissue Cultures'. *Physiologia Plantarum* 15 (3): 473–97. https://doi.org/10.1111/j.1399-3054.1962.tb08052.x.

Nishida, Sho, Chisato Tsuzuki, Aki Kato, Ayaka Aisu, Junko Yoshida, and Takafumi Mizuno. 2011. 'AtIRT1, the Primary Iron Uptake Transporter in the Root, Mediates Excess Nickel Accumulation in Arabidopsis Thaliana'. *Plant & Cell Physiology* 52 (8): 1433–42. https://doi.org/10.1093/pcp/pcr089.

Nziguheba, Generose, and Erik Smolders. 2008. 'Inputs of Trace Elements in Agricultural Soils via Phosphate Fertilizers in European Countries'. *The Science of the Total Environment* 390 (1): 53–57. https://doi.org/10.1016/j.scitotenv.2007.09.031.

O'Malley, Ronan C., Cesar C. Barragan, and Joseph R. Ecker. 2015. 'A User's Guide to the Arabidopsis T-DNA Insertional Mutant Collections'. *Methods in Molecular Biology (Clifton, N.J.)* 1284: 323–42. https://doi.org/10.1007/978-1-4939-2444-8_16.

Omega.chemwatch.net. 2015. *Chemwatch*. http://omega.chemwatch.net/chemwatch.web/dashboard.

Piñeros, M., and M. Tester. 1997. 'Characterization of the High-Affinity Verapamil Binding Site in a Plant Plasma Membrane Ca2+-Selective Channel'. *The Journal of Membrane Biology* 157 (2): 139–45.

Platt, Alexander, Matthew Horton, Yu S. Huang, Yan Li, Alison E. Anastasio, Ni Wayan Mulyati, Jon Ågren, et al. 2010. 'The Scale of Population Structure in Arabidopsis Thaliana'. *PLOS Genetics* 6 (2): e1000843. https://doi.org/10.1371/journal.pgen.1000843.

Pottier, Mathieu, Ronald Oomen, Cristiana Picco, Jérôme Giraudat, Joachim Scholz-Starke, Pierre Richaud, Armando Carpaneto, and Sébastien Thomine. 2015. 'Identification of Mutations Allowing Natural Resistance Associated Macrophage Proteins (NRAMP) to Discriminate against Cadmium'. *The Plant Journal: For Cell and Molecular Biology* 83 (4): 625–37. https://doi.org/10.1111/tpj.12914.

Purcell, Shaun, Benjamin Neale, Kathe Todd-Brown, Lori Thomas, Manuel A. R. Ferreira, David Bender, Julian Maller, et al. 2007. 'PLINK: A Tool Set for Whole-Genome Association and Population-Based Linkage Analyses'. *American Journal of Human Genetics* 81 (3): 559–75. https://doi.org/10.1086/519795.

Rees, Jonathan D., Robert A. Ingle, and J. Andrew C. Smith. 2009. 'Relative Contributions of Nine Genes in the Pathway of Histidine Biosynthesis to the Control of Free Histidine Concentrations in Arabidopsis Thaliana'. *Plant Biotechnology Journal* 7 (6): 499–511. https://doi.org/10.1111/j.1467-7652.2009.00419.x.

Remans, Tony, Sofie Thijs, Sascha Truyens, Nele Weyens, Kerim Schellingen, Els Keunen, Heidi Gielen, Ann Cuypers, and Jaco Vangronsveld. 2012. 'Understanding the Development of Roots Exposed to Contaminants and the Potential of Plant-Associated Bacteria for Optimization of Growth'. *Annals of Botany* 110 (2): 239–52. https://doi.org/10.1093/aob/mcs105.

Sachan, Priti, and Nand Lal. 2017. 'Nickel Essentiality and Toxicity in Plants'. *Indian Farmer*. http://www.academia.edu/34301732/Nickel_Essentiality_and_Toxicity_in_Plants.

Sağlam, Coşkun. 2017. 'Heavy Metal Concentrations in Serpentine Soils and Plants from Kizildag National Park (Isparta) in Turkey'. *Fresenius Environmental Bulletin 26(6):3995-4003*. https://www.researchgate.net/publication/319528236_HEAVY_METAL_CONCENTRATIONS_IN_SERPENTINE_SOILS_AND_PLANTS_FROM_KIZILDAG_NATIONAL_PARK_ISPARTA_IN_TURKEY.

Sakai, Tatsuya, Susumu Mochizuki, Ken Haga, Yukiko Uehara, Akane Suzuki, Akiko Harada, Takuji Wada, Sumie Ishiguro, and Kiyotaka Okada. 2012. 'The Wavy Growth 3 E3 Ligase Family Controls the Gravitropic Response in Arabidopsis Roots'. *The Plant Journal: For Cell and Molecular Biology* 70 (2): 303–14. https://doi.org/10.1111/j.1365-313X.2011.04870.x.

Satbhai, Santosh B., Christian Göschl, and Wolfgang Busch. 2017. 'Automated High-Throughput Root Phenotyping of Arabidopsis Thaliana Under Nutrient Deficiency Conditions'. *Methods in Molecular Biology (Clifton, N.J.)* 1610: 135–53. https://doi.org/10.1007/978-1-4939-7003-2_10.

Schaaf, Gabriel, Annegret Honsbein, Anderson R. Meda, Silvia Kirchner, Daniel Wipf, and Nicolaus von Wirén. 2006. 'AtIREG2 Encodes a Tonoplast Transport Protein Involved in Iron-Dependent Nickel Detoxification in Arabidopsis Thaliana Roots'. *The Journal of Biological Chemistry* 281 (35): 25532–40. https://doi.org/10.1074/jbc.M601062200.

Schat, and W. M. Ten Bookum. 1992. 'Genetic Control of Copper Tolerance in *Silene Vulgaris*'. *Heredity* 68 (3): 219–29. https://doi.org/10.1038/hdy.1992.35.

Schat, Henk, Riet Vooijs, and Eric Kuiper. 1996. 'Identical Major Gene Loci for Heavy Metal Tolerances That Have Independently Evolved in Different Local Populations and Subspecies of Silene Vulgaris.' *Evolution; International Journal of Organic Evolution* 50 (5): 1888–95. https://doi.org/10.1111/j.1558-5646.1996.tb03576.x.

Schneeberger, Korbinian, Stephan Ossowski, Christa Lanz, Trine Juul, Annabeth Høgh Petersen, Kåre Lehmann Nielsen, Jan-Elo Jørgensen, Detlef Weigel, and Stig Uggerhø Andersen. 2009.

'SHOREmap: Simultaneous Mapping and Mutation Identification by Deep Sequencing'. *Nature Methods* 6 (8): 550–51. https://doi.org/10.1038/nmeth0809-550.

Serino, Giovanna, and Davide Marzi. 2018. '*Arabidopsis Thaliana* as an Experimental Organism'. In *ELS*, edited by John Wiley & Sons Ltd, 1–9. Chichester, UK: John Wiley & Sons, Ltd. https://doi.org/10.1002/9780470015902.a0002031.pub3.

Singh, Pooja, Samir Sharma, and Vivek Prasad. 2011. 'Verapamil, a Calcium Channel Blocker, Induces Systemic Antiviral Resistance in Susceptible Plants: Verapamil-Induced Systemic Antiviral Resistance in Plants'. *Journal of Phytopathology* 159 (2): 127–29. https://doi.org/10.1111/j.1439-0434.2010.01738.x.

Slovak, Radka, Christian Göschl, Xiaoxue Su, Koji Shimotani, Takashi Shiina, and Wolfgang Busch. 2014. 'A Scalable Open-Source Pipeline for Large-Scale Root Phenotyping of Arabidopsis'. *The Plant Cell* 26 (6): 2390–2403. https://doi.org/10.1105/tpc.114.124032.

Spedding, M., and R. Paoletti. 1992. 'Classification of Calcium Channels and the Sites of Action of Drugs Modifying Channel Function'. *Pharmacological Reviews* 44 (3): 363–76.

'Stainless Steel - General Information - Alloying Elements in Stainless Steel'. n.d. Accessed 17 February 2019. http://www.aalco.co.uk/datasheets/Stainless-Steel_Alloying-Elements-in-Stainless-Steel_98.ashx.

The International HapMap Consortium, David Altshuler, and Peter Donnelly. 2005. 'A Haplotype Map of the Human Genome'. *Nature* 437 (7063): 1299–1320. https://doi.org/10.1038/nature04226.

Visioli, Giovanna, Mariolina Gullì, and Nelson Marmiroli. 2014. 'Noccaea Caerulescens Populations Adapted to Grow in Metalliferous and Non-Metalliferous Soils: Ni Tolerance, Accumulation and Expression Analysis of Genes Involved in Metal Homeostasis'. *Environmental and Experimental Botany* 105 (September): 10–17. https://doi.org/10.1016/j.envexpbot.2014.04.001.

Weng, Liping, Theo M. Lexmond, Anke Wolthoorn, Erwin J. M. Temminghoff, and Willem H. van Riemsdijk. 2003. 'Phytotoxicity and Bioavailability of Nickel: Chemical Speciation and Bioaccumulation'. *Environmental Toxicology and Chemistry* 22 (9): 2180–87. https://doi.org/10.1897/02-116.

White, Philip J., and Martin R. Broadley. 2003. 'Calcium in Plants'. *Annals of Botany* 92 (4): 487–511. https://doi.org/10.1093/aob/mcg164.

Yi, Hankuil, and Eric J Richards. 2008. 'Phenotypic Instability of Arabidopsis Alleles Affecting a Disease Resistance Gene Cluster'. *BMC Plant Biology* 8 (April): 36. https://doi.org/10.1186/1471-2229-8-36.

Yu, Qilin, Chenpeng Xiao, Kailun Zhang, Chang Jia, Xiaohui Ding, Bing Zhang, Yu Wang, and Mingchun Li. 2014. 'The Calcium Channel Blocker Verapamil Inhibits Oxidative Stress Response in Candida Albicans'. *Mycopathologia* 177 (3–4): 167–77. https://doi.org/10.1007/s11046-014-9735-7.

Yusuf, M., Q. Fariduddin, S. Hayat, and A. Ahmad. 2011. 'Nickel: An Overview of Uptake, Essentiality and Toxicity in Plants'. *Bulletin of Environmental Contamination and Toxicology* 86 (1): 1–17. https://doi.org/10.1007/s00128-010-0171-1.

Zhou, J., and P. B. Goldsbrough. 1995. 'Structure, Organization and Expression of the Metallothionein Gene Family in Arabidopsis'. *Molecular & General Genetics: MGG* 248 (3): 318–28.

Zhou, Xiang, and Matthew Stephens. 2012. 'Genome-Wide Efficient Mixed-Model Analysis for Association Studies'. *Nature Genetics* 44 (7): 821–24. https://doi.org/10.1038/ng.2310.

Zientara, Katarzyna, Anna Wawrzyńska, Jolanta Lukomska, José Rafael López-Moya, Frantz Liszewska, Ana G. L. Assunção, Mark G. M. Aarts, and Agnieszka Sirko. 2009. 'Activity of the AtMRP3 Promoter in Transgenic Arabidopsis Thaliana and Nicotiana Tabacum Plants Is Increased by Cadmium, Nickel, Arsenic, Cobalt and Lead but Not by Zinc and Iron'. *Journal of Biotechnology* 139 (3): 258–63. https://doi.org/10.1016/j.jbiotec.2008.12.001.

Zimeri, Anne Marie, Om Parkash Dhankher, Bonnie McCaig, and Richard B. Meagher. 2005. 'The Plant MT1 Metallothioneins Are Stabilized by Binding Cadmiums and Are Required for Cadmium Tolerance and Accumulation'. *Plant Molecular Biology* 58 (6): 839–55. https://doi.org/10.1007/s11103-005-8268-3.

9. Appendix

- *Supplemental Data*

***Data 1**: Calculation to prepare the $NiSO_4.6H_2O$ stock solution*

- Molecular weight ($NiSO_4.6H_2O$) = 262g/mol =1M= 262g/L
- Stock solution required: 100mM Ni
- Final volume: 50ml

Calculation:

- For 1mM of $NiSO_4.6H_2O$ (1000 times less): 0.262g/L
- For 100mM of $NiSO_4.6H_2O$ (x100) : 100 x 0.262g/L = 26.2g/L = 26.2g/1000ml
- For a volume of 10ml (%100) : 0.262g/10ml
- For a volume of 50ml (x5): 13.1g/50ml

$NiSO_4.6H_2O$ weight = 13.1g into 50ml

I added 13.1g of $NiSO_4.6H_2O$ (powder) into 50ml demi water in order to obtain 100mM Ni stock solution

***Data 2**: Volume taken from the 100mM stock solution $NiSO_4.6H_2O$ and added in the nutrient solution for calculation of the EC50. Example of a calculation for a final concentration of 16* µM Ni and a final volume of 1L from a stock solution of 100mM Ni

Ni concentration (µM)	0	16	32	64	128	256
Volume Ni (µl)	0	160	320	640	1280	2560

- Stock concentration (C1): 100mM
- Volume to take (V1): ?
- Final concentration (C2): 16 µM
- Final volume (V2): 1 L

C1 x V1 = C2 x V2 100mM x V1 = 16 µM x 1L

V1= (16 µM x 1L)/ 100mM = (16 µM x $1x10^3$ ml) / ($100x10^3$) = 0.16ml = 160 µl

***Data 3**: Calculation for the volume of $NiSO_4.6H_2O$ to add in the nutrient solution*

- Stock concentration (C1): 100mM
- Volume to take (V1): ?
- Final concentration (C2): 44 µM
- Final volume (V2): 10 L

C1 x V1 = C2 x V2 100mM x V1 = 44 µM x 10L

V1= (44 µM x 10L)/ 100mM = (44 µM x $10x10^3$ ml) / ($100x10^3$) = 4.4 ml

I added 4.4 ml of stock solution of 100mM of $NiSO_4.6H_2O$ into 10L half strength Hoagland solution.

Supplemental Figures

```
#Gwas_settings.R
#1) SPECIFY DATA-FOLDER AND SCRIPT FOLDER

data.path      <- "D:/GWAS_Biometris/data_files/"  #
script.path    <- "D:/GWAS_Biometris/script_folder/"

# 2) CHOOSE THE DATA

r.image.name     <- "LFN350acc_000_new_gene_annotation_ibd_kinship.RData"
add.phenotypic.data <- T
csv.file.name   <-  'Phenotype_random.csv'
which.columns.as.factor <- integer(0)#c(2,4,5) #integer(0)
trait.numbers   <- 5:5
covariables        <- F
cov.cols          <- 8

# 3) Choose a threshold for the selection of candidate loci (BT= bound type)

BT     <- 1
alpha   <- 0.10
LOD.thr <- 4
K      <- 4

# 4) TASKS TO BE PERFORMED, AND OUTPUT OPTIONS

suffix  <- "_withinR"
reml.algo     <- "emma"
GLS.method <- 3
MAF          <- 0.05
size.of.included.region <- 0 # N.B. the region will be size.of.included.region on BOTH sides !
min.r2 <- 0.5   # If size.of.included.region is larger than zero,
extra.output.file <- F
kinship.type    <- 1
alternative.kinship.name <- "drops_identity.csv"
h2.fixed    <- F
jpeg.only         <- F
genomic.control <- F
```

Figure S1*: Script to perform a GWAS on R studio with 215.000 SNPs made by Dr. Willem Kruijer*

```
/GEMMA$ gemma –bfile INPUT –k INPUT .kinship.cXX.txt –lmm 1 –maf 0.05 –o INPUT
```

Figure S2*: Script to run a GWAS on GEMMA with the imputed data set (1 million SNPs), correction with the kinship, with a linear mixed model and with a minimum allele frequency (MAF) of 0.05%.*

```
D:/>cd LD/data_files/

D:\LD\data_files>plink --bfile LFN350 --r2 --ld-snp m66557 --ld-window-kb 99 --ld-window 9999 --ld-window-r2 0
```

***Figure S3**: Script to display the LD region (with r^2 as a measurement of the LD) for a specific SNPs).*

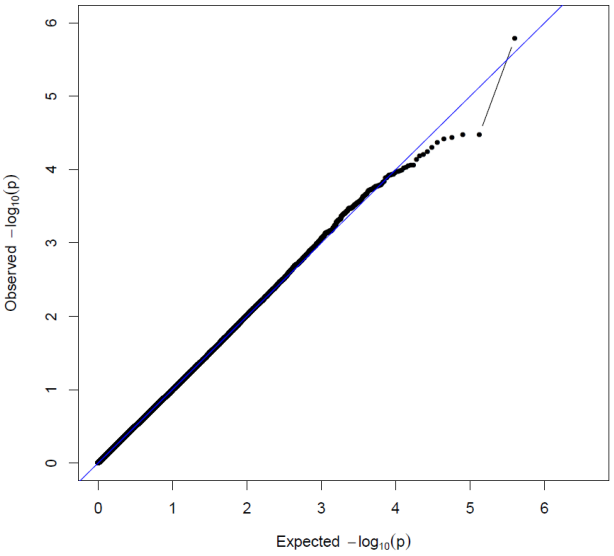

***Figure S4**: QQplot of the relative change in root growth obtained with R studio showing a normal symmetric distribution with some outliers.*

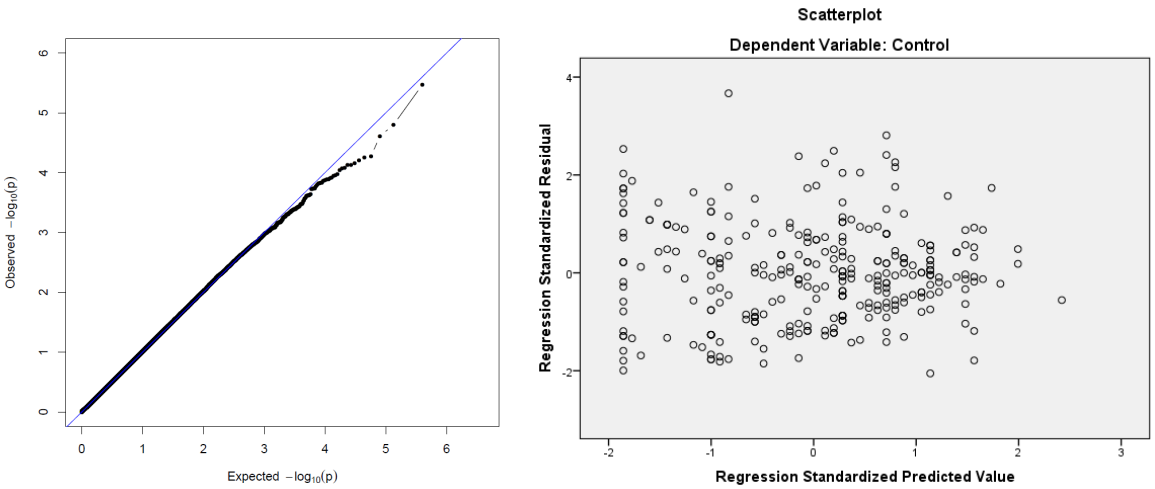

***Figure S5**: (A) QQplot of the residuals obtained with R studio displaying a normal symmetric distribution. (B) Scatterplot for testing homogeneity of error variance distribution obtained with SPSS displaying that 0 is the center of the trend and, therefore, the linearity assumption is accepted.*

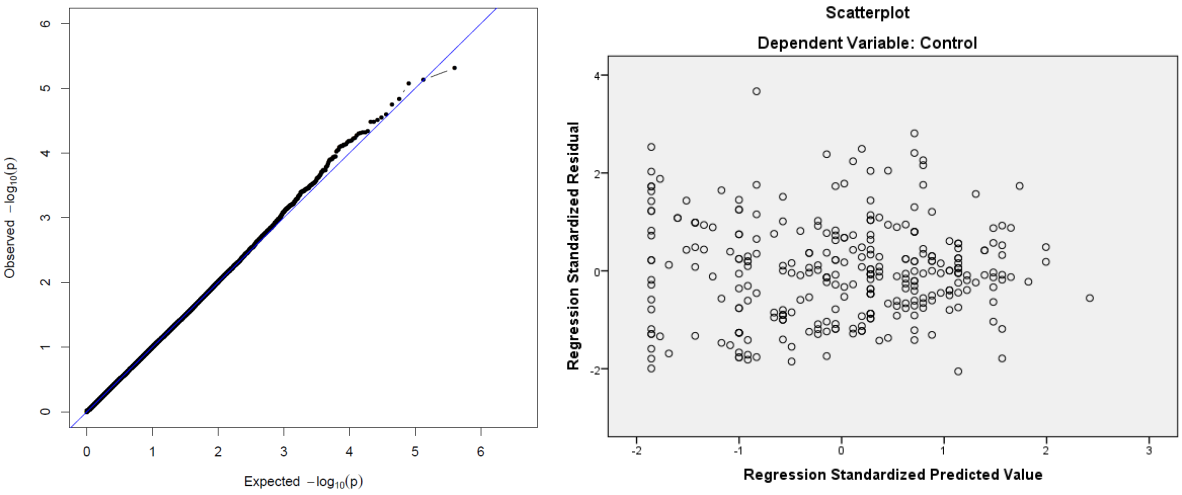

***Figure S6**: (A) QQplot of the residuals obtained with R studio displaying a normal symmetric distribution. (B) Scatterplot for testing homogeneity of error variance distribution obtained with SPSS displaying that 0 is the center of the trend and, therefore, the linearity assumption is accepted.*

A/ Genotype	Total root length (mm)	Groups
Col0b	37.07605	a
Col0c	34.96977	ab
C24	34.50524	ab
St0	26.11021	abc
Cvi0	22.52847	abc
Ler1	18.68036	bc
Be1	11.14241	c

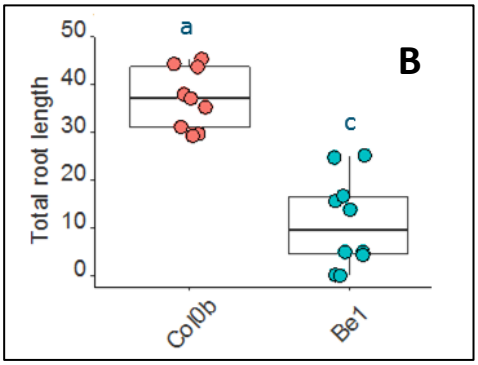

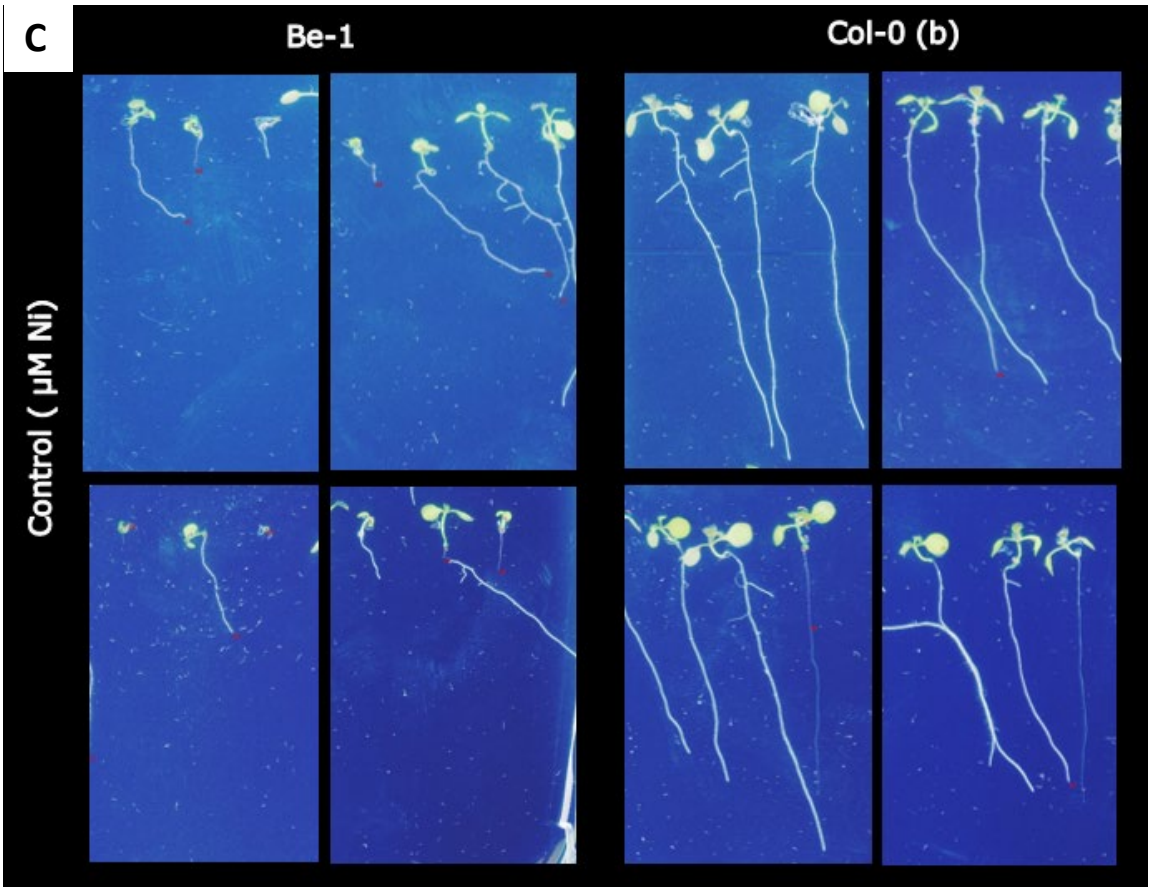

***Figure S7**: Root length analysis of A. thaliana plants (10 days old) grown on agar plate with 20 µM Ni (A) Total root length measurement determined by BRAT V1 for each genotype and their significant differences calculated with the post-hoc test Bonferroni (α=0.05 Boxplot (B) representing means and standard error for root length calculated per genotype obtained with R studio. Each scan photo (C), after segmentation by BRAT1, display three plants from the same genotype (Be-1 or Col-0) on an agar plate.*

A/ Genotype	Total root length (mm)	Groups
C24	8.561076	a
Col0c	6.405260	ab
Col0b	6.311648	ab
St0	5.554912	ab
Ler1	4.615112	b
Cvi0	4.599557	b
Be1	3.918819	b

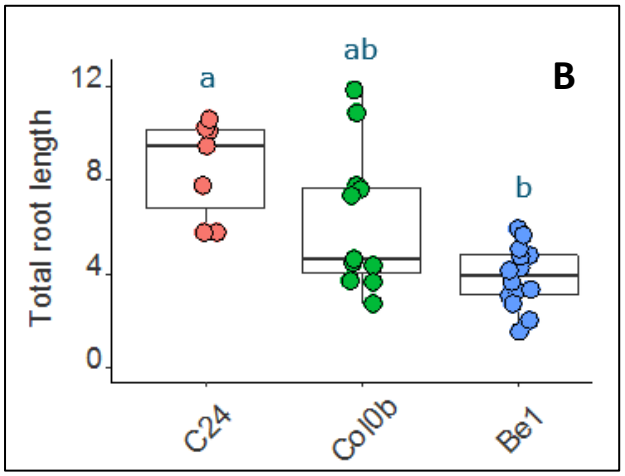

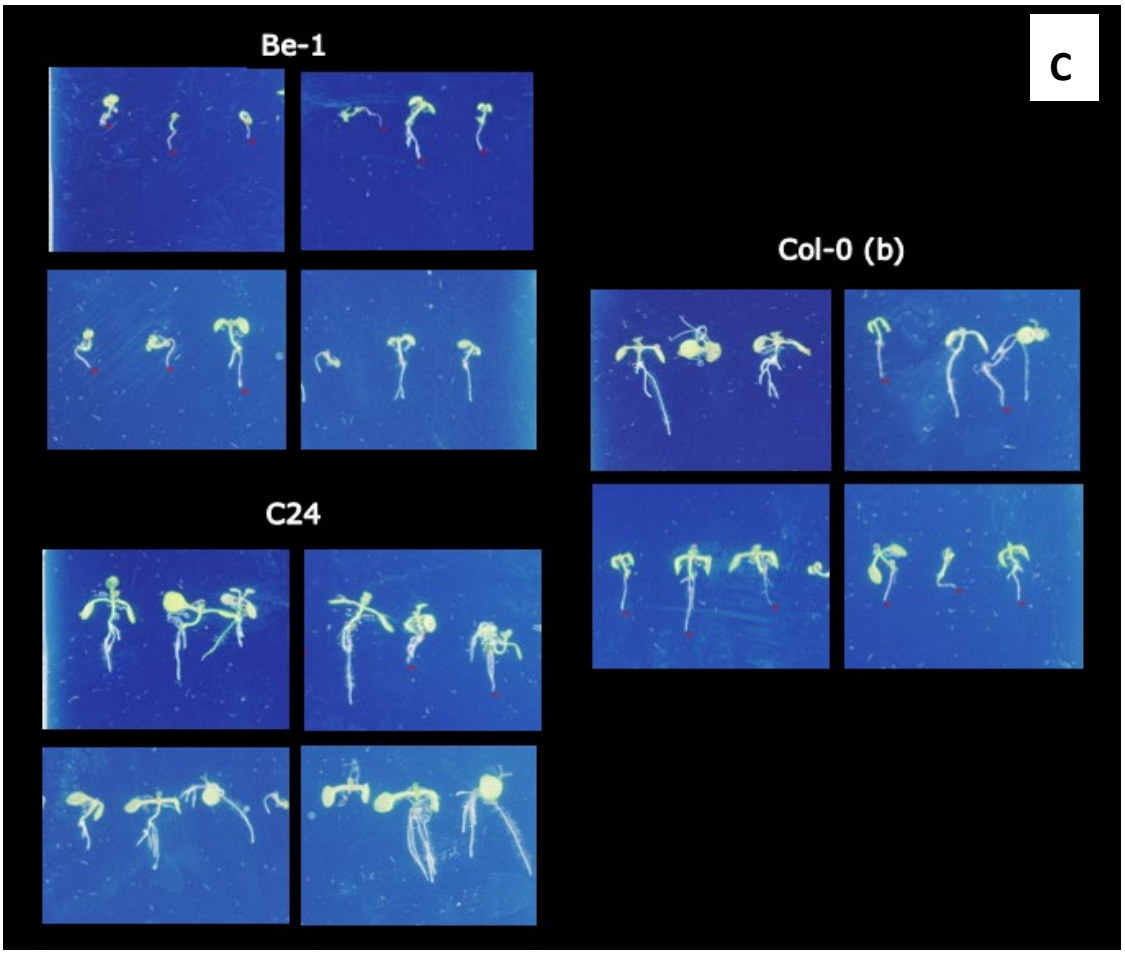

Figure S8: *Root length analysis of A. thaliana plants (10 days old) grown on 80 µM Ni on agar plate. (A) Total root length measurement determined by BRAT V1 for each genotype and their significant differences calculated with the post-hoc test Bonferroni (α=0.05). (B) Boxplot representing means and standard error for root length calculated per genotype obtained with R studio. (C) Each scan photo, after segmentation by BRAT1, display three plants from the same genotype (Be-1 or Col-0 or C24) on an agar plate.*

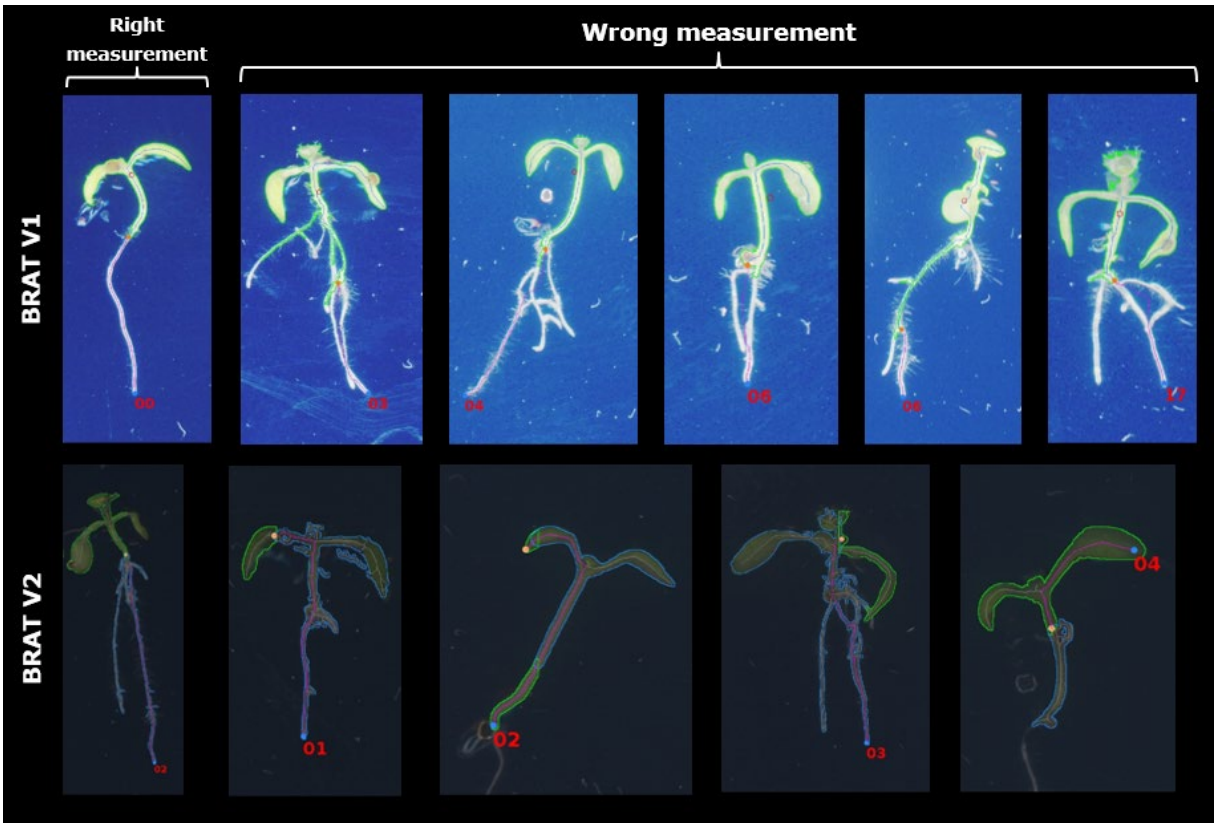

***Figure S9**:* Comparison *of between wrong and right root measurement for BRAT V1 and BRAT V2.*

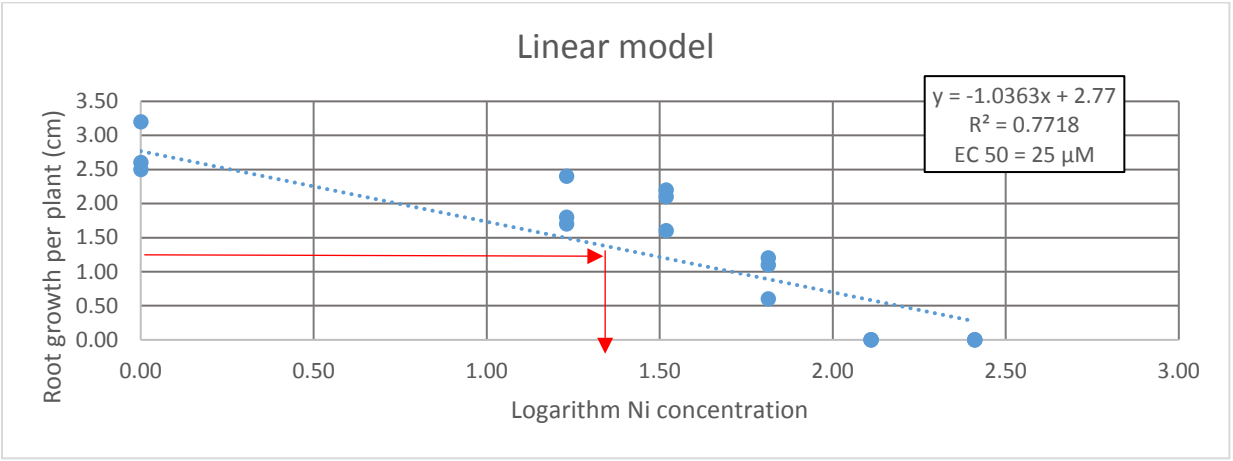

Figure S10: *Graphic displaying the data distribution of root growth in the function of the logarithm Ni concentration with a linear model. A. thaliana plants (17 days old) were grown in hydroponic condition and root growth was measured manually 4 days after dipping roots into active charcoal., A determined Ni concentration was applied for each treatment and this concentration was transformed with the logarithm function. Each data point represents the root growth measurement of one plant in one pot along different logarithm Ni concentration. With only three repeats per treatment, it was decided to set up the intercept (maximum root growth) of the equation at 2.77 which represents the average of*

the three root growth measurements in the control condition. The equation and R^2 were determined with Excel (2016) and the EC50 were calculated with the equation of the linear model.

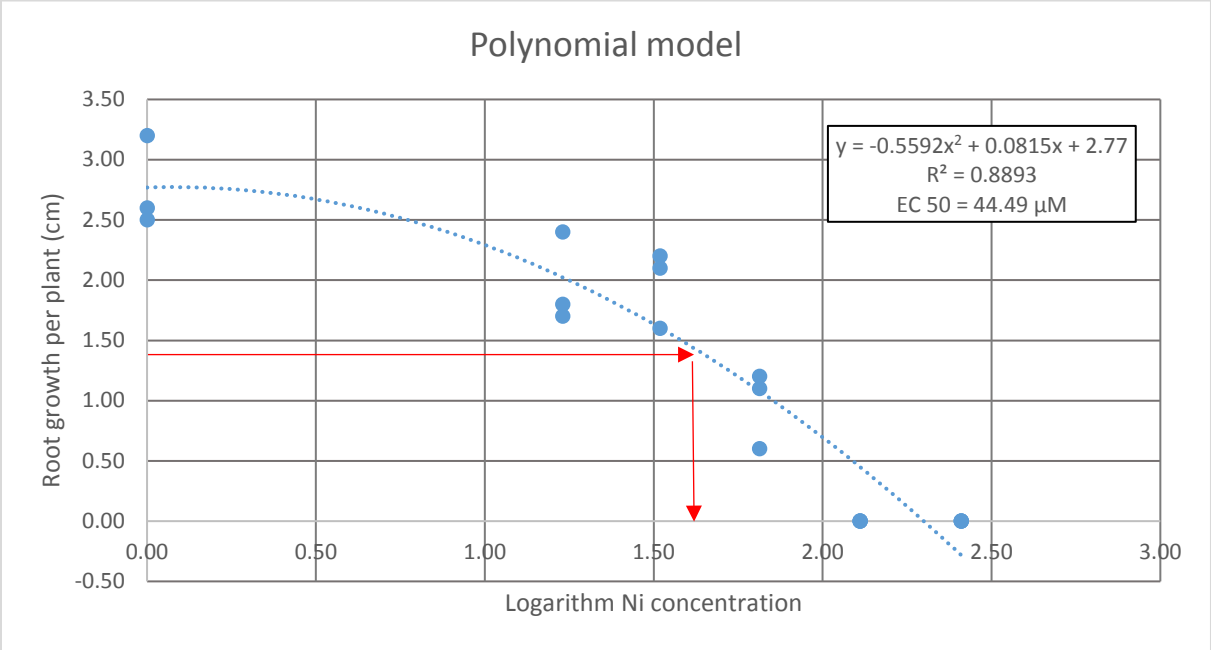

***Figure S11**: Graphic displaying the data distribution of root growth in the function of the logarithm Ni concentration with a polynomial model. A. thaliana plants (17 days old) were grown in hydroponic condition and root growth was measured manually 4 days after dipping roots into active charcoal., A determined Ni concentration was applied for each treatment and this concentration was transformed with the logarithm function. Each data point represents the root growth measurement of one plant in one pot along different logarithm Ni concentration. With only three repeats per treatment, it was decided to set up the intercept (maximum root growth) of the equation at 2.77 which represents the average of the three root growth measurements in the control condition. The equation and R^2 were determined with Excel (2016) and the EC50 were calculated with the equation of the polynomial model.*

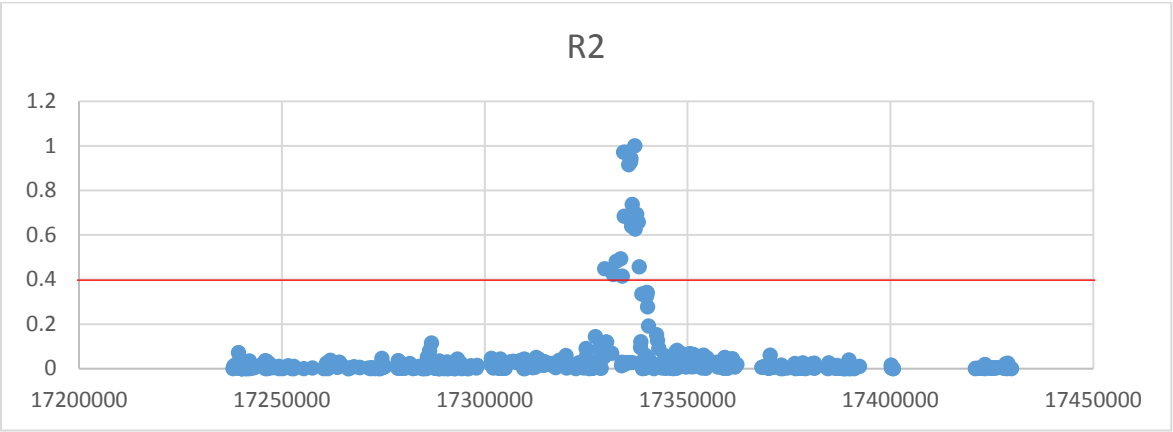

Figure S12: *Example of LD region checked for a SNP with a graphic of r^2 values with the 215.000 SNPs set. The red line represents an arbitrary threshold (=0.4) for the LD. All SNPs located upper this threshold are considered to be in the LD region with the selected SNP.*

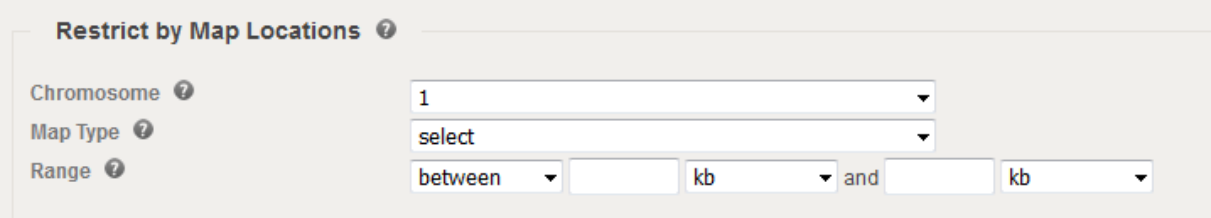

Figure S13*: Screenshot from the website TAIR Gene Search where it is possible to get the list of all genes located at a specific locus (https://www.arabidopsis.org/servlets/Search/).*

Supplemental Tables

Table S1*: Different component and parameter used to produce the Hyponex solution given by Mr Geurt Versteeg.*

EC	1,4				Hyponex - standard				
pH	5,8								
NH4	1,70	mmol							
K	4,13								
				pH is set with: Kali lye					
Na							Acide sulfurique		
Ca	1,97		**with**	**Liquid fertilizers per 100 liters**					
				42.1 ml Calsal					
Mg	1,24			21.3 ml Amnitra					
				52.24 ml sulfacal					
NO3	4,14			15.1 ml fosforzuur 59%					
				36.8 ml bascal					
Cl				57.58 ml magnesul					
			with	**Liquid fertilizers per 100 liters**					
SO4	3,14			47.2 gram Ca(NO3)2.H2O				mm	236,15 gr.
				3.2 gram NH4NO3				mm	80,04 gr.
HCO3				72.1 gram K2SO4				mm	174,27 gr.
				30.6 gram MgSO4.7H2O				mm	246,47 gr.
P	1,29			15 gram NH4H2PO4				mm	115,03 gr.
Si									
Fe	21	umol	Consists of 50% Fe-DTPA 3%						
Mn	3.4			50% Fe- EDDHSA 3%					
Zn	4.7								
B	14								
Cu	6.9								
Mo	0.5								

Table S2: *Statistical results for the germination rate obtained with a two-way ANOVA from R Studio.*

Tests of Between-Subjects Effects

Dependent Variable: % Germinationrate

Source	Type III Sum of Squares	df	Mean Square	F	Sig.
Corrected Model	15329.630[a]	24	638.735	13.016	.000
Intercept	612008.333	1	612008.333	12471.113	.000
Accession	12931.481	4	3232.870	65.877	.000
Treatment	283.333	4	70.833	1.443	.234
Accession * Treatment	2114.815	16	132.176	2.693	.004
Error	2453.704	50	49.074		
Total	629791.667	75			
Corrected Total	17783.333	74			

a. R Squared = .862 (Adjusted R Squared = .796)

***Table S3**: List of genes found for each significant SNPs (log> 4) for each selected QTLs and their characteristics without the genes in the LD region. Genes were detected with the SNPs position by the genome browser Salk Arabidopsis 1,001 Genomes (http://signal.salk.edu/atg1001/3.0/gebrowser.php). Information related to genes were determined with The Arabidopsis Information Resource (Tair) (https://www.arabidopsis.org/index.jsp), National Center for Biotechnology Information (NCBI) (https://www.ncbi.nlm.nih.gov/) and UniProt (https://www.uniprot.org/). Each color in the table represents a different QTL. There are two genes for one SNP position when the SNP was detected between these two genes.*

QTLs	Chromosome	Position	Log	Genes	Significant SNP or in LD region	Name of the gene	The function of the gene	Gene expression
QTL3	2	9649576	4.74	AT2G22690	Significant SNP			
	2			AT2G22680	Significant SNP	WAVH1	metal ion binding (zinc), ubiquitin-protein transferase activity, involved in root gravitropism (regulation of root growth)	Expressed in root tips and leaf primordia
	2			AT2G22670	LD region	IAA8	Aux/IAA proteins: short-lived transcriptional factors that function as repressors of early auxin response genes at low auxin concentrations	Highly expressed in the whole plant
	2	9629882	4.27	AT2G22660	Significant SNP	ATGRDP1, GLYCINE-RICH DOMAIN PROTEIN1	GRDP1 is involved in germination and response to ABA. Loss of function mutants have reduced germination in the presence of osmotic stressors.	

	2	9621504	4.04	AT2G22630	Significant SNP	AGAMOUS-LIKE 17, AGL17	Encodes a MADs domain containing protein involved in promoting flowering. Loss of function mutations show delayed flowering in long days and reduced levels of LFY and AP1 expression.	
	2			AT2G22610	LD region	KIN14R	Di-glucose binding protein with Kinesin motor domain-containing protein;(source:Araport11)	
	2			AT2G22620	LD region		Rhamnogalacturonate lyase family protein	
	2			AT2G22640	LD region	ATBRK1, BRICK1, BRK1, HSPC300	Component of the WAVE protein complex which act as activators of ARP2/3 complex involved in actin nucleation. Required for trichome morphogenesis. Required for accumulation of SCAR1 protein in vivo. Selectively stabilizes SCAR2.	Expressed in roots, root hairs, hypocotyls, cotyledons, stems, leaves, trichomes, and flowers.
	2			AT2G22650	LD region		FAD-dependent oxidoreductase family protein	
QTL4	3	11042876	4.79	AT3G29060	Significant SNP	PHO1-H9	EXS (ERD1/XPR1/SYG1) family protein phosphate ion transmembrane transporter activity	
				AT3G29050	Significant SNP	CRRSP14	receptor-like protein kinase-like protein	
	3	10986443	4.12	AT3G28960	Significant SNP			
	3	11280097	4.30	AT3G29375	Significant SNP		XH domain-containing protein	

				AT3G28970	LD region	AAR3, ANTIAUXIN-RESISTANT 3	Identified in a screen for mutants resistant to an anti-auxin. Encodes a protein with unknown function that shares homology with DCN protein family.	
				AT3G28980	LD region	AXX17_At3g28980	mediator of RNA polymerase II transcription subunit-like protein,	carpel, collective leaf structure, flower, flower pedicel, petal, plant embryo, pollen, pollen tube cell, sepal, stamen
				AT3G28990	LD region	AXX17_At3g28990	Acts as a Mg2+ transporter. Can also transport other divalent cations such as Fe2+, Sr2+, Ba2+, Mn2+ and Co2+ but to a much less extent than Mg2+	
				AT3G29000	LD region	CML45	Potential calcium sensor, Calcium-binding EF-hand family protein	
				AT3G29010	LD region		Biotin/lipoate A/B protein ligase	carpel, cauline leaf, collective leaf structure, cotyledon, flower, flower pedicel, guard cell, hypocotyl, inflorescence meristem, leaf

								apex, leaf lamina base, petal, petiole, plant embryo, root, seed, sepal, shoot apex, shoot system, stamen, stem, vascular leaf
				AT3G29020	LD region	MYB110	Encodes a putative transcription factor (	
				AT3G29030	LD region	EXPA5	Causes loosening and extension of plant cell walls by disrupting non-covalent bonding between cellulose microfibrils and matrix glucans. No enzymatic activity has been found (By similarity).	
				AT3G29040	LD region	CRRSP13		
	3	11852064	5.25	at3g30213	Significant SNP		TE pseudo gene	
				AT3G06025	LD region		long_noncoding_rna	
				AT3G30210	LD region		protein_coding	
				AT3G30214	LD region		pseudogene	
				AT3G30214	LD region		pseudogene	
				AT3G30216	LD region		transposable_element_gene	
				AT3G30218	LD region		transposable_element_gene	
				AT3G30219	LD region		transposable_element_gene	
				AT3G30220	LD region		protein_coding	
				AT3G30222	LD region		protein_coding	
				AT3G30230	LD region		protein_coding	
				AT3G30235	LD region		protein_coding	

				AT3G30240	LD region		transposable_element_gene	
				AT3G30245	LD region		pseudogene	
				AT3G30247	LD region		protein_coding	
				AT3G30250	LD region		transposable_element_gene	
	3			at3g30212	Significant SNP		TE pseudo gene	
	3	11844594	4.73	at3g30211	Significant SNP		TE pseudo gene	
	3	11999657	4.09	at3g30393	Significant SNP		TE pseudo gene	
				AT3G30387	LD region		protein_coding	
				AT3G30388	LD region		pseudogene	
				AT3G30390	LD region		protein_coding	
				AT3G30390	LD region		protein_coding	
				AT3G30390	LD region		protein_coding	
				AT3G30393	LD region		transposable_element_gene	
				AT3G30396	LD region		transposable_element_gene	
				AT3G30400	LD region		transposable_element_gene	
				AT3G30405	LD region		transposable_element_gene	
				AT3G30410	LD region		transposable_element_gene	
				AT3G30411	LD region		transposable_element_gene	
				AT3G30413	LD region		transposable_element_gene	
				AT3G30415	LD region		pseudogene	
				AT3G30416	LD region		transposable_element_gene	
				AT3G30418	LD region		transposable_element_gene	
				AT3G30420	LD region		transposable_element_gene	
				AT3G30430	LD region		protein_coding	
				AT3G30433	LD region		transposable_element_gene	
				AT3G30436	LD region		transposable_element_gene	
				AT3G30440	LD region		transposable_element_gene	
				AT3G30450	LD region		transposable_element_gene	

				AT3G30455	LD region		transposable_element_gene	
QTL7	1	5486002	4.26	**AT1G15940**	Significant SNP	T24D18.4	One of 5 PO76/PDS5 cohesion cofactor orthologs of Arabidopsis.	
				AT1G15960	Significant SNP	**NRAMP6**	Metal transporter, Probable intracellular cadmium (Cd) transporter that participates in the distribution or availability of Cd within the cell.	Expressed in the vascular bundles of shoots, cotyledons, young leaves, sepals and petals, at the top of the flower stem and in the style. Expressed in the peduncle of developing siliques as well as in the septum and the funiculi.
		5488194	4.67	**AT1G15970**	Significant SNP		DNA-3-methyladenine glycosylase activity	
		5489294	4.67	**AT1G15980**	Significant SNP		Involved in cyclic electron flow around photosystem I to produce ATP.NAD(P)H DEHYDROGENASE SUBUNIT 48, NDF1, NDH-DEPENDENT CYCLIC ELECTRON FLOW 1, NDH48, PHOTOSYNTHETIC NDH SUBCOMPLEX B 1, PNSB1	
				AT1G16000	Significant SNP	GAG1At, OEP9.1, OUTER ENVELOPE PROTEIN 9.1	Member of the Arabidopsis 7-kDa OEP family. Tail-anchored (TA) membrane protein which possesses a single C-terminal transmembrane domain targeting post-translationally to plastids.	

		5495293	4.67	**AT1G16010**	Significant SNP	ATMGT2, ATMRS2-1, MAGNESIUM TRANSPORTER 2, MGT2, MRS2-1	Transmembrane magnesium transporter. One of nine family members.	mesophyll vacuoles
		5499180	4.67	**AT1G16020**	Significant SNP	CALCIUM CAFFEINE ZINC SENSITIVITY 1A, CCZ1A	vesicle-mediated transport	
		5506701	4.64	**AT1G16040**	Significant SNP		phosphatidylinositol-glycan biosynthesis class F-like protein, chloroplast, endoplasmic reticulum membrane, integral component of membrane	
				AT1G16060	Significant SNP	AP2-like ethylene-responsive transcription factor At1g16060	Probably acts as a transcriptional activator. Binds to the GCC-box pathogenesis-related promoter element. May be involved in the regulation of gene expression by stress factors and by components of stress signal transduction pathways	
				AT1G05213	LD region			
				AT1G15910	LD region			
				AT1G15920	LD region			
				AT1G15930	LD region			
				AT1G15950	LD region			
				AT1G15990	LD region			

				AT1G16022	LD region			
				AT1G16025	LD region			
				AT1G16030	LD region			
				AT1G16070	LD region			
QTL11	**3**	11852064	5.25	AT3G30213	IAA8		TE pseudo gene	
				AT3G30212	IAA8		TE pseudo gene	
		11844594	4.73	AT3G30211	IAA8		TE pseudo gene	
		11999657	4.09	AT3G30393	IAA8		TE pseudo gene	
QTL12	**2**	10911372	4.54	AT2G25640	Significant SNP	ENOC	SPOC domain / Transcription elongation factor S-II protein;	
				AT2G25660	Significant SNP	emb2410	Embryo defective 2410	
		10938838	4.02	AT2G25670	Significant SNP		hypothetical protein	
		10954985	4.1	AT2G25710	Significant SNP	HCS1, HOLOCARBOXYLASE SYNTHASE 1	Plays a major role in biotin-dependent carboxylase biotinylation. Catalyzes the addition of biotin to the biotin carboxyl carrier protein (BCCP) subunit of acetyl-CoA carboxylase and can also biotinylate methylcrotonyl-CoA carboxylase. Is responsible for most, if not all, biotin--protein ligase activity in Arabidopsis.	Expressed in roots, leaves, stems, flowers, siliques and seeds.

							Is essential for plant viability and required for ovule development	
QTL14	3	17336284	5.13	AT3G47060	Significant SNP	FTSH7	Probable ATP-dependent zinc metallopeptidase.	carpel, cauline leaf, collective leaf structure, cotyledon, flower, flower pedicel, guard cell, hypocotyl, inflorescence meristem, leaf apex, leaf lamina base, petal, petiole, plant embryo, plant sperm cell, pollen, root, seed, sepal, shoot apex, shoot system, stamen, stem, vascular leaf
	3	17337787	4.84	AT3G47070	Significant SNP	F13I12.120	Thylakoid soluble phosphoprotein	
				AT3G47050	LD region	F13I12.100		

				AT3G47080	LD region	AXX17_At3g47079	Tetratricopeptide repeat (TPR)-like superfamily protein;(source:Araport11)	
QTL15	2	19396129	5.77	AT2G47240	Significant SNP	LACS1	Activation of long-chain fatty acids for both synthesis of cellular lipids, and degradation via beta-oxidation. Acts in both the wax and cutin pathways. Preferentially uses palmitate, palmitoleate, linoleate and eicosenoate. Seems to have a specific activity against very long-chain fatty acid (VLCFA) class with acids longer than 24 carbons (C(24)).	
				AT2G47270	LD region			
	2	19397901	**6.69**	AT2G47250	Significant SNP		Probable pre-mRNA-splicing factor ATP-dependent RNA helicase DEAH3	carpel, cauline leaf, collective leaf structure, cotyledon, flower, flower pedicel, guard cell, hypocotyl, inflorescence meristem, leaf apex, leaf lamina base, petal, petiole, plant embryo, plant sperm cell, pollen, root, seed, sepal,

								shoot apex, shoot system, stamen, stem, vascular leaf
				AT2G47260	Significant SNP	WRKY23	Transcription factor. Interacts specifically with the W box (5'-(T)TGAC[CT]-3'), a frequently occurring elicitor-responsive cis-acting element (By similarity).	
				AT2G47245	LD region			
QTL16	5	13406723	5.08	AT5G35148	Significant SNP		transposable_element_gene	
				AT5G05175			long_noncoding_rna	
				AT5G35111			pseudogene	
				AT5G35113			transposable_element_gene	
				AT5G35116			transposable_element_gene	
				AT5G35118			transposable_element_gene	
				AT5G35120			protein_coding	
				AT5G35130			transposable_element_gene	
				AT5G35140			transposable_element_gene	
				AT5G35142			transposable_element_gene	
				AT5G35145			transposable_element_gene	
				AT5G35146			transposable_element_gene	

	5	13406872	5.03	AT5G35090	Significant SNP	AXX17_At5g35090	E3 ubiquitin-protein ligase that mediates ubiquitination and subsequent proteasomal degradation of target proteins. E3 ubiquitin ligases accept ubiquitin from an E2 ubiquitin-conjugating enzyme in the form of a thioester and then directly transfers the ubiquitin to targeted substrates.	
				AT5G35080		OS10	Encodes a protein involved in the endoplasmic reticulum-associated degradation of glycoproteins.Lectin which functions in endoplasmic reticulum (ER) quality control and ER-associated degradation (ERAD). May bind terminally misfolded non-glycosylated proteins as well as improperly folded glycoproteins, retain them in the ER, and possibly transfer them to the ubiquitination machinery and promote their degradation. Targets the misfolded LRR receptor kinase BRI1 and the misfolded receptor-like kinase EFR.	carpel, cauline leaf, collective leaf structure, cotyledon, flower, flower pedicel, guard cell, hypocotyl, inflorescence meristem, leaf apex, leaf lamina base, petal, petiole, plant embryo, pollen, root, seed, sepal, shoot apex, shoot system, stamen, stem, vascular leaf
	5	13408215	5.03	AT5G35150	Significant SNP		transposable_element_gene	
	5	13412405	5.08	AT5G35150	Significant SNP			

	5	13414267	5.03	AT5G35160	Significant SNP	TMN11	carpel, cauline leaf, collective leaf structure, cotyledon, flower, flower pedicel, guard cell, hypocotyl, inflorescence meristem, leaf apex, leaf lamina base, petal, petiole, plant embryo, plant sperm cell, pollen, root, seed, sepal, shoot apex, shoot system, stamen, stem, vascular leaf	